UNIVERSAL CLOCKING OFF ROTATING NEUTRON STARS

An initial mathematical analysis of pulsar spin-down dynamics for use in time-keeping technology

Joshua Carroll
M.S.T., Applied Mathematics
B.S., Physics

Table of Contents

Executive Summary

This paper discusses the initial feasibility analysis of an invention that utilizes pulsars as a timing source for network communications and potentially other position and timing applications. The main idea is to develop a way to calculate a pulsar's decay curve so that it may eventually be used to make reference time predictions based on pulse period measurements. This paper provides an outline of said invention, the theoretical background on timekeeping, pulsars and their intrinsic properties, methods and applications of collecting the necessary data, and a mathematical analysis of the equations used to model said data. Furthermore, this paper addresses future needs for this project, and potential targets for the work done. Our team has been able to successfully implement code that captures and parses pulsar data that is then run through a mathematical program to generate a curve of best fit. The model is able to generate parameter estimations with high confidence ($p < 0.05$) provided our assumptions on the local stellar environment are correct. The successful prediction of a viable magnetic field and estimation of the pulsar's braking index is an indicator that this model is worth further study and analysis. We also briefly look into the market space that this technology could play a role in and identify key areas of interest and potential solutions for competition.

1: The Invention

We will first briefly go over the invention that is driving this research and development. For a full breakdown of the invention, see Appendix A.

This piece of technology seeks to use pulsars as a reference clock that can act as a failsafe to synchronize networks. This invention will determine a reference time that can synchronize networks with minimum human involvement to a high degree of precision. It will be incredibly useful not only as a good backup for keeping accurate and secure network timing, but it could also serve as a way for human-made objects in deep space to ensure they are able to stay within network timing thresholds so they do not lose communication with either each other or Earth in the event of power loss or other unforeseen circumstances. Below is a brief summary of each component of said invention.

1) The first component of this invention will be a database of known pulsars containing their coordinates and the decay function for each pulsar. This database will be periodically updated by something we call the Database Decay Function Processor to provide new decay functions for each targeted pulsar.

2) The second component is a high-precision clock that will be used to increment both the measured and estimated reference time. This could be a local, chip-sized atomic clock or the pulsar clock itself.

3) The third component will be a set of sensors to detect the radiation pulses from any select set of pulsars. This component could be an array of sensors that is able to measure various types of electromagnetic radiation to provide more data collecting capabilities when scanning for pulsars.

4) The fourth component will be a signal processor that allows the invention to isolate the pulsar's signal from background noise. In general, the signal processor uses a low-pass filter to remove noise above the observed signal's frequency. It can then down-modulate the signal to a more manageable frequency. It can then further isolate the pulsar's signal by passing this down-modulated signal through another band-pass or low-pass filter. It will then fold the pulsar's signal at the frequency of the pulsar's rotational rate of rotation to generate a running average or "pulse profile" of the pulsar. This feature will be the first line of verification of the pulsar being observed to match it with the data in the pulsar database.

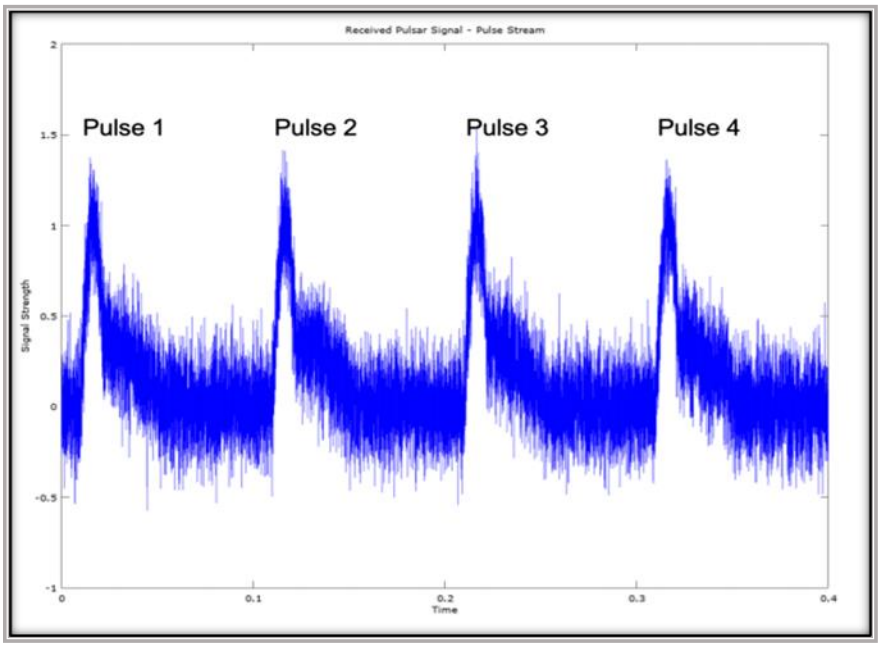

Figure 1: Recording pulses from a simulated pulsar

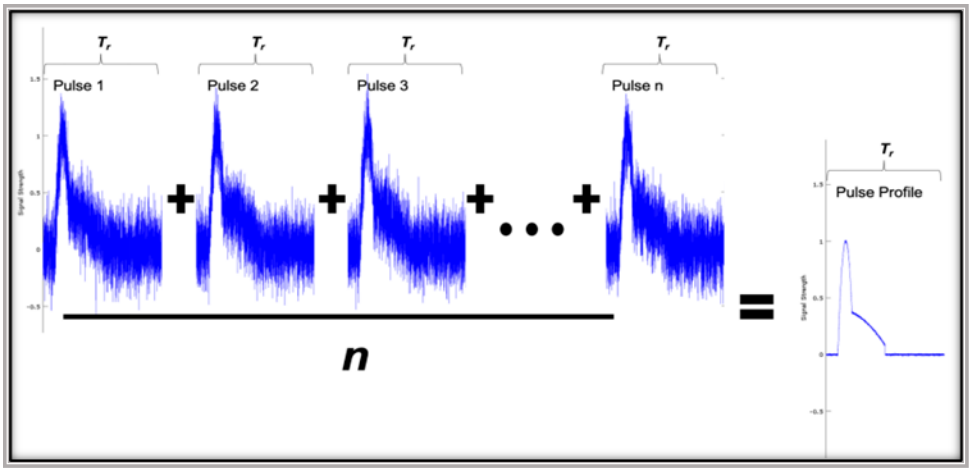

Figure 2: Folding pulse signals to generate a pulse profile

5) The fifth component will be the Time Processor, which takes a pulsar's rotational frequency and uses it to calculate a reference time. This is done via a calculated Decay Function for the targeted pulsar. Initially, these decay functions will be provided via human interaction, but over time the invention seeks to have the system "learn" and calculate the Decay Function at the time the measurement is taken. This processor stores and maintains these Decay Functions for all selected pulsars and uses them to average their calculated reference time.

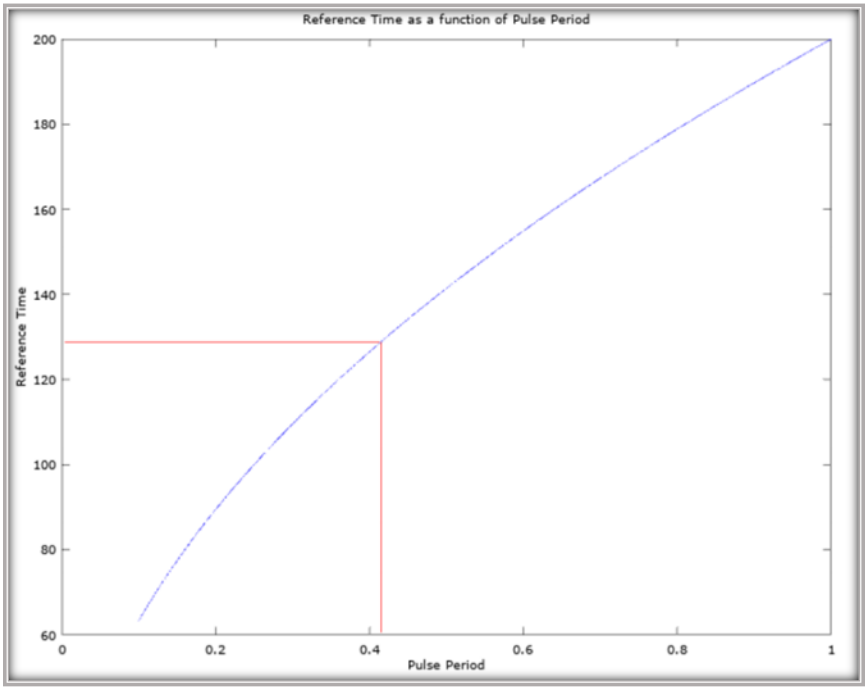

Figure 3: Solving a pulsar's Decay Function for a measured pulse period

6) The sixth component will be the Glitch Processor, which is responsible for detecting changes in a pulsar's rotational decay that the Decay Function cannot predict. Whereas we do not understand fully what causes these events to occur, they do so with a large enough effect that we must take them into account when using the star for a reference time. Essentially, the invention will be monitoring multiple pulsars and checking the Decay Function against the observed pulses. If a glitch occurs in one of the pulsars being measured, this Glitch Processor flags that particular star as needing to be re-baselined before using it again.

7) The seventh component will be the Decay Function Processor. When a glitch is identified and a particular Decay Function is no longer valid, the Glitch Processor tells the Decay Function Processor to create a new Decay Function for the glitched pulsar. Collecting enough measurements to fit a decay curve to a pulsar may take a while, so the Glitch Processor will ensure the glitched pulsar remains flagged, so as not to be used in the Time Processor. This component will re- baseline the pulsar by collecting data from the pulsar in question (the star's pulse profile and frequency of rotation) to calculate the new decay curve.

2: Theoretical Background- Timing and Networks

Timing is a crucial component in networked systems as the application of it allows for the successful transfer of information, the use of troubleshooting techniques, and as a means of security for the system as a whole. Furthermore, accurate timing is a crucial component for positioning systems such as our GPS network of satellites. Accurate timing allows for location services that is integral in much of our modern-day technologies, and will be on the forefront of future deep space technologies that can no longer rely on Earth-based positioning systems. Developing a way for networked systems to remain time-synced using pulsar rotational decay curves is the subject of this research that is being done by Booz Allen Hamilton in conjunction with the University of Utah, with the idea of providing a different and potentially more secure way to keep any network time-synced, even over vast distances. This may also play a role in positioning systems in which it can provide a common time and distance calculation for technology that is beyond low-Earth orbit. In this section, we will establish a simple overview of basic timekeeping and its role in networks

2.1: A Simple Scenario

We will begin to understand timekeeping and network communication with the simplest case. Let's say you have two clocks that need to read the same time, perhaps a wristwatch and a well- established clocktower. Since the clocktower is the agreed upon (well-established) timeframe that you wish to use, you will want to sync your wristwatch to the tower, so that your personal time matches what the clocktower says. Now let's introduce another clock, say your friend's wristwatch. If you want to be able to communicate with them for an agreed upon time, they will also need to sync with the clocktower. In

this way, you have a basic communication network in that you and your friend can speak using the same reference time. If you want to meet at 2pm for lunch, their watch and yours will allow you to meet up at the agreed upon time without needing to each look at the reference clock. Whereas this is a very simple scenario, it will allow us to elucidate some issues that arise with network timing that we have today.

The simplest issue that arises is that of a specific watch falling out of sync with the reference clock. If over time your watch is slightly slower than your friends, your watch's time will "drift" with respect to the reference clock's time and eventually it will not read the same time as your friend's watch. As such you risk an inability to communicate with your friend as your time wouldn't be what theirs is when agreeing to meet at a specific time. To remedy this, it would be incumbent upon you to sync your watch with the clocktower every so often to correct this drift. For this simple scenario that could be once a month, but for realistic networks today this is done on the millisecond scale and is done often to ensure all systems within the network have the correct time to avoid communication issues.

Another issue would be loss of connection to the reference time source. This could be due to a mechanical issue with the communication equipment, or from malicious intent. Either scenario presents a path to losing communication capabilities. In our simple scenario, let's say that one of our friends likes to travel long distances and can no longer make it back to the reference clock tower often. If their watch runs out of batteries and they can no longer reestablish the correct time by using the clock tower, they will not be in sync with you and your watch. Or you could have a scenario where someone wants to disrupt your communication by either tampering with your friend's watch or by "spoofing" the reference time to throw off your communication system. Both of these are situations in which your simple network could break down and communication could be lost.

Our simplified scenario is meant to present to you the basics of network timing and the issues that can and do present themselves. For most systems that are Earth-based, losing reference time isn't that big of a deal (outside of malicious intent) in that you can reestablish communication with the reference time via something called a Network Time Protocol (NTP) server, which is sometimes called a Network Time Server (NTS). In many large-scale networks this server is connected to a commonly recognized time source via a satellite. This time source is defined as Coordinated Universal Time (UTC) and is maintained via a system of atomic clocks (more on this in the following section).

However, let's say our network is not Earth-based and reestablishing communication with a UTC-based network may take some time. In a situation like that, it would be quite useful to have access to a reference time so you can resynchronize your network, or even to introduce a separate "universal" time that doesn't rely on Earth-based timing sources. As humanity moves out into the solar system, addressing the issues raised above for more remote locations will become a priority. Having a reference source that is not attached to any human-based systems and instead uses natural phenomena to increment time would be a great way to ensure you can maintain network timing even when removed from communication with Earth-based systems no matter the cause of the interruption.

2.2: Timekeeping and Atomic Clocks

The essence of time keeping comes down to agreeing upon how long a base unit of time lasts. The ability to keep track of something that occurs repeatedly with as little variation as possible is what enables us to increment time forward and assign values to this incrementation. The standard unit of time is the second, and this has been defined in many different ways throughout time. For a deeper discussion on this, see Chapter 9, *From Sundials to Atomic Clocks: Understanding Time and Frequency* (Jespersen & Fitz-Randolph, 1999). As mentioned above, our large-scale networks use UTC. UTC is built from a combination of International Atomic Time (TAI) and Universal Time (UT1). TAI is time kept by 400 atomic clocks around the world and it provides the exact "speed" our clocks should "tick". UT1 (also known as a solar time) is based on the Earth's rotation. The combination of the two are used to compare the atomic "tick speed" and the length of a day on Earth, with the output being UTC.

Let us now focus our attention on the second and how we define that using atoms. Just as you can create a system of time based on how long it takes for a pendulum to swing back and forth one time (one oscillation), you can also use other periodic behavior. In essence, a clock consists of two parts; an oscillator and something to count the oscillations. In the mid-20th century, humanity set up an official definition for a second based on the atom. Prior to this, the second was based on the Earth's rotation (a solar day), or precisely $\frac{1}{86{,}400}$ of the mean solar day. However, the Earth's rotation is variable due to different factors such as the change of the seasons and tidal friction with the sun and moon.

One of the primary things we do within the science of measurements is establish standards to measure things by. These standards should seek to achieve two things: your standard should strive to have no variability in it, and you should seek to remove the "human element" from them as much as possible. You can achieve this by using natural phenomena and constants of nature to base your measurements off. In this way, you can eliminate ambiguity when it comes to human error and ensure that your standards are based on fundamental and cosmological principles that do not vary.

Atoms possess many features, but the oscillatory nature of the electrons in its various orbitals are what we are after when seeking to define a second. As mentioned above, you can use anything with periodic behavior to increment time, however in order to have a very accurate and precise definition of time you need highly stable oscillations. As written in *Atomic Clocks: A Brief History and Current Status of Research in India*, "The quality of an oscillator is determined by its degree of stability and accuracy and its capacity to remain immune to environmental changes. Any uncertainty or change in the frequency of the oscillator will result in a corresponding uncertainty or change in the timekeeping accuracy of the clock." (Arora, et al., 2014)

Understanding that atomic oscillations are stable, accurate, and have resistance to environmental changes, the standard second was defined using the atom at the 13th General Conference of Weights and Measures. The atom chosen was Cesium due to its atomic structure (see below).

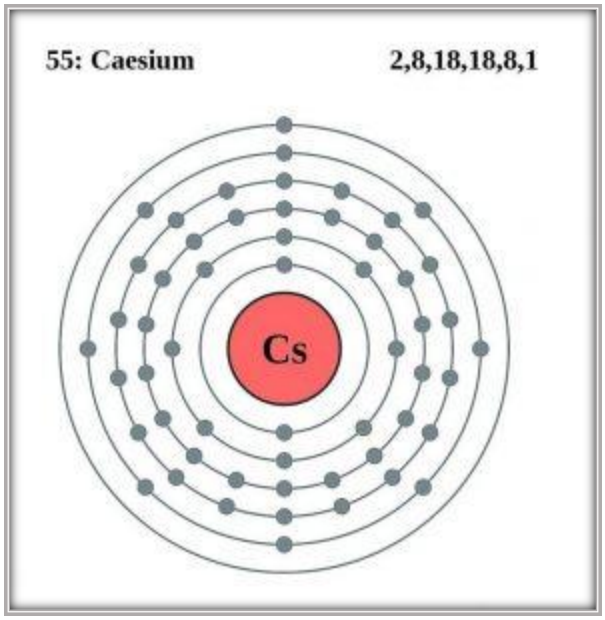

Figure 4: Bohr model of the Cesium atom
Image source: https://www.chemistrylearner.com/cesium.html

Cesium is an alkali metal and it exists in the first column of the periodic table of elements. That means that it contains one electron in its outermost orbital, and it is that electron that we seek to obtain our highly accurate oscillations from. To be specific, the isotope Cesium-133 is what is used within atomic clocks. There is only one stable isotope for Cesium, so when you utilize the isotope, you know that every atom within your atomic clock will have the same hyperfine structure.

These Cesium atoms are fed through a radiation chamber that is tuned to the resonate frequency of the atoms, which is exactly 9,192,631,770 Hz. When this radiation hits the atoms, it causes the outer electron to jump to a higher orbital and then settle back down to its ground state. This releases radiation that we detect and count, which provides us the oscillatory behavior necessary to measure a second (see Figure 5). In particular, the second was defined by the 13th General Conference of Weights and Measures as "the duration of 9,192,631,770 periods of the radiation corresponding to the transition between the two hyperfine levels of the ground state of the Cesium-133 atom". (Arora et. al., 2014, pg. 175).

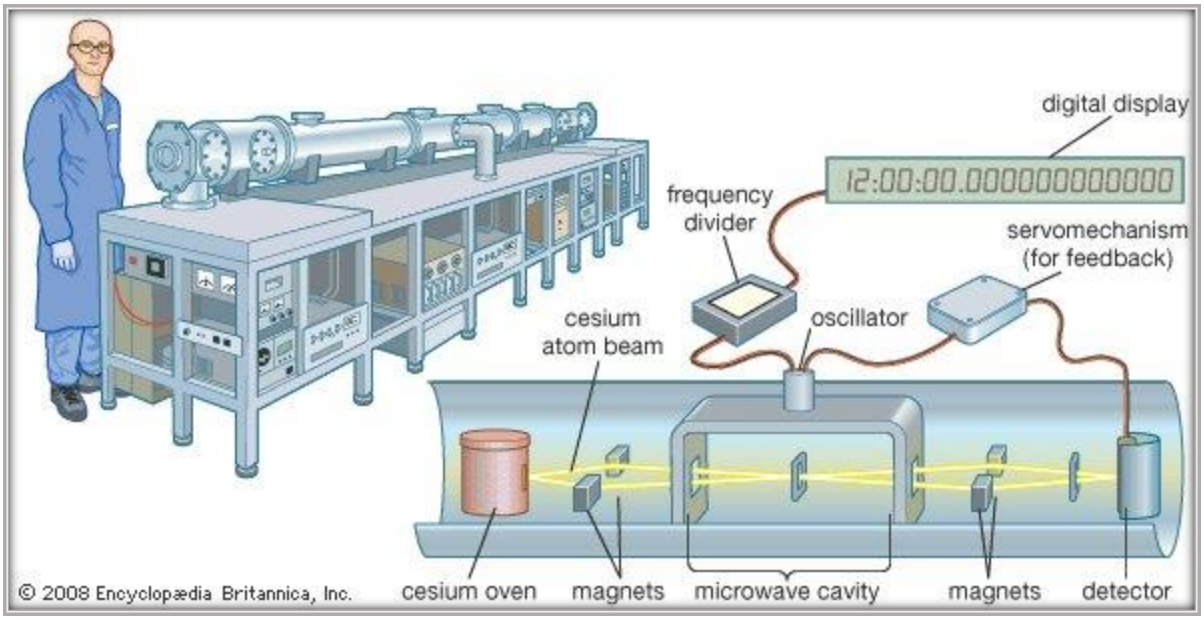

Figure 5: Cesium clock
Source: Encyclopædia Britannica,
https://www.britannica.com/technology/atomic-clock#/media/1/41652/107848

Our usage of atomic clocks allows us to have very accurate measures of time that we can base all our time measurements off. In fact, some of the Cesium clocks we operate today will neither lose nor gain a second in around one million years (Arora et. al., 2014, pg. 177). Other clocks, such as the one at the National Physics Laboratory in the UK can achieve an accuracy that will only falter once in approximately 158 million years! (Rowlatt, 2014)

2.2: Network Time Protocol

With our standard for a second defined quite accurately, we can use this to increment UTC forward, and as such we have developed a very accurate reference "clock tower". Today's networks can access this reference time via satellite and their NTP servers. In a typical network structure, you will have access to UTC through different methods such as a GPS-antennae or a radio broadcast. The structure of the node receiving and sharing the time is broken down into stratums 0-7, with the numbers representing how "close" to the source time the node in a network is. Stratum 0 is the reference time itself, so a typical network topology will have your NTP server as stratum 1 (see below graphic). For a more complete breakdown of NTP and how it operates, see *Internet Time Synchronization: The Network Time Protocol* (Mills, 1989).

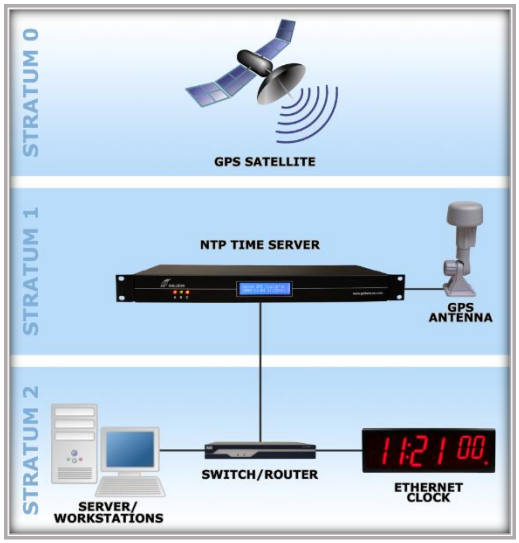

Figure 6: NTP distribution
Source: Galleon Systems

The reference time is broadcast to any network that is requesting the time, and then that network uses it to keep each node within the network timed. In this way, all the systems within the network can effectively communicate with each other and if needed can communicate with other networks outside of its immediate domain (such as various interconnected networks across multiple server locations). If a system falls out of time sync with the rest of the network, communication can be lost. Typically, lower stratum nodes will have their times checked and corrected by higher stratum nodes using the stratum 0 reference time (UTC).

2.3: Potential Issues

Now that we have established how timing within networks works and its importance, we can discuss issues that arise. As mentioned above, loss of connection to the reference time source, such as your GPS-antennae malfunctioning, a spacecraft's onboard Cesium clock suffering a mechanical failure, or being too-far away from Earth-based timing sources, your networked systems that rely on timing will no longer be able to accurately function. In some instances, malicious attacks that target the NTP server or a system that requires time to function properly (such as with anything GPS related) can bring down networks and pose as a real threat.

The former case is fairly straight forward: if a failure in your equipment disrupts the timing of your system, you can experience loss of communication capabilities. There are many factors that can cause this, but the end results are the same in that if you cannot successfully increment your time forward and keep the systems synced, you lose communication capabilities between different nodes within a network. The latter is a bit more nuanced and presents real threats to our networks, nationally and internationally.

2.3.1: Time Spoofing

On January 12th, 2016 two U.S. Navy patrol boats and 10 sailors were captured by Iranian forces after the boats strayed into Iranian waters. The story from the U.S. Navy was a "mechanical failure", however it has been speculated that the U.S. Navy's GPS system was spoofed and caused it to stray into unfriendly waters. Another case occurred on December 4th, 2011 when a U.S. drone crashed in Iran. There has been speculation that Iran had spoofed the GPS signal to trick the drone, which caused the crash landing. Each of these are discussed by the U.S. Naval Institute as a means to elucidate the threats that our security faces due to our reliance on GPS. (Goward, 2016)

GPS spoofing is a very real threat that has been studied extensively. The basic idea behind spoofing a GPS involves mimicking the signals of the GPS constellation. A malicious actor can make their fake signals slightly stronger than the ones coming from the GPS satellites. Once the receiver of these signals aligns with the fake signals, the spoofer can tamper with the time shift between the fake signal and the receiver, which results in the receiver being tricked into thinking it is somewhere where it is not. This method (among others) has been demonstrated to trick aerial drones into thinking they are in one place when they are not (Horton & Ranganathan, 2018). A deep dive into the workings of GPS and spoofing methodologies and research is also given in the paper *On GPS spoofing of aerial platforms: a review of threats, challenges, methodologies, and future research directions* (Khan, Mohsin, & Iqbal, 2021) and a decent overview of time service spoofing and solutions is also given in the Meinberg Knowledge Base (Burnicki, 2019).

There are multiple solutions being researched now (Khalajmehrabadi, Gatsis, Akopian, & Taha, 2018), but having access to a backup reference time source is a common solution. A network that suspects itself to be the target of a time spoofing attack can switch to a backup reference time until the threat has been removed. In fact, having a backup reference time not only helps in mitigating the threat of time spoofing, but also provides a solution for the simpler problem of having a malfunction with your hardware and/or software that receives a time signal. As described by Burnicki in the Meinberg Knowledge Base, "A good way to detect and avoid spoofing is to use different, independent time sources as backup sources. The receiver can then check the time offsets between these sources to determine if they all agree on the same current time."

However, you also must be sure that your backup time cannot also be spoofed. The mode of attack is to create a fake signal that can alter the time signals of the fake GPS signal, so you would need something that can keep track of time that isn't easily spoofed or that can be easily cross-referenced with known values so the system can be sure that it can increment the time correctly with the backup time source. It turns out that trying to spoof pulsar signals (especially in the X-Ray band) would be incredibly difficult to achieve, and as such our pulsar timing mechanism could find market viability along these lines.

3: Theoretical Background- Pulsars

In this section we will discuss the theoretical background of pulsars and their intrinsic properties that we are seeking to exploit. The first requirement for a good timing source is not needing much human

interaction to perform oscillatory behavior, which a pulsar provides by the fact that its rotation is due to fundamental principles of physics. The second requirement is that the oscillations you are using maintain a high degree of accuracy over time. This is what remains in question with using pulsars as a timing source and one that this paper seeks to answer. In essence, can we develop a mathematical way to predict accurate time using data collected from any given pulsar based on the fundamental laws of physics?

3.1: Pulsars-The Birth of a Dead Star

For the following analysis, we will be relying on knowledge supported from the textbook *Foundations of Astrophysics.* (Ryden & Peterson, 2010)

The way a pulsar achieves its rotational properties that we want to use for keeping time emerges from the following physics. Every star's fate is determined by its mass (known as the Russell-Vogt Theorem), with smaller stars becoming white dwarfs and the larger stars becoming either neutron stars or black holes. It will be helpful if we discuss the mass of stars using solar masses ($M_\odot$), with one solar mass being roughly 1.989×10^{30}kg. Stars that have an initial mass between $7M_\odot$ and $18M_\odot$ are fated to become neutron stars.

Once core collapse begins in a star, the resulting outputs are fantastic. When a star exhausts all its fuel, it begins to collapse under its own gravity. During the main sequence phase, a star is fusing hydrogen in its core into helium. Once this fuel source is exhausted, the star will begin to collapse down, and the increase in pressure on the core due to this causes the helium to begin to fuse into carbon. For stars with mass $7M_\odot \leq m \leq 18M_\odot$, this fusion process will continue from helium all the way up to iron. During these core phases, the star expands into what we call a supergiant. In the final moments of the star's life, the star will have many layers with iron at its center (see image below). The outer layers of this star fuse themselves into the elements of the layers below them, with the inevitable conclusion of the iron core growing. Once this dense iron core reaches what is known as the Chandrasekhar mass (named for the astrophysicist who first made these calculations, Subramanyan Chandrasekhar), it completely collapses.

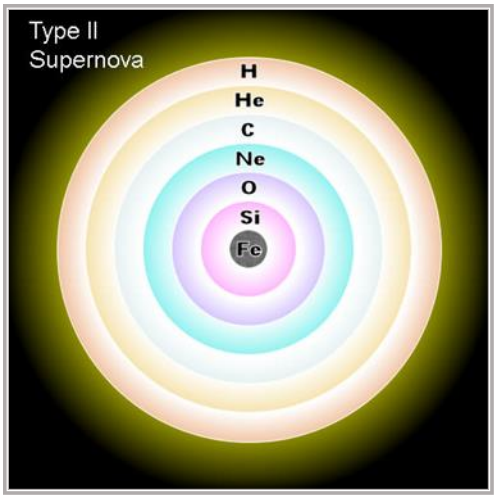

Figure 7: High mass star prior to collapse
Source: Wikimedia Commons

When the iron core collapses, its density rises rapidly with the freefall time being

$$t_{ff} < \frac{1}{10} s \, .$$

During this rapid collapse, protons and free electrons are forced together unimaginably quickly. The result of this interaction is the formation of neutrons as follows:

$$p + e^{-} = n + v_e$$

The electron neutrinos (v_e) that are created in this interaction carry away a massive amount of energy (approximately 10^{46}J, which is more energy than our sun will create during the entirety of its main sequence phase). The neutrons that remain are still in freefall and crashing towards themselves with the only thing stopping them being neutron degeneracy pressure.

Degenerate neutrons produce a pressure of

$$p_n \sim \hbar^2 \left(\frac{n_n^{5/3}}{m_n} \right)$$

where the mass of the neutron (m_n) is 1,839 times the mass of an electron and n_n is the number density of neutrons. This pressure keeps these neutrons from falling into infinity and creating a black hole (stars that have an initial mass $m > 18 M_{\odot}$ will collapse to a singularity required for a black hole). This dense

ball of degenerate neutrons (roughly 2×10^{57} of them) is what we call a neutron star and is among the most-dense objects in the known universe, only surpassed by that of a black hole. One of the amazing things about this process is that the stages prior to this strange feature of nature are incredibly large (many hundreds to even thousands of times the radius of our own sun), and the resulting neutron star will roughly be 20km in diameter, or just large enough to fit the island of Manhattan inside of it!

3.2: The Useful Nature of Pulsars

The discussion above about the process of stellar collapse and the density of the remaining object leads into the feature we are looking for: oscillatory behavior. As the core of our dying star collapses, angular momentum is conserved. As the star rapidly collapses, it begins to rotate incredibly quickly. Rotational velocities of $v \sim 0.1c$ are entirely possible as a maximum with a corresponding rotational period $p_{ns} \sim 2 \times 10^{-3} s$. This hyperdense ball of neutrons also contains a very strong magnetic field that is also conserved in the collapse. For reference, our star has $B_{\odot} \approx 10^{-4}\ Tesla\ (1\ Gauss)$ and a typical neutron star has $B_{ns} \approx 10^{11}\ Gauss$. The rotational nature of the neutron star and the conserved, intense magnetic field it carries classifies the neutron star as a pulsar.

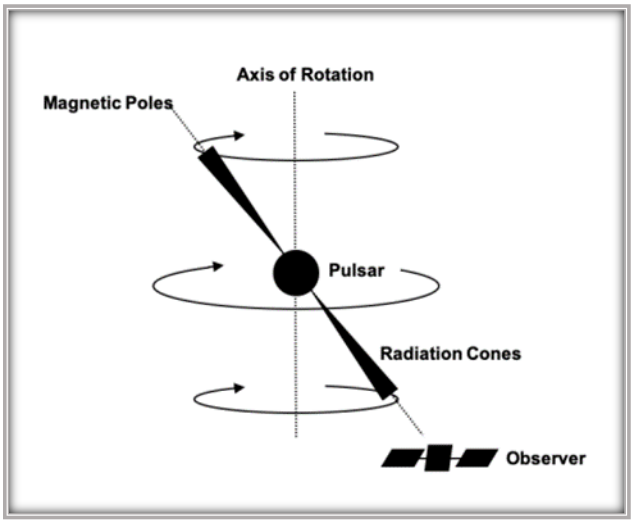

Figure 8: General pulsar diagram

As seen in the above diagram, as the pulsar rotates, the magnetic poles sweep around the axis of rotation by some angle Φ. The rotating magnetic field generates a very strong electric field that rips electrons and ions out of the star's atmosphere and accelerates them along the magnetic field lines. This acceleration creates synchrotron radiation and it is beamed around and out of the magnetic poles. If Φ = 0, this radiation beam wouldn't sweep out any area around the star's poles and would be aligned perfectly with the axis of rotation. However, if Φ ≠ 0, these radiation beams will sweep out an area

around the star as it rotates. If an observer happens to be aligned with this beam (as seen in Figure 8), they will see the radiation "flash" as the beam passes over them.

The following information and equation derivations can be looked over in detail in the *Handbook of Pulsar Astronomy* (Lorimer & Kramer, 2005). As this beam passes over us, it appears as a periodic pulse of radiation from which we can ascertain information about the pulsar emitting the beams. Pulse periods are directly related to the rotation of the pulsar itself; the faster the star rotates, the shorter the period. Over time it has been observed that pulse periods increase, which corresponds to the star's rotation slowing down. We can represent this behavior by looking at the loss of rotational kinetic energy by a pulsar with the following relation:

$$\dot{E} = -\frac{dE_{rot}}{dt} = -\frac{d\left(\frac{I\Omega^2}{2}\right)}{dt} = -I\Omega\dot{\Omega} = 4\pi^2 I\dot{P}P^{-3}$$

Where $\dot{E}$ is the "spin down luminosity" (total power output by the star), I is the moment of inertia, Ω is the rotational angular frequency, and $\dot{P} = \frac{dP}{dt}$, or is the rate at which the pulse period changes with respect to time.

This $\dot{P}$ is of particular interest for this research in that each pulsar will have its own period of slowing directly related to its local environment and the star's intrinsic properties. $\dot{P}$ gives us a dimensionless value that categorizes the pulsar's rotational decay over time, and if we then plot P vs t, we will be able to observe this slowing or "braking". With sufficient measurements, it would be possible to fit a curve to a particular pulsar and extract a "rotational decay function" that can be used to identify a star within a given database and be a useful tool to ensure that we can accurately use the star's oscillatory nature to increment time.

This "braking" of a pulsar's spin can be described by something called a Braking Index. This feature of pulsar rotational decay is currently being studied extensively by many researchers. Of the various things that can drive this rotational decay, we will look at one feature: the emission of the magnetic radiation from the rotating dipolar magnetic field. For a full treatment of this process, see the papers *Braking index of isolated pulsars* (Hamil, Stone, Urbanec, & Urbancova, 2015) and *A high braking index for a Pulsar* (Archibald, et al., 2016), as well as Chapter 3 from Lorimer's and Kramer's textbook mentioned above. The energy loss is considered a proportional model-dependent power of Ω. For the ideal case of an isolated pulsar in the vacuum of space, we can observe this power law by looking at how the energy produced by this dipole changes with respect to time:

$$\dot{E} = \frac{2}{3c^3}|\boldsymbol{m}|^2\Omega^4 sin^2(\Phi)\ .$$

Here, $|\boldsymbol{m}|$ is the rotating magnetic dipole moment, and as discussed above Φ is the angle between the rotation axis of the pulsar and the magnetic moment. You can relate this equation with the equation we

had above for the loss in rotational kinetic energy to arrive at a way to equate the expected evolution of the rotational frequency:

$$\dot{\Omega} = -\left(\frac{2|\boldsymbol{m}|^2 sin^2(\Phi)}{3Ic^3}\right)\Omega^3$$

We can see a generalized power law relationship if we simplify this using $\nu = \frac{1}{P}$ (rotational frequency):

$$\dot{\nu} = -K\nu^n$$

where n is our braking index. For the ideal case that we've discussed above, n is equal to 3. However, this would represent a rotational decay due purely to the outflow of energy from to the magnetic dipole. In reality, there are many other mechanisms that can decay a rotation for a pulsar which are being researched today (Archibald, et al., 2016). The reason we dove into these equations and explanations is to elucidate the fact that each pulsar will have many factors that play into their decay curves that we can fit to the aforementioned P vs t plot. This will help provide a sort of "data signature" that may be useful to ensure validation of the data that is collected in order to increment time forward for this reference pulsar.

Furthering their usefulness for this project, there are a vast number of pulsars that are aligned in ways that allow us to see their energy pulses and we have created vast catalogues to track them. These pulsars are far enough away that we have decent visibility of them despite our location within the solar system (provided we select pulsars that are high enough above or below the ecliptic plane) and they are objects that would prove difficult to spoof, thus providing a robustness in their use for reference timekeeping. Within these catalogues, we can track things such as the frequency of the pulse, the velocity of the star's rotation, the distance to that pulsar, etc. The data surrounding these known quantities will be vital in developing a way to exploit these stars to develop a way to use them for timekeeping purposes.

4: Analysis of the Pulse Period

To begin, we will focus in on the parameters of what we are selecting as a governing equation for this project. When presented with a set of data, you need to identify an equation that is theoretically sound that governs the curve of our fit. For this, we turn to an equation discussed in the paper *PsrPopPy: An Open-Source Package for Pulsar Population Simulations* (Bates, Lorimer, Rane, & Swiggum, 2014). The equation

$$P(t) = \left[{P_0}^{(n-1)} + \left(\frac{n-1}{2}\right) t_d k B^2 \sin^2\left(\Phi_0\left(1 - e^{\frac{-2t}{t_d}}\right)\right)\right]^{\frac{1}{n-1}} \quad (1)$$

is from a differential equation for $\dot{P}$ taken from Lorimer and Kramer's work in aforementioned textbook. (Lorimer & Kramer, 2005) As we have discussed, this equation is assuming the pulsar is predominantly slowing due to dipole radiation with no external influences (such as a thick gas cloud or an unseen binary companion). It is, however, allowing the angle between the radiation beams and the spin-axis to vary with time, which can affect the rotation's slowing.

4.1: Exploring the Parameters

The above equation for the pulse period contains a few parameters that will be discussed. This will help shape the remainder of our analysis when we get into the methods used for fitting our selected pulsar's data.

Parameter	Name	Units
P_0	Initial pulse period	s
B	Magnetic Field	$\sqrt{\frac{g}{cm}}s^{-1}$
n	Braking index	Dimensionless
t_d	Characteristic time for rotation-radiation axes alignment	s
k	Scaling constant	$\frac{cm(s^3)}{g}$
Φ_0	Initial angle between rotation-radiation axes	Dimensionless

Table 1: Parameters

The parameters of interest for this initial analysis are B and n, the magnetic field strength and braking index respectively. The magnetic field strength is being measured in Gauss (cgs), and the braking index is a dimensionless quantify that characterizes the manner in which any given pulsar slows down over time. These quantities take on different roles for the analysis that are both important in discussing and classifying the pulsar, and determining how effective (if at all) this model is as a governing equation for our data.

In order to evaluate the model's effectiveness during this initial analysis, we seek to use this model to extract values for the parameters that are unknown to us from the given data. Our data provides us with our initial pulse period measurement and a potential starting point for the characteristic alignment time. As mentioned in S.D. Bates paper, we assume an initial angle of $\frac{\pi}{2}$ radians that then transitions to align with the rotation of the pulsar over that characteristic time. For the purposes of using our model, this alignment occurs during or close to the measurement period to infer the long-term behavior of the pulsar, with longer measurement periods coinciding with more accurate outputs for the model. The k parameter is a combination of constants canonical pulsar estimations, such as the moment of inertia

being around 10^{45} g(cm^2) and radius to be 10^6 cm. That leaves us with B, n, and t_d to be estimated using the assumptions of the model and the output of the curve fitting algorithm respectively.

4.2: Dimensional Analysis

To discuss n, we must first discuss equation (1). As mentioned, this model is assuming pure dipole-braking. For that, we must take $n = 3$. Being that this equation represents a physical system, we can use dimensional analysis to see why this must be the case.

Let's establish the dimensions for each term by looking at their units and reconstructing the equation in terms of said dimensions. We will rewrite the equation to simplify the analysis a bit so that we elucidate the important terms:

Set

$$t_d k B^2 = \Lambda \quad , \quad \Phi_0\left(1 - e^{\frac{-2t}{t_d}}\right) = \Phi(\mathrm{t})$$

Now, we rewrite (1) as

$$P(t) = \left[{P_0}^{(n-1)} + \left(\frac{n-1}{2}\right)\Lambda \sin^2(\Phi(\mathrm{t}))\right]^{\frac{1}{n-1}} \qquad (2)$$

One more simplification we can make is set $\left(\frac{n-1}{2}\right)\sin^2(\Phi(t)) = \eta$, remove the t dependence, and raise each side to the $n-1$ power to arrive at

$$P^{(n-1)} = {P_0}^{(n-1)} + \eta\Lambda \qquad (3)$$

where η is a function of n and t whose output is unitless.

With (3) and Table 1 above, we can now construct this equation in terms of its dimensions.

Unit	Description	Dimension
s	Second	T (time)
cm	Centimeter	L (length)
g	Gram	M (mass)

Table 2: Base units and their dimensions

Term	Dimension
$P^{(n-1)}$	$[T]^{(n-1)}$
$P_0^{(n-1)}$	$[T]^{(n-1)}$
Λ	$[T]^2$

Table 3: Dimensions of key parameters

When we are discussing and equation that represents a physical system, we want to be sure that the units within the relationship work out to make physical sense. Here, we have an equation dealing with seconds, so we need to ensure that the units on the left-hand side (LHS) of the equation equals the same units on the right-hand side (RHS) with the same dimensions.

If we rewrite (3) in terms of its dimensions, we get

$$[P]^{(n-1)} = [P_0]^{(n-1)} + \eta[\Lambda] \quad (4)$$

$$[T]^{(n-1)} = [T]^{(n-1)} + \eta[T]^2 \quad (5)$$

In (4) we've dropped the unitless term to illustrate the dimensional relationship between the LHS and the RHS. As you can see, two of the three key terms in this relationship are dependent upon the braking index, and one term has a fixed dimension (time squared). This "forced" dimension follows directly from Λ, where:

$$\Lambda = t_a k B^2$$

If we input the units for each term in Λ, we get

$$(s)\left(\frac{cm(s^3)}{g}\right)\left(\sqrt{\frac{g}{cm}}s^{-1}\right)^2 = s^2$$

As such, this then forces $n = 3$,

$$[T]^{(3-1)} = [T]^{(3-1)} + [T]^2$$

$$[T]^2 = [T]^2 + [T]^2$$

$$[seconds]^2 = [seconds]^2$$

If $n \neq 3$, then we wouldn't arrive at the same dimensions for our base units, and the physical interpretation of the numerical output wouldn't make sense. In this sense, the braking index is forced to be 3.

4.2.1: Variable Braking Index

We will briefly cover an area of active research about braking index measurements and how restricting $n = 3$ fails to capture information about a pulsar's long-term behavior. In Archibald's paper on pulsar braking indexes (Archibald, et al., 2016), the authors go over determining a pulsar's index. In a model that assumes pure dipole-braking, if you fix the magnetic properties of the pulsar and assume no effects from particle wind interaction, electrodynamics predicts our assumed value of 3. However, if you relax the constraints on the model, such as allowing for the angle between the magnetic poles and the spin to evolve over time (as ours does in equation (1)) the braking index can vary as well. As shown above in (3),

we see that the value for n is required to be 3 to satisfy our equation's dimensions, which presents a problem if our model is also assuming a varying beam-rotation angle. Active research (like the work done by Archibald et. al.) is currently being done to find n for known pulsars.

A method used to find the value for n follows from an equation we mentioned previous in Section 3.2:

$$\dot{\nu} = -K\nu^n \qquad (6)$$

Here, ν represents the spin frequency, and $\dot{\nu}$ the frequency derivative. With knowledge of the relationship shown in (6), we can perform some analysis to arrive at an equation that predicts the braking index for any pulsar:

$$n = \frac{\nu\ddot{\nu}}{\dot{\nu}^2} \qquad (7)$$

(Archibald, et al., 2016)

Since this equation contains quantities that can be measured directly, we theoretically have a means of determining the value for n by observing the spin frequency. However, as Archibald et. al. discusses, this is only possible for extremely young pulsars due to needing a large enough $\ddot{\nu}$ to detect on human timescales. As the paper mentions, out of the thousands of known pulsars, we've only been able to accurately measure the braking index for eight of them.

The n values for these pulsars range from 0.9 to 2.84 (see Figure 2, page 2 in Archibald et. al.'s paper). Given the small sample size, we cannot definitively say whether or not this is representative of all known pulsars, however from a mathematical perspective we must accept that clearly $n = 3$ is not the only value to consider. Leaving our governing equation only able to accept a braking index of 3 is not sufficient if we wish to test out other values for n. For this proof of concept, we need to ensure our model is pliable and able to use n values other than just 3 without altering the assumptions of a dipole-dominant braking mechanic which is typically what we expect for long term pulsar behavior. However, if we adjust n without taking the dimensions into consideration, the outputs won't hold physical meaning.

Furthermore, we have accepted that for dipole-braking dominant pulsars, $n\epsilon(1,3]$ with 3 being the "upper limit" for a braking index. The eight pulsars with an actual measured braking index almost all fall within that range (one being measured around 0.9), and the pure dipole-braking assumption would lead us to believe that 3 was this upper limit. However, mathematically n can take on any value above 1. 3 is merely an upper-bound based upon the assumed physics of the situation. But in this paper by Archibald et. al, they have calculated a braking index of $n \approx 3.15$ for PSR J1640-4631. We bring this up here to further illustrate why our model needs to be able to account for n values other than just 3, especially if we are wanting our invention to be able to fit curves at-will while accounting for new measurements.

4.3: Generalizing the Dipole-Braking Model

For this proof of concept, we want to ensure that our model has the best chance at delivering accurate parameter estimates. For that we want to allow our values of n to be other than just 3 when running our curve fitting algorithm. To do this, we will use the dimensional analysis from above to make a slight change to the dipole-braking model we see in (2). Let's start with equation (3):

$$P^{(n-1)} = {P_0}^{(n-1)} + \eta\Lambda$$

Again, the units on the LHS work out to $s^{(n-1)}$, so each term on the RHS also need their respective units to work out to $s^{(n-1)}$. For P_0 this works out fine, but our second term, $\eta\Lambda$, still contains units of s^2 (with η being unitless). This squared term is what is forcing our braking index to be 3 in order to preserve an output from this model that makes physical sense. In wanting to perturb this equation as little as possible, we want to only allow the dimensions of our term with units (Λ) to change such that its units also work out to $s^{(n-1)}$.

To accomplish, the following is proposed:

$$(\Lambda)^{\frac{(n-1)}{2}} \quad (8)$$

This allows our second term to become *n*-dependent like the first on the RHS and the dimensions work out as follows:

$$[\Lambda]^{\frac{(n-1)}{2}} = ([T]^2)^{\frac{(n-1)}{2}}$$

$$= [T]^{2\left\{\frac{(n-1)}{2}\right\}}$$

$$= [T]^{(n-1)}$$

With this change, our proposed equation now becomes

$$P^{(n-1)} = {P_0}^{(n-1)} + \eta\Lambda^{\frac{(n-1)}{2}}$$

and the dimensions work out as follows

$$[T]^{(n-1)} = [T]^{(n-1)} + [T]^{(n-1)}$$

As you can see, our dimensions now work out so that if we choose $n > 1$, the output of our function will have matching dimensions with units that physically make sense. To ensure that our change doesn't introduce a contradiction in logic, we can check this new model with the familiar value of $n = 3$ and see if the resulting output collapses back to our known equation (3). First, set $n = 3$

$$P^{(3-1)} = {P_0}^{(3-1)} + \eta\Lambda^{\frac{(3-1)}{2}}$$

$$P^2 = {P_0}^2 + \eta\Lambda$$

When we look at the dimensions:

$$[P]^2 = [P_0]^2 + \eta[\Lambda]$$

$$[T]^2 = [T]^2 + [T]^2$$

whereas before in (4) we drop the unitless term to illustrate the equivalence of the dimensions. Here, we have shown that when we fix our braking index to 3, we recover the known equation (3) from our proposed model. As such, we have achieved a more generalized model for a pulsar that is

predominantly braking due to dipole radiation with a variable rotation-radiation angle. This generalized dipole-braking model can be written as follows:

$$P(t) = \left[P_0{}^{(n-1)} + \left(\frac{n-1}{2}\right)\Lambda^{\frac{(n-1)}{2}}\sin^2(\Phi(t))\right]^{\frac{1}{n-1}},\ \forall n > 1 \quad (9)$$

4.4: Discussing the Magnetic Field Strength

The other parameter we will discuss is the magnetic field strength (B). Pulsars are known to have incredibly strong magnetic fields. These magnetic fields range from 10^{11} Gauss (G) for the weaker radio pulsars up to a massive 10^{15} G for a special class of pulsars known as magnetars. The magnetic fields of neutron stars are an important property, so being able to identify them and understand how they behave is crucial when working with them, be it for attempting to understand their structure and evolution academically, or working to incorporate their properties for a piece of technology (as we are). The paper *Evolution of Neutron Star Magnetic Fields* (Igoshev, Popov, & Hollerbach, 2021) does a deep dive into the generation of the magnetic fields produced by neutron stars and their evolution over time. This paper has many examples of the way the magnetic field of a pulsar can evolve, and being that it is known that a pulsar slows due in large part to the dipole-radiation beams, the insights this paper provides may prove useful in future model tweaking.

In Chapter 3 of *Handbook of Pulsar Astronomy*, the magnetic field strength at the surface of a canonical pulsar can be estimated using the following equation

$$B_s = 3.2 \times 10^{19}\sqrt{P\dot{P}} \quad (10)$$

where again we are taking the assumptions for the moment of inertia and radius to be 10^{45} g(cm^2) and 10^6 cm respectively (still using cgs units). From this, you can measure the pulse period and calculate its derivative to give you a good idea of what the magnetic field strength at the moment of measurement is. This is used in countless texts as a means to verify if the pulsar is in fact a pulsar or a magnetar. What this means is that we should be able to use the magnetic field strength parameter in our models (equations (1) and (9)) to verify, at least initially, if our model is a good representation of the physical situation.

Our governing equation will eventually be used to generate time estimations for the invention, but before we can say anything about the accuracy of the time being estimated, we must first ensure our selected model can provide accurate measurements of known (or "easily" estimated) parameters. Our model is only taking in a pulse period per measurement time, so the input is simpler than the input for equation (10) in which you need to calculate $\dot{P}$ from the frequency measurement. For our model, you only need to run the various measures of the pulse period (directly measured) and the model should reveal the magnetic field strength of the pulsar based on those measurements. With this in mind, we can develop a sort of "test" for how well the model should work based on this parameter estimate. If our chosen model provides a decent estimation of the magnetic field strength, it can be taken as a signpost that we have a viable equation for making future time predictions that will be required for this technology to work.

5: Modeling the Data

This next section we'll focus on gathering the data needed to perform this proof of concept, and then performing the mathematical analysis required to obtain outputs from our curve fitting methods. The first major task of this phase of our development required was to identify a source of pulsar data that contained enough information to allow us to attempt fitting curves. For this, we turned to the Australia Telescope National Facility and its Data Access Portal. (Manchester, Hobbs, Tech, & Hobbs, 2005) (ATNF Pulsar Catalogue, 2021) Using this database, we were able to identify a pulsar to study for our proof of concept, collect the necessary data, parse and operate on it to get it into a useable format, and finally apply a curve fitting algorithm to it to produce results.

5.1: Pulsar Selection

For our proof of concept, we wanted to select a pulsar with a large $\dot{P}$ and that had enough data collected so that our model could be tested on its parameter estimation. The reason for selecting for the largest $\dot{P}$ was that we wanted a more pronounced pulse period change in the measurements so that our curve would be more pronounced. The ATNF Pulsar Catalogue has over 1500 pulsars' data within it, so we had plenty to choose from. We sorted the pulsars based on their most recent frequency and pulse period measurements, sorting for the pulsars with the largest $\dot{P}$ at the top. Once this was accomplished, we then began going through each pulsar at the top of this list to find pulsars that had enough projects to account for many years of measurements. We wanted enough information to be sure that our sample wasn't small, but not too large that download times would be unnecessarily long. With these constraints in mind, we settled upon the pulsar J1550-5418. This pulsar had over 200 measurements made over roughly 10 years of observations across multiple different projects[1]. The values for $P = 2.0968$ and $\dot{P} = 2.318 \times 10^{-11}$ that helped us select this pulsar were provided by data collected and analyzed by a group of researchers. (Camilo, Ransom, Halpern, & Reynolds, 2007).

5.1.1: FITS Data and Parsing

The data provided by the ATNF Pulsar Catalogue were in a FITS format, which is a specific type of file format commonly used for astronomical data collection. The first hurdle the team had to overcome within the data collection process was learning how to pull this data and extract the values we needed. What we needed from the FITS files was a frequency measure and the date-time group that the particular frequency measurement was taken. We would collect all of the frequency measurements over

[1] The projects that contributed to this data are P236, P456, P501, P574, and P602 and a list of all contributors can be found at https://data.csiro.au/domain/atnf/results?p=1&rpp=25&showFacets=true&so=ASC&observationMode=All%20including%20calibration%20files&sb=projectId&pulsarName=J1550-5418_R

the 7 years of data collected on J1550-5418, then put all of that information into a table that we could manipulate and perform mathematical operations on. The major challenge was trying to parse this data and put it into a useable format.

To do this, we began building a Python script (see Appendix B) that would take data downloaded from the catalogue, parse it for the necessary values, remove any unnecessary characters, and then build an Excel spreadsheet containing only what we needed. In the first iteration of our code base, we manually went to the ATNF Catalogue site and selected all of the files from the collected projects on J1550-5418 and stored that raw data in a pre-selected file location. Then, a Python script was written using the Astropy package to be able to manipulate and extract the values for the date-time group and the frequency measures. (Robitaille, et al., 2013) (Price-Whelan, et al., 2018)

Our script had to recognize the date-time group in the FITS file structure and then manually manipulate it into a date-time group format that was recognizable by Excel. This was done line by line for each character in the date-time group header for each file so that our Excel spreadsheet would have the appropriate coding to recognize the incoming data. The script also operated on the file structure (called an "hdul") where the frequency measures were stored. This operation was an iterative loop that systematically stripped off extra characters and spaces from the actual numerical values desired. Our script then exported these numbers to Excel, and instructed Excel to perform a calculation turning the frequency measures into pulse period measures ($P = \frac{1}{f}$). This process looked at each file that was pulled directly from ATNF that was collected for J1550-5418 and then saved it all to a final Excel sheet for our analysis.

This first version worked well enough to transform the raw data we manually downloaded from the ATNF Pulsar Catalogue into a useable format that we could then operate on. However, this script was refined by integrating an API provided by the ATNF. In the second version of our script for data collection, you are now queried by the script to input the J-name of the pulsar of interest. The script then utilizes the API to navigate to the ATNF database and retrieve a file list for that pulsar. It asks you how many files you want, and then it downloads them all to a specified file location. The rest of the script operates the same as above; parsing the data, extracting the desired information, and organizing it into an Excel sheet. With a working script that now is able to automate the data collection and organization, we were able to begin using it to fit a curve.

5.2: Results from Fitting the Data

With the data collected and organized, we began the process of generating a curve of best fit on the data. To do this, we employed RStudio and its nonlinear curve fitting function, nls(). The packages needed to perform this analysis in RStudio were *tidyverse* and *lubridate* (see Appendix C). For a first pass on this data, we wanted to see if actually obtaining any sort of curve with decent parameter estimation was possible considering all we were allowing ourselves to use was the data on the pulse period and the time that measurement was taken. The idea behind this was to go into the curve generation and parameter estimation with only one observed value and its time stamp to see how well our model would perform without any extra "help". This technology eventually aims to be able to take a

measurement of a pulsar and then using a decay curve, predict a time based on the pulse period seen in the observation.

5.2.1: Using RStudio to Organize and Fit the Data

Once the data was exported to an Excel sheet via our Python script, we were able to import the necessary information into RStudio. This was done by converting the data on the Excel sheet into a dataframe in RStudio. We then performed a few operations on the dataframe, such as putting the data into sequential order via the data, and then generated a new column that turned the date-time group column into a measure of seconds with our first measurement being taken as $t = 0$. This operation allowed us to iterate time forward using the "t.seconds" function within RStudio. Once this was accomplished, we did a simple plot of the dataframe to observe the structure of the data.

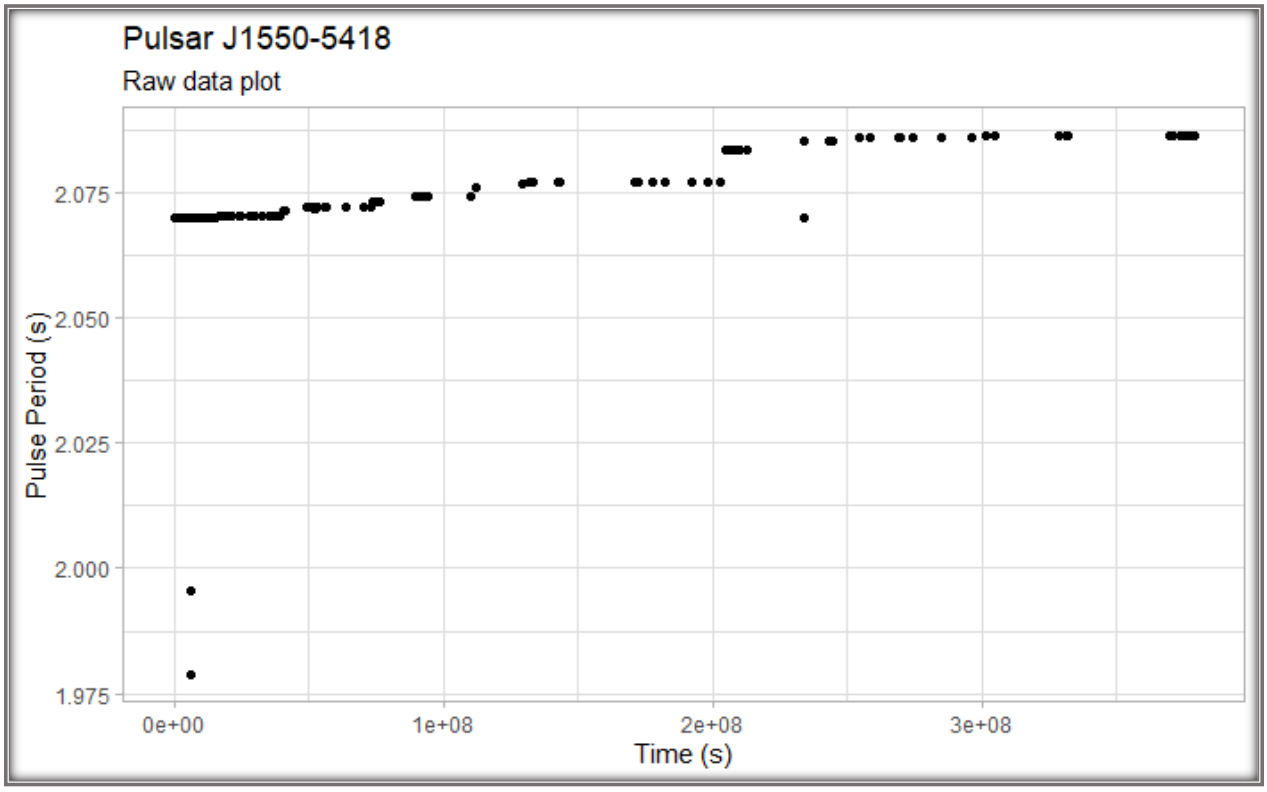

Figure 9: Plotting the raw data imported from the Python script

The immediate structure allows us to see that the pulsar is in fact slowing down over time, albeit with a few extreme values. Investigating the few outliers reveals that these could potentially be glitches that pulsars sometimes experience. A glitch event in a typical pulsar is usually seen as a brief "spin-up" in which we'd observe a sudden decrease in the pulse period, followed by an exponential recovery period that brings the pulsar back into a regular rotational period (Basu, Char, Nandi, Joshi, & Bandyopadhyay,

2018). This is thought to be due to the physical structure of the neutron star, in which angular momentum from a superfluid core is transferred to the crustal lattice (van Eysden & Melatos, 2010). The exponential recovery phase is believed to be brought about by physical processes that restore the superfluid-lattice corotation (van Eysden & Melatos, 2010).

When looking at the pulse period for J1550-5418, we can see some of the datapoints appear to imply that the pulsar may have glitched, although it is difficult to tell if there is an exponential recovery period afterwards. If we are to accept that these glitches and recovery periods are due to incredibly sensitive physical situations within the neutron star, then a glitch should be paired with some form of an exponential recovery. Closer inspection of these datapoints doesn't reveal one way or another if these values are due to a glitch. However, regardless of whether they are glitches or encoding errors, removing them to explore the data's structure and calculate our curve of best fit should not affect our end result, and we will test this assumption in a future section. Upon sub-setting the data within RStudio to remove the outliers, we wind up with the following plot:

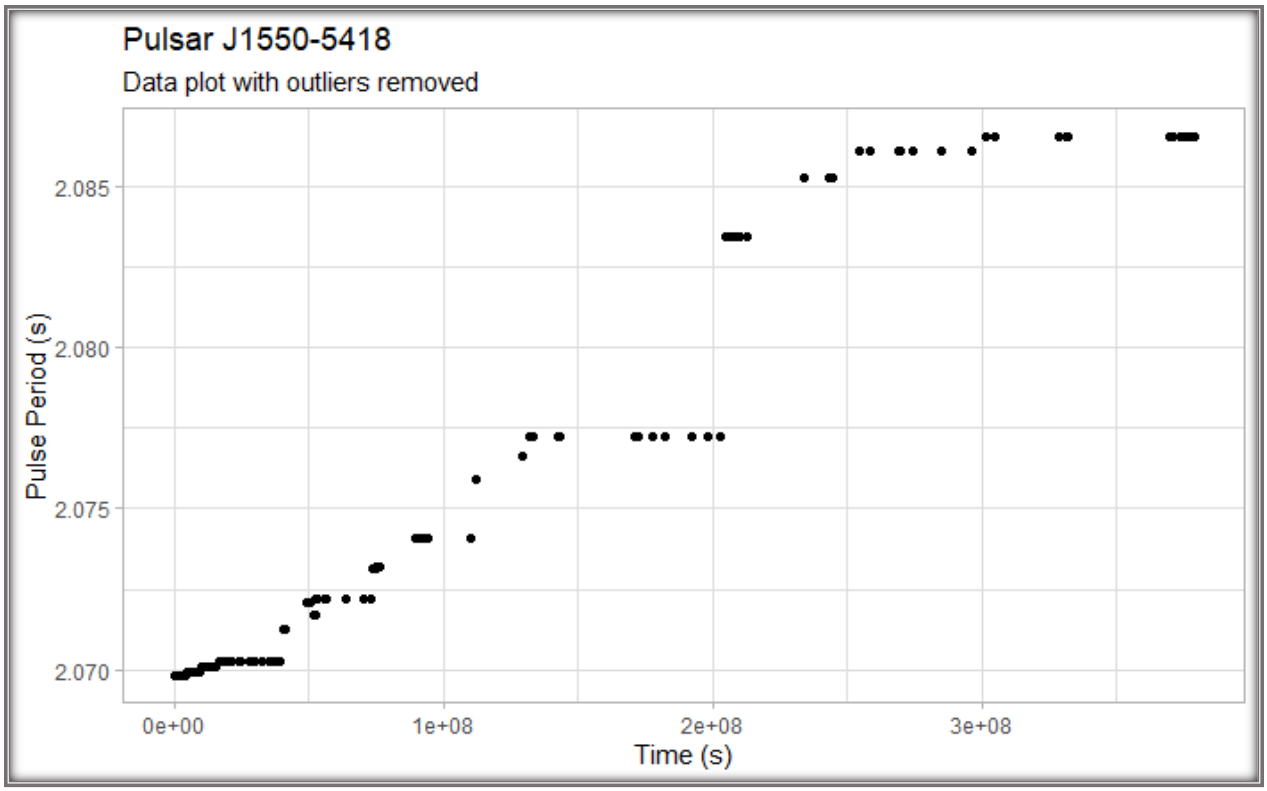

Figure 10: Plotting the subset data without outliers

With the outliers removed, we can see a better picture of the structure of the pulsar's slowing rotation. The odd structure of this data would suggest some peculiar behavior is going on with this star where the star appears to maintain a steady pulse period for quite a bit of time, only to then appear to slow down drastically and then level off again. This resembles what could be described as an "anti-glitch", in which the pulsar goes through a sudden period of slowing followed by a relatively stable period. Researchers are currently studying this strange behavior, but it is thought to be due to either "an impulse-like

angular-momentum transfer between regions of more slowly spinning superfluid and the crust" or "outflow along the open field lines of the magnetosphere, or a sudden twisting of the field lines..." (Archibald, et al., 2013) Either of these imply very peculiar and not-well understood behaviors, but may point towards more exotic structures within this pulsar that could help us further understand our model.

Despite the peculiar data structure, we proceeded with our analysis in the hopes that our governing model would be able to provide a decent parameter estimate for the magnetic field strength. With our subset dataframe and the necessary operations done to the data so that our nonlinear curve fitting algorithm could work with it, we set about generating our first proof-of-concept curve.

We employed our generalized model (9) with the breaking index $n = 3$ for this first curve, allowed both the magnetic field strength (B) and the characteristic time of alignment (t_d) to vary, and arrived at the following plot and statistics:

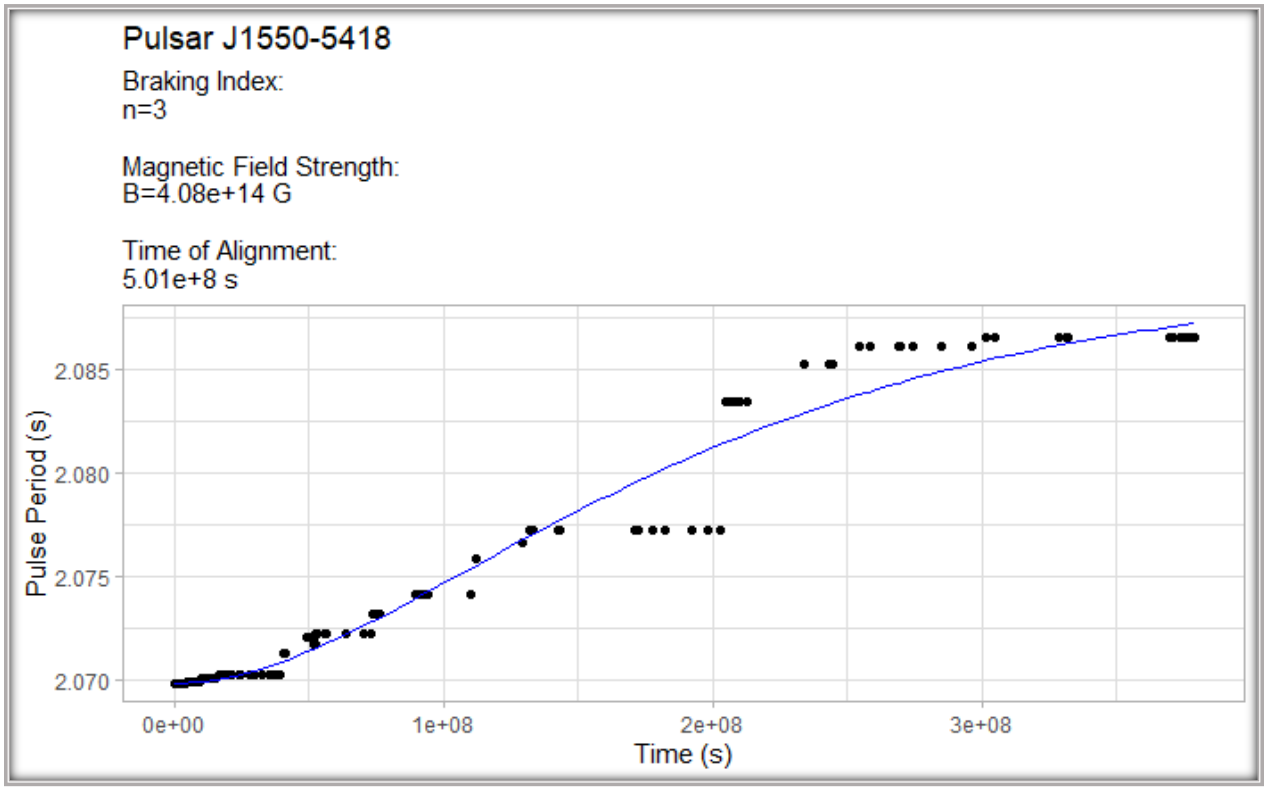

Figure 11: Fitted data with theoretical braking index

```
Formula: P ~ (P0^(n - 1) + ((n - 1)/2) * ((td * k * B^2)^((n - 1)/2)) *
    (sin(X0 * (1 - exp(-2 * t.seconds/td))))^2)^(1/(n - 1))

Parameters:
    Estimate Std. Error t value Pr(>|t|)
B  4.083e+14  2.558e+12  159.62   <2e-16 ***
td 5.007e+08  1.343e+07   37.28   <2e-16 ***
---
Signif. codes:  0 ‘***’ 0.001 ‘**’ 0.01 ‘*’ 0.05 ‘.’ 0.1 ‘ ’ 1

Residual standard error: 0.001023 on 223 degrees of freedom

Number of iterations to convergence: 6
Achieved convergence tolerance: 1.786e-06
```

Figure 12: Statistics from the governing model with theoretical braking index

Our first pass attempt assuming the theoretical braking index of 3 and the canonical values for the pulsar's radius and moment of inertia provided an estimate for the magnetic field strength $B = 4.1 \times 10^{14} G$ and a time of alignment (t_d) of approximately $5 \times 10^8 s$. This is a rather large estimate for a pulsar's magnetic field strength, which would (if correct) mean this star is a rare object known as a magnetar. In fact, of the 2,000+ known pulsars, we've only identified around 30 of them to be magnetars. What that means is that if this magnetic field strength is accurate, it would identify this pulsar as a magnetar and be a strong sign that our model is performing well.

The estimated alignment time appears to be slightly longer than the time period of the dataset (we have measurements for about $3.8 \times 10^8\ s$), which could imply that the rotation axis and the radiation beam axis have yet to align, although they are close. We have a small snapshot of this pulsar's life, and our model is only "aware" of the data we can provide it. As such, we can extrapolate from this that a pulsar will have an alignment near the "end" of its lifetime, which for our model is the end of this dataset. In a sense, our model may me telling us something intrinsic about alignment behavior.

Exploring this further, we can try to analyze this outcome and justify if our model is representing the long-term behavior of this pulsar accurately (i.e.: what we would see if we had data on the entirety of the pulsar's lifespan). Typically, alignment is thought to be roughly on the order of $10^{14}\ s$. However, there are a lot of assumptions with that value, such as assuming typical pulsar parameters. The typical pulsar has magnetic field strengths on the order of $10^{11}\ G$. We are three orders of magnitude larger than that with J1550-5418, which could imply that if we are dealing with a magnetar, their radiation axis may align faster than that of a smaller pulsar's magnetic field or even that magnetars may go radio-silent faster. There could be an intrinsic connection between how fast alignment occurs and the strength of the magnetic field over the lifetime of the pulsar. This may be further linked to how long a pulsar is thought to "live" before going radio silent.

However, let us just take for granted the canonical estimate for alignment and see if our model is representative of that. If we take radio silence to be the "death" of a pulsar, this occurs anywhere from 10 to 100 million years ($10^{14}s - 10^{15}s$). If we accept the value for alignment of the radiation axis and rotation axis to occur on the order of $10^{15}\ s$, this would imply that alignment takes nearly the entire

active period of a pulsar's life. Our model's estimate is suggesting this same phenomenon with alignment appearing to occur close to the end of the dataset, which our model is "seeing" as the end of the lifetime of the star. We will further explore this parameter in a later section when discussing orders of magnitude.

Getting back to our curve fit, it appears to align well with the data. Checking our statistics pulled from the governing model, we see we have statistically significant parameter estimates, with their t-values being "large" (implying significance). However, as mentioned above with our dimensional analysis, the braking index is not theoretically locked to 3. 3 assumes that the only form of braking comes from radiation and that no other variables are present. Our model assumes that the rotation-radiation angle is variable, which could imply that $n = 3$ is not the true braking index and it could be less. If this is the case and n is lower, then our parameter estimates will change and our curve may look slightly different. We can use this to our advantage to formulate a test for the braking index and the model's ability to estimate accurate parameters. In fact, if we can formulate a way to estimate the braking index for this particular pulsar assuming it is not equal to 3, we can use this to check how well our model does absent of knowledge about these parameters a priori. In particular, we can check our estimated magnetic field strength via purely manipulating the model graphically against a calculated and researched value to determine how well this model does.

Once we do this, we can then develop a method for estimating the braking index given our now-known parameter estimates (both from our curve and from independent sources). This is being done in this way to ensure we don't bias our adjustments to the model, and therefore ensuring our results reflect its validity. First, we begin with varying the braking index to account for our model's assumptions of a variable rotation-radiation angle.

We proceed with this by using our t-value for the magnetic field as a means of estimating a braking index. If we shrink the index by a set amount and observe this t-value, we can gain some insight into whether or not a smaller braking index better fits this particular pulsar. If we can find a maximized t-value for the magnetic field, we can make a prediction about the magnetic field and then compare that to independent calculations of the field. Once we have that complete, we can then set out to try and validate the estimated braking index using this method with an analytical one.

Figure 12 presents the statistics for a braking index $n = 3$, and a t-value for B being 159.62. Given our assumptions of a variable rotation-radiation angle, let's drop the braking index by 0.2 and see what happens to our magnetic field.

Statistics for $n = 2.8$:

```
Parameters:
    Estimate Std. Error t value Pr(>|t|)
B  3.275e+14  1.970e+12   166.2   <2e-16
td 5.004e+08  1.341e+07    37.3   <2e-16
---
```

Figure 13: n=2.8

We can see that our t-value went up, implying a more significant value for B. We then drop n again and observe what happens.

Statistics for $n = 2.6$:

```
Parameters:
    Estimate Std. Error t value Pr(>|t|)
B  2.486e+14  1.489e+12  166.99   <2e-16
td 5.001e+08  1.340e+07   37.33   <2e-16
---
```

Figure 14: n=2.6

Our t-value is still increasing, so we continue to drop it.

Statistics for n=2.4:

```
Parameters:
    Estimate Std. Error t value Pr(>|t|)
B  1.744e+14  1.119e+12  155.96   <2e-16
td 4.999e+08  1.339e+07   37.35   <2e-16
---
```

Figure 15: n=2.4

As we can see, once our braking index drops below 2.6, our t-value for the magnetic field begins to decrease, which implies that there must be an optimum value for the braking index. It would also appear that our t-value for t_d is still slightly increasing, but seems to be fixed around $5 \times 10^8\ s$, whereas the magnetic field is changing by larger quantities. Table 4 summarizes each iteration so we can make a prediction about what we think the braking index should be:

Braking Index	Magnetic Field Estimate (G)	t-value
3.0	4.08×10^{14}	159.62
2.9	3.68×10^{14}	163.3
2.8	3.28×10^{14}	166.2
2.7	2.88×10^{14}	167.71
2.6	2.49×10^{14}	166.99
2.5	2.11×10^{14}	163.26
2.4	1.74×10^{14}	155.96

Table 4: Various braking indexes and their associated magnetic field strengths

Given the data above, we can clearly see that we get slightly more significance for the magnetic field parameter as we drop away from 3, but stay above 2.6. This is a good indicator that assuming $n = 3$ and using it for parameter estimates is not a good idea. For the sake of making a prediction, we choose $n = 2.65$ and fit that curve.

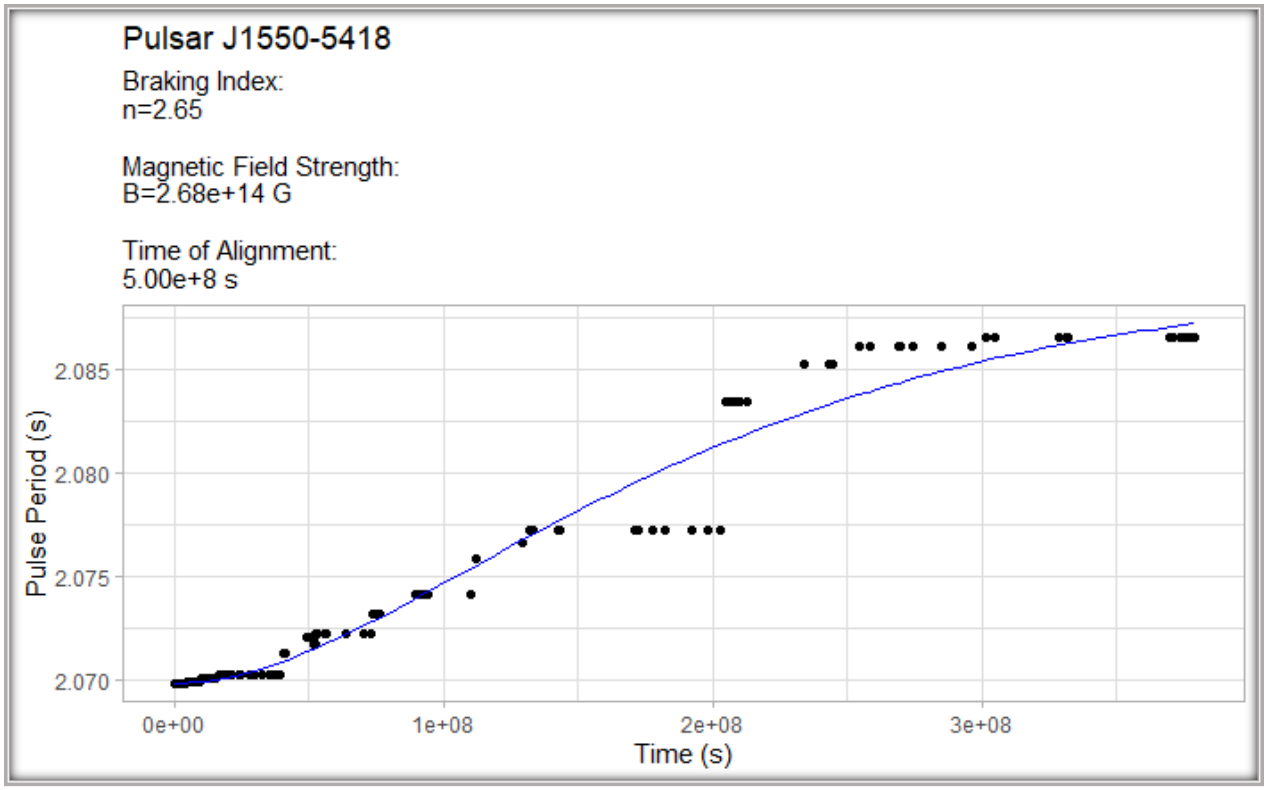

Figure 16: Our estimated curve for predictions

```
Formula: P ~ (P0^(n - 1) + ((n - 1)/2) * ((td * k * B^2)^((n - 1)/2)) *
    (sin(X0 * (1 - exp(-2 * t.seconds/td))))^2)^(1/(n - 1))

Parameters:
    Estimate Std. Error t value Pr(>|t|)
B  2.681e+14  1.599e+12  167.68   <2e-16 ***
td 5.002e+08  1.340e+07   37.32   <2e-16 ***
---
Signif. codes:  0 ‘***’ 0.001 ‘**’ 0.01 ‘*’ 0.05 ‘.’ 0.1 ‘ ’ 1

Residual standard error: 0.001023 on 223 degrees of freedom

Number of iterations to convergence: 6
Achieved convergence tolerance: 3.478e-06
```

Figure 17: Statistics from our model with predicted braking index

This method for determining a better fit for our braking index has yielded a smaller magnetic field, but still within the same order of magnitude as the original estimate. Whereas this has been a more “manual” way of adjusting our parameters, it allows us to now make a prediction and then check that against an independent calculation. From there, we can proceed with a more formal and analytic way of estimating the braking index. All of this will be put together to formulate a final estimation of the

parameter values and then fit against the unaltered data, which will more closely resemble data seen by this invention.

Our estimates are as follows:

$$B \approx 2.68 \times 10^{14}\ G$$

$$n \approx 2.65$$

5.2.2: Model/Parameter Comparisons

Now that we have a magnetic field strength estimate for our selected pulsar, we wanted to check it against external estimations using measurements prior to proceeding with our analytical solve for the braking index. We discussed above in Section 4 how we can estimate the magnetic field strength of a given pulsar with the following equation:

$$B_s = 3.2 \times 10^{19}\sqrt{P\dot{P}} \quad (10)$$

As previously mentioned, to avoid any bias in our selection for braking index values or the model in general, we avoided any research into our chosen pulsar before running our model and exploring various parameter values. A good check on our model would be to see if it could accurately predict (within the same order of magnitude) the magnetic field strength of the pulsar. If our model's estimate aligns with researched and calculated values, it can be taken as a good sign that our work is headed in the right direction.

When researching this pulsar, we found that the magnetic field strength for J1550-5418 was estimated as:

$$B = 2.2 \times 10^{14}\ G$$

(Lin, et al., 2012)

We can also calculate an estimate for the magnetic field strength using (10) with the values for P and $\dot{P}$ mentioned earlier (Camilo, Ransom, Halpern, & Reynolds, 2007):

$$P = 2.0968$$

$$\dot{P} = 2.318 \times 10^{-11}$$

$$B_s = 2.231 \times 10^{14}\ G$$

Not only does our model estimate the magnetic field strength parameter close to independently determined values, but it also correctly identifies J1550-5418 as a magnetar known as a Soft Gamma Repeater. We mentioned earlier that magnetars are rare objects, so the fact that our model was able to identify this object as a magnetar even with various values for the braking index ($n \in (1,3)$) is a good sign that we are on the right path.

These parameter estimates, however, are due to the braking index being selected at $n = 2.65$. As we said above, this analysis was meant to verify our model selection, but not meant to be how we proceed

with an analytical path towards estimating the braking index. If n changes, so too do these parameters. Since we can independently check the estimated magnetic field strength using either equation (10) or the field strength calculated by Lin, et. al., we can now proceed with our attempt to find a way to calculate the braking index without this method and perhaps make our model stronger. This will be done to further verify what we are seeing in our model, and a successful outcome would be a braking index close to the estimated values.

In future work with this invention, we would move quickly to estimate any and all parameters possible, and then proceed to estimate the best braking index using the following analysis. Since we know our model is producing a parameter estimate near to the now-calculated magnetic field based on the current pulse period and its derivative, we can adjust our braking index so as to have our model produce the independently estimated parameter B.

When we do this, we arrive at the following curve fit and statistics:

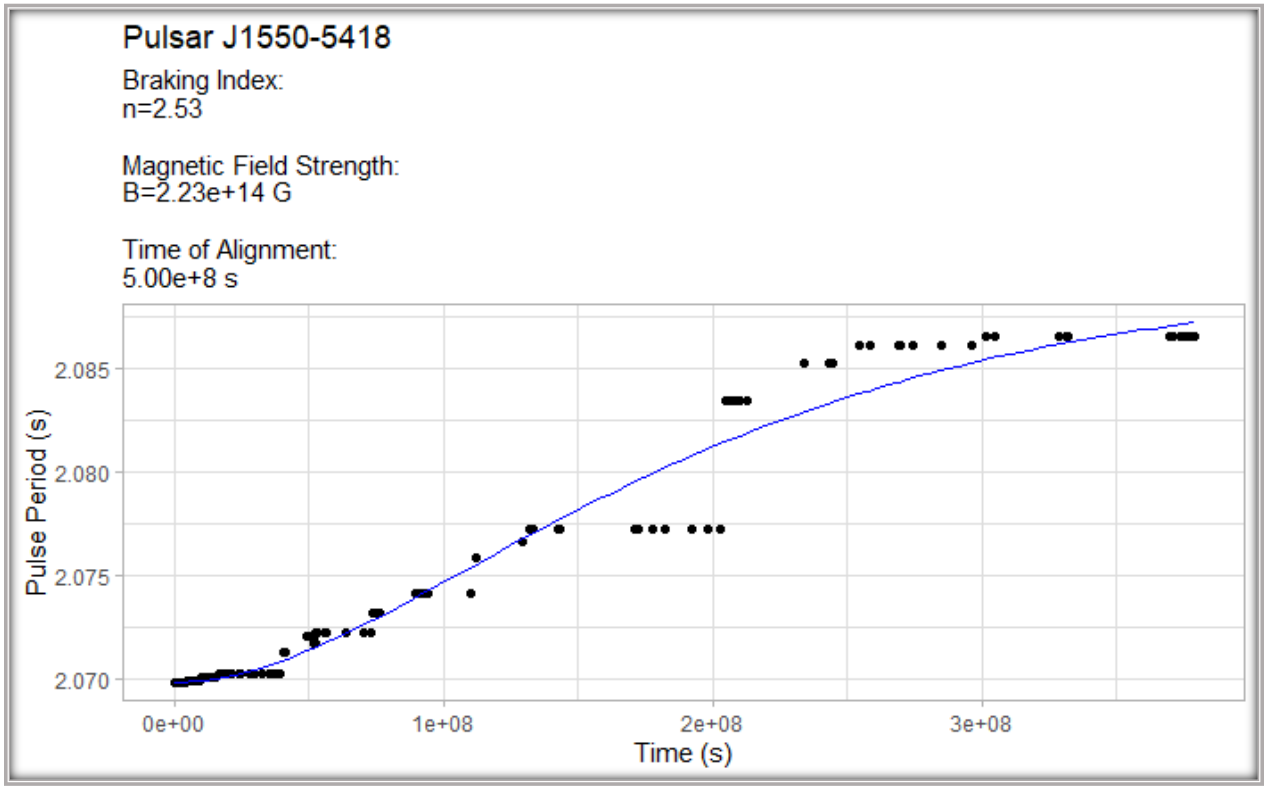

Figure 18: Fitted data with estimated magnetic field strength

```
Formula: P ~ (P0^(n - 1) + ((n - 1)/2) * ((td * k * B^2)^((n - 1)/2)) *
    (sin(X0 * (1 - exp(-2 * t.seconds/td))))^2)^(1/(n - 1))

Parameters:
    Estimate Std. Error t value Pr(>|t|)
B  2.232e+14  1.354e+12  164.88   <2e-16 ***
td 5.001e+08  1.339e+07   37.33   <2e-16 ***
---
Signif. codes:  0 ‘***’ 0.001 ‘**’ 0.01 ‘*’ 0.05 ‘.’ 0.1 ‘ ’ 1

Residual standard error: 0.001023 on 223 degrees of freedom

Number of iterations to convergence: 6
Achieved convergence tolerance: 1.283e-06
```

Figure 19: Statistics for our fitted data with known magnetic field strength

The braking index given our estimated magnetic field strength is still close to what we initially predicted using our t-value iterative process. The magnetic field strength that equation (10) estimates it to be means the braking index for the magnetar J1550-5418 is estimated to be roughly

$$n \approx 2.53$$

The analysis thus far has been done in an attempt to verify our model selection and as a means of exploring the behavior of an unknown pulsar. The values we have been obtaining are crucial in attempting to put together the best model we can for J1550-5418, but future pulsars should have a more standardized approach to parameter estimation.

5.2.3: Estimating the Braking Index Using a Least Squares Minimization Technique

As mentioned in 4.2.1, calculating the braking index for a pulsar is incredibly difficult and has only been possible for 8 pulsars. This further motivates us to develop a method to estimate the braking index without needing the information in equation (7) and only using the collected data on the pulsar's pulse period. This is not an easy task, but if we want to make our model more robust and accurate, we must venture into this analysis. To do this, we will utilize a least squares minimization for the braking index to see if we can estimate a good value for n. This estimated value should follow the same "rules" as what the model requires, such as $1 < n \leq 3$. However, as mentioned in 4.2.1, a braking index greater than 3 has been calculated, which means that n could be greater than 3. Either way, our estimation will ultimately be tested by comparing parameter estimates with independent calculations from other sources to verify its accuracy and arrive at a good model for our data.

We'll start with our generalized equation for the pulse period, simplify, and then work through the algebra.

$$P(t) = \left[{P_0}^{(n-1)} + \left(\frac{n-1}{2}\right) \Lambda^{\frac{(n-1)}{2}} \sin^2\left(\phi_0 (1 - e^{\frac{-2t}{t_d}})\right)\right]^{\frac{1}{n-1}}$$

We set

$$n - 1 = m$$

$$P(t) = \left[{P_0}^{m} + \left(\frac{m}{2}\right) \Lambda^{\frac{m}{2}} \sin^2\left(\phi_0 (1 - e^{\frac{-2t}{t_d}})\right)\right]^{\frac{1}{m}}$$

Simplify with the following:

$$\phi_0 \left(1 - e^{\frac{-2t}{t_d}}\right) = \Phi_{(t)}$$

and raise each side to the m^{th} power to arrive at:

$${P_{(t)}}^{m} = {P_0}^{m} + \frac{m}{2} \Lambda^{\frac{m}{2}} \sin^2\left(\Phi_{(t)}\right) \quad (11)$$

Since P_0 and Λ are constants with respect to our data, we can further simplify:

$$\frac{{P_{(t)}}^{m}}{{P_0}^{m}} = 1 + \frac{m}{2} \frac{\Lambda^{\frac{m}{2}}}{{P_0}^{m}} \sin^2\left(\Phi_{(t)}\right)$$

$$\left(\frac{P_{(t)}}{P_0}\right)^{m} = 1 + \frac{m}{2} \frac{\left(\sqrt{\Lambda}\right)^{m}}{{P_0}^{m}} \sin^2\left(\Phi_{(t)}\right)$$

$$\left(\frac{P_{(t)}}{P_0}\right)^{m} = 1 + \frac{m}{2} \left(\frac{\sqrt{\Lambda}}{P_0}\right)^{m} \sin^2\left(\Phi_{(t)}\right)$$

We now can set

$$\frac{P_{(t)}}{P_0} = P_T, \quad \frac{\sqrt{\Lambda}}{P_0} = \beta$$

and we get the simplified equation

$${P_T}^{m} = 1 + \frac{m}{2} \beta^{m} \sin^2\left(\Phi_{(t)}\right) \quad (12)$$

Now, we take the natural log of each side to get

$$m \ln(P_T) = \ln\left[1 + \frac{m}{2} \beta^{m} \sin^2\left(\Phi_{(t)}\right)\right] \quad (13)$$

Looking at the right-hand side (RHS) of equation (13), we must perform a bit of analysis.

Let's first set

$$\frac{m}{2}\beta^m \sin^2\left(\Phi_{(t)}\right) = \mu \quad (14)$$

Now, we rewrite the RHS of (13) as

$$\ln(1+\mu) \ (15)$$

This simplification is important because if we can determine the behavior of μ, we may be able to take advantage of the approximation

$$\ln(1+x) \approx x \quad 0 < x \ll 1 \quad (16)$$

This approximation can be shown using a Maclaurin series expansion:

$$f(x) = \ln(1+x)$$

$$P(x) \approx f(0) + xf'(0) + \frac{x^2 f''(0)}{2!} + \frac{x^3 f'''(0)}{3!} + O(x^4)$$

$$P(x) \approx x - \frac{1}{2}x^2 + \frac{1}{3}x^3 \mp O(x^4)$$

Our approximate polynomial implies that as our exponent increases, we'll be adding and subtracting smaller and smaller terms. Given $x \ll 1$, we can ignore the 2nd-order terms and beyond to arrive at

$$P(x) \approx x \quad 0 < x \ll 1$$

$$\ln(1+x) \approx x \quad 0 < x \ll 1 \quad \therefore$$

Given the above analysis, let's look at each term in μ to see if we can use this approximation. Since we have some variability in this term, we will want to set some constraints and evaluate the terms at their approximate maximums so we can see just how large μ could theoretically get for J1550-5418.

For $\sin^2\left(\Phi_{(t)}\right)$, we must consider what our model is saying. For the variable rotation-radiation angle, we are assuming that over the lifetime of our star, the rotation axis and the radiation beam will align. Recall that

$$\Phi_{(t)} = \phi_0\left(1 - e^{\frac{-2t}{t_d}}\right)$$

The exponential term in this function is meant to be scaled by the rotation-radiation alignment over a specific amount of time, t_d. Physically speaking, the pulsar's beams align with the rotation axis when $t = t_d$. Even if t_d is some incredibly large number, the idea behind this physical model is that at some finite point in the future, the variable rotation-radiation angle will align and at that point this function will evaluate to a specific number. Knowing this, we will first calculate limit as $t \to t_d$ to see what this term evaluates to at this alignment regardless of what those values are:

$$\lim_{t \to t_d}\left[\phi_0\left(1 - e^{\frac{-2t}{t_d}}\right)\right] = \phi_0(1 - e^{-2})$$

Evaluating our sine function in this limit give us

$$\sin^2[\phi_0(1 - e^{-2})] \approx 0.955484657$$

In reality, the pulsar's radiation beams will align with the rotation axis at some finite time in the future, but after this, the age of the pulsar will continue to increase. In effect, our t value will become equal with t_d, the two axes will align, and then t will grow larger than t_d. What will happen is that for a brief moment the pulsar will hit our calculated value of 0.95548... and then continue to increase for an incredibly long time. So, for a more generalized maximum we must evaluate the limit as $t \to \infty$:

$$\lim_{t\to\infty} \Phi_{(t)}$$

$$\lim_{t\to\infty}\left[\phi_0\left(1-e^{\frac{-2t}{t_d}}\right)\right] = \phi_0\left(1-e^{\frac{-2\infty}{t_d}}\right)$$

$$= \phi_0(1-0)$$

$$= \phi_0$$

Given $\phi_0 = \frac{\pi}{2}$, then

$$\sin^2(\phi_0) = 1$$

What this shows is that once the radiation beam axis and rotation axis align, the value for this function will slowly climb from 0.95548... to 1 over many years. This is assuming the radiation beam starts off orthogonally to the rotation axis, which is an assumption we've made for our model but is not guaranteed to happen. In order to ensure we are allowing for the largest this term can be, we will set it equal to 1 and proceed with the other terms in our calculation.

For β^m (and $\frac{m}{2}$ for that matter), this is a bit more nuanced as we need to consider both the case for the pulsar we are using (J1550-5418) and for any pulsar in general. We can do some calculations to determine if we are allowed to use the approximation in (16) for our pulsar, but for any pulsar in general, we will need a deeper analysis. Let us start with our pulsar to determine if the approximation is valid. As discussed in previous sections, the braking index for a pulsar is theoretically maximized at $n = 3$. We simplified our model with $n - 1 = m$, so therefore if we accept that 3 is our maximum value for the braking index, then

$$m = 2$$

is our maximized value for m. Given that we have now have measured a braking index potentially above 3 (Archibald, et al., 2016), this may be a point of contention, however this analysis may actually render this development inconsequential.

For now, we will take the upper bound for m to be 2 and turn our attention to β. For any given pulsar, this value should be relatively constant on the timescale of our data. Recall,

$$\frac{\sqrt{\Lambda}}{P_0} = \beta$$

and that

$$\Lambda = \mathrm{k}\, t_d B^2$$

where $k = 9.768 \times 10^{-40}$ and is defined by physical constants and assumed canonical values for the pulsar, t_d is some finite time value, and B^2 is the square of the magnetic field strength. Our current model assumes these values to be constant all with respect to the timescale that we are interested in, so therefore we can consider Λ as a constant of some particular magnitude. We need to pry Λ open a little and try and justify what values we will use to calculate its magnitude.

While considering t_d, we need to fix it as some value with respect to the timescale of our data. When we set $n = 2.53$ (which is what value it needed to be in order to get the calculated magnetic field strength), we arrived at $t_d = 5 \times 10^8$ which is slightly longer than our data exists for, but within the same order of magnitude. As we discussed in 4.1, we should be able to safely use this value given how our modeling process works. If we are to assume alignment occurs at some point late in a canonical pulsar's lifecycle, then our model is accurately predicting this behavior given its estimate for t_d.

To further verify if this is valid, we can take a look at the canonical value for t_d ($\approx 10^{14}\ s$). Recall, this is being estimated for a typical pulsar. Typical pulsars are not magnetars in the sense that their magnetic fields hover around $10^{11}\ G$. There may be some intrinsic link worthy of exploring between the behavior of how long a pulsar typically "lives" and the strength of its magnetic field. This has been looked into by some researchers and is very much an area of active research. (Igoshev, Popov, & Hollerbach, 2021) This will be brought up later when discussing general assumptions. For now, we will assume $t_d \approx 5 \times 10^8\ s$ so as to allow our values to match what our data is describing. In essence, we need a scaled value for the estimated alignment time given our measured initial pulse period and length of data.

Regarding P_0, this is the initial pulse period (either measured or estimated) and can be treated as a constant. As just discussed, we do not have the data that stretches back to when this pulsar was formed, and estimations for this value are loaded with assumptions about the early behavior of the pulsar. As far as our model is concerned, this is the first value in our data that it will be slowing from, so we must use our first measured pulse period and proceed from there. This will be an active area of research going forward that will require expert input and data on other pulsars with well documented ages and pulse periods.

The magnetic field B is yet another complication in this effort. Unlike the other two values, we do have a way to estimate the magnetic field given recent measurements. We need to employ this external estimation for the magnetic field to seed our calculation for β to help us develop an analytical solution to estimate the braking index. For this we return to equation (10)

$$B_s = 3.2 \times 10^{19}\sqrt{P\dot{P}}$$

Using the values $P = 2.0968$ and $\dot{P} = 2.318 \times 10^{-11}$ that were calculated by Camilo et. al. for J1550-5418, we can estimate the magnetic field as

$$B_{est.} = 2.231 \times 10^{14}\ G$$

It is acknowledged that these parameter assumptions are done for the sake of attempting a general estimate, but our model is attempting to extrapolate the general behavior of the pulsar from a sample. This means we need to use the values calculated with our data and then verify if they make physical sense once our analysis is complete. With our selected values for k, t_d, B, and P_0, we can treat β as a constant. Therefore, we need only find the value of β to observe its magnitude.

For our pulsar and the given data set we are modeling it with, the values for each term above are

$$\Lambda = 0.024327784, \qquad P_0 = 2.069833010$$

This means that

$$\beta = 0.075355676$$

and if we are taking $n = 3$ to be a maximum value for the braking index,

$$\beta^m = \beta^2 = 0.005678478$$

As it was mentioned earlier, we have recently measured a braking index above 3, meaning that we cannot rule out an arbitrarily large index for any pulsar, including ours. If we allow m to grow arbitrarily large, our value for β will get arbitrarily small. So even in the limit of large values for the braking index, the magnitude of β will remain very small, or $\beta^m \ll 1$.

Consequentially, if we fix our braking index n to be 3,

$$\frac{m}{2} = 1$$

If we were content to allow the braking index to remain at 3, then $\frac{m}{2}\beta^m \sin^2\left(\Phi_{(t)}\right) = \mu$ would result in

$$\mu = (1)(0.005678478)(1) = 0.005678478$$

But is this the maximized value for any braking index? What about allowing n (and as such m) to grow arbitrarily large for this relation? Surely as the braking index gets large, the ratio $\frac{m}{2}$ will also grow large. The question then becomes how does this ratio and β^m behave together as m grows arbitrarily large?

We know that β is a specific number determined by the constants of the pulsar we are measuring, and with our pulsar's data, the result is $\beta \ll 1$. Starting with the extreme case, we can look at the behavior of these two terms in the limit of m getting arbitrarily large.

$$\lim_{m\to\infty}\left[\frac{m\beta^m}{2}\right] = 0, \quad \forall\, \beta < 1$$

So, for J1550-5418 we are covered in that if the braking index were to be very large, this term would shrink to 0. However, what we must also consider is the magnitude of $\mu = \frac{m}{2}\beta^m \sin^2\left(\Phi_{(t)}\right)$ if any value of the braking index will cause μ to get too close to some critical value before m gets arbitrarily large, or even when $1 < m \leq 3$ thus rendering our approximation invalid. The idea behind this analysis is to justify the approximation in equation (16) for our pulsar, so we must first identify this critical value where our approximation becomes invalid, if anywhere.

Let's again consider our relation from (14)

$$\frac{m}{2}\beta^m \sin^2\left(\Phi_{(t)}\right) = \mu$$

and the approximation in (16)

$$\ln(1 + x) \approx x$$

(16) is only true when x is smaller than 1. But how much smaller? To find out, we can plot $\ln(1+x)$ and x and look at where they begin to significantly diverge with respect to the magnitude of μ.

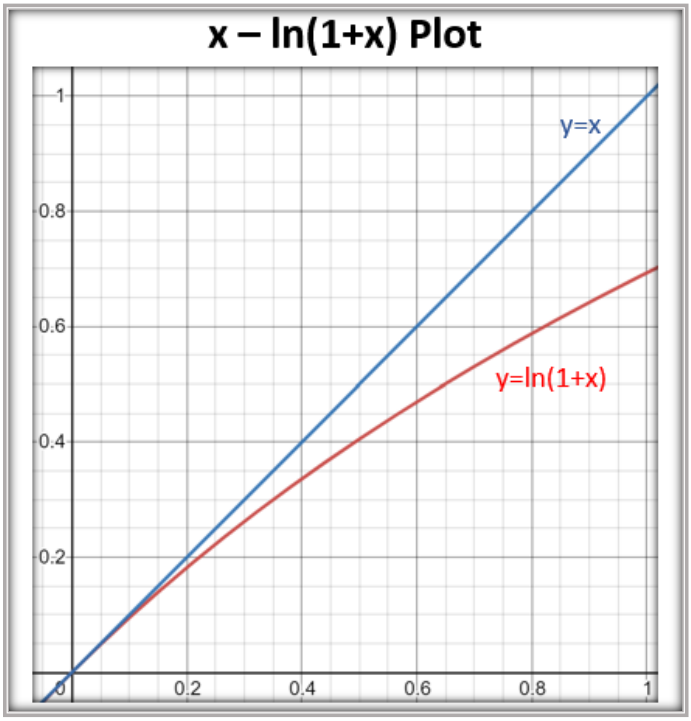

Figure 20: Plotting x and ln(1+x)

We can see that a significant divergence between the two plots begins around $x = 0.3$, which we can set as our critical value, $f_{critical}$. If our μ term in (14) exceeds this critical value at any point as m approaches infinity, it will invalidate our approximation. To see how μ behaves as m grows, we can calculate the various parameters in μ and use that to describe a function $\mu = f(m) = \frac{m}{2}\beta^m \sin^2(\Phi_{(t)})$. We can then find the value for m that maximizes this function and check to ensure this value does not cause μ to exceed 0.3.

Generalizing μ as the function $f(m)$ (while knowing our sine term will be a constant between 0 and 1),

$$f(m) = amb^m$$

calculating its derivative,

$$f'(m) = ab^m(1 + m\ln(b))$$

and setting this derivative equal to 0, we get the maximum occurs at either

$$ab^m = 0 \quad (17)$$

or

$$1 + m\ln(b) = 0 \quad (18)$$

We know that $\beta = 0.075355676$ and the maximum of our sine term is equal to 1. Plugging our known values into the generalized terms, we get the following:

$$a = \frac{1}{2} = 0.5 \quad b = \beta = 0.075355676$$

$$f'(m) = (0.5)m(0.075355676)^m(1 + m\ln(0.075355676))$$

Since (17) can only equal zero when either $m \to -\infty$ or $a = 0$, and we know $m > 0$ and $a \neq 0$ for our model, we must use (18) to determine our maximum. Performing the necessary algebra, we find that

$$m = -\frac{1}{\ln(b)}$$

$$= -\frac{1}{\ln(0.075355676)}$$

$$m \approx 0.386766995$$

This value for m should maximize our function. When we plug this m back into our function, we get

$$f(m) = \mu \approx 0.071141813$$

Looking at our plot in Figure 20 and the critical value for which we see the outputs of x and $\ln(1 + x)$ diverge ($f_{critical} \approx 0.3$), we observe

$$\mu < f_{critical}$$

which means that as $m \to \infty$, the largest μ will get is smaller than our critical value we've defined for when our approximation in (16) is no longer valid. So, even if our braking index is allowed to grow to arbitrarily large values, the behavior of μ will never exceed our critical value and will eventually vanish altogether in the limit.

Putting all of this together, we can safely say that for magnetar J1550-5418

$$\mu = \frac{m}{2}\beta^m \sin^2\left(\Phi_{(t)}\right) \ll 1 \ \ \forall m > 0$$

As such we can employ the approximation in (16) and say that

$$\ln(1 + \mu) \approx \mu$$

which leads us back to equation (13):

$$m\ln(P_T) = \ln\left[1 + \frac{m}{2}\beta^m \sin^2\left(\Phi_{(t)}\right)\right]$$

Armed with our validated approximation, we can rewrite this as

$$m\ln(P_T) \approx \frac{m}{2}\beta^m \sin^2\left(\Phi_{(t)}\right) \quad (19)$$

We will now proceed to minimize this relationship for m as follows:

$$m\ln(P_T) = \frac{m}{2}\beta^m \sin^2\left(\Phi_{(t)}\right)$$

$$2\ln(P_T) = \beta^m \sin^2\left(\Phi_{(t)}\right)$$

$$\ln[2\ln(P_T)] = \ln\left[\beta^m \sin^2\left(\Phi_{(t)}\right)\right]$$

$$\ln(2) + \ln[\ln(P_T)] = m\ln(\beta) + \ln\left[\sin^2\left(\Phi_{(t)}\right)\right]$$

We can identify constant values as

$$\ln(2) = b \quad \ln(\beta) = a$$

Now simplify and rearrange as

$$am = \ln[\ln(P_T)] - \ln\left[\sin^2\left(\Phi_{(t)}\right)\right] + b \qquad (20)$$

Our remaining terms inside the natural logs are both functions of time that will always result in real, positive numbers once evaluated, so we can rewrite each of these logs as functions of time:

$$\ln[\ln(P_T)] = F(t)$$

$$\ln\left[\sin^2\left(\Phi_{(t)}\right)\right] = G(t)$$

Rewrite (20) as

$$am = F(t) - G(t) + b$$

From here, we want to apply a least-squares minimization for m given that we have a finite data set where we will obtain our values for our functions of time. We sum over each output for our functions of time $\forall\ t$ in the dataset. More mathematically speaking,

$$\sum_{k=1}^{N} [am - (F(t_k) - G(t_k) + b)]^2 \rightarrow \min_m \qquad (21)$$

To minimize this, we take the derivative of this summation and set it equal to zero as follows:

$$\frac{d}{dm}\sum_{k=1}^{N} [am - (F(t_k) - G(t_k) + b)]^2 = 0$$

taking the derivative inside our summation and evaluating we arrive at

$$\sum_{k=1}^{N} 2a(am - F(t_k) + G(t_k) - b) = 0$$

Applying our summation,

$$aN\ m - \sum_{k=1}^{N} F(t_k) + \sum_{k=1}^{N} G(t_k) - Nb = 0$$

Solving for m we get

$$m = \frac{1}{aN}\sum_{k=1}^{N} F(t_k) - \frac{1}{aN}\sum_{k=1}^{N} G(t_k) + \frac{b}{a} \quad (22)$$

Given (22), we can now evaluate our summations to find the minimized value for m. Recalling that we initially set $n - 1 = m$, we can rewrite this for the braking index n as

$$n = \frac{1}{aN}\sum_{k=1}^{N} F(t_k) - \frac{1}{aN}\sum_{k=1}^{N} G(t_k) + \frac{b}{a} + 1 \quad (23)$$

When we supply this equation with the necessary values for our summations and plug in the constants, we arrive at the estimated braking index for magnetar J1550-5418 to be

$$n = 2.71$$

What is interesting is that if we use this value for the braking index but leave our estimated magnetic field strength as calculated by (10), our curve will undershoot the data as it forces the model to predict that this magnetar is spinning down slower than the data suggests:

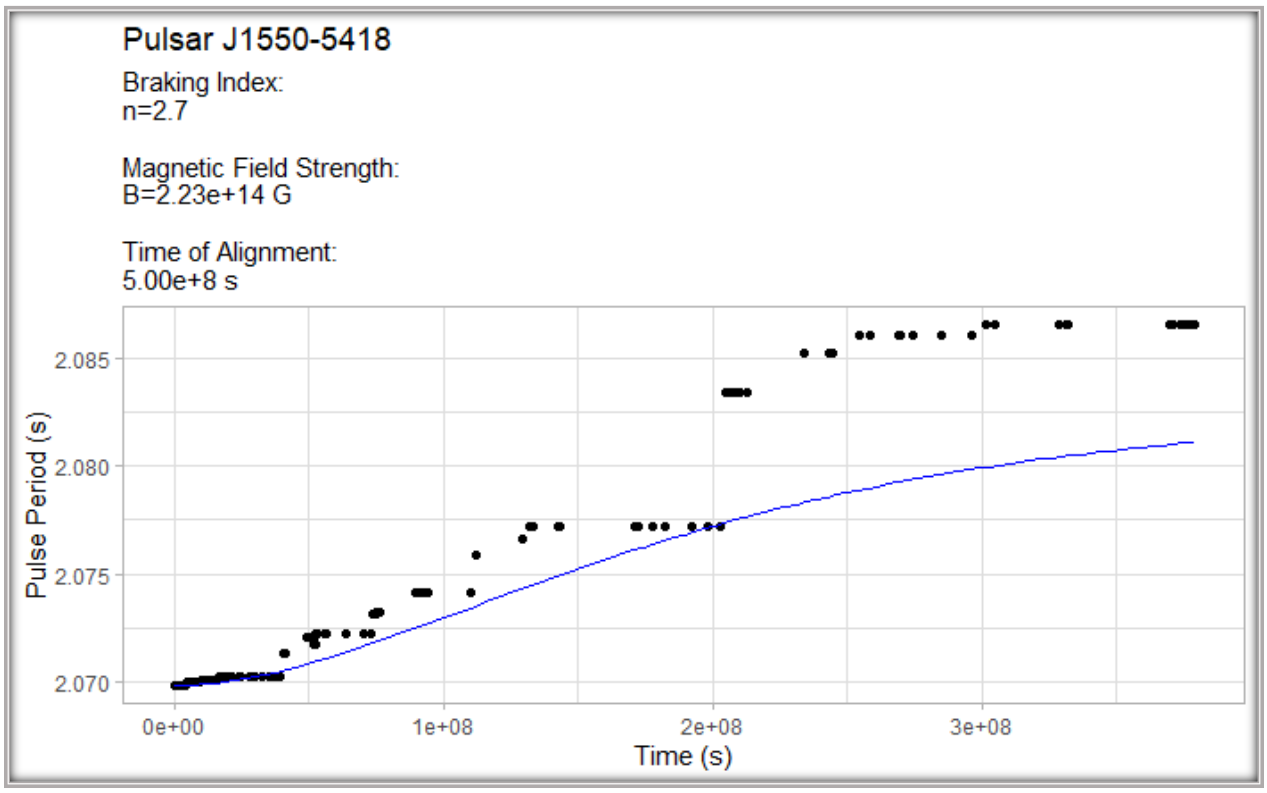

Figure 21: Forcing the braking index to be 2.7 with our calculated value for the magnetic field remaining the same

This clearly is a "worse fit" as the model is predicting the pulse period to be approximately .007s (7 milliseconds) below what the data shows it to be at its worst. However, all we did was calculate what the estimated magnetic field was using equation (10), set our alignment time to what occurs with that value for B (which happens to remain relatively constant regardless of what we set n and B as), and then plug all of that into equation (23). With those parameter estimates, (23) tells us that the braking

index should be closer to 2.7, not 2.53. So, what could be going on? If you look back at Table 9, you can see that a braking index of 2.7 yielded a magnetic field $B \approx 2.88 \times 10^{14}\ G$, which is roughly 1.3 times more than what our calculated estimate was. Considering our model is only using the pulse period data, it is tough to discern what properties are causing this shift. If we refit our data with $n = 2.71$ we get the following curve and statistics

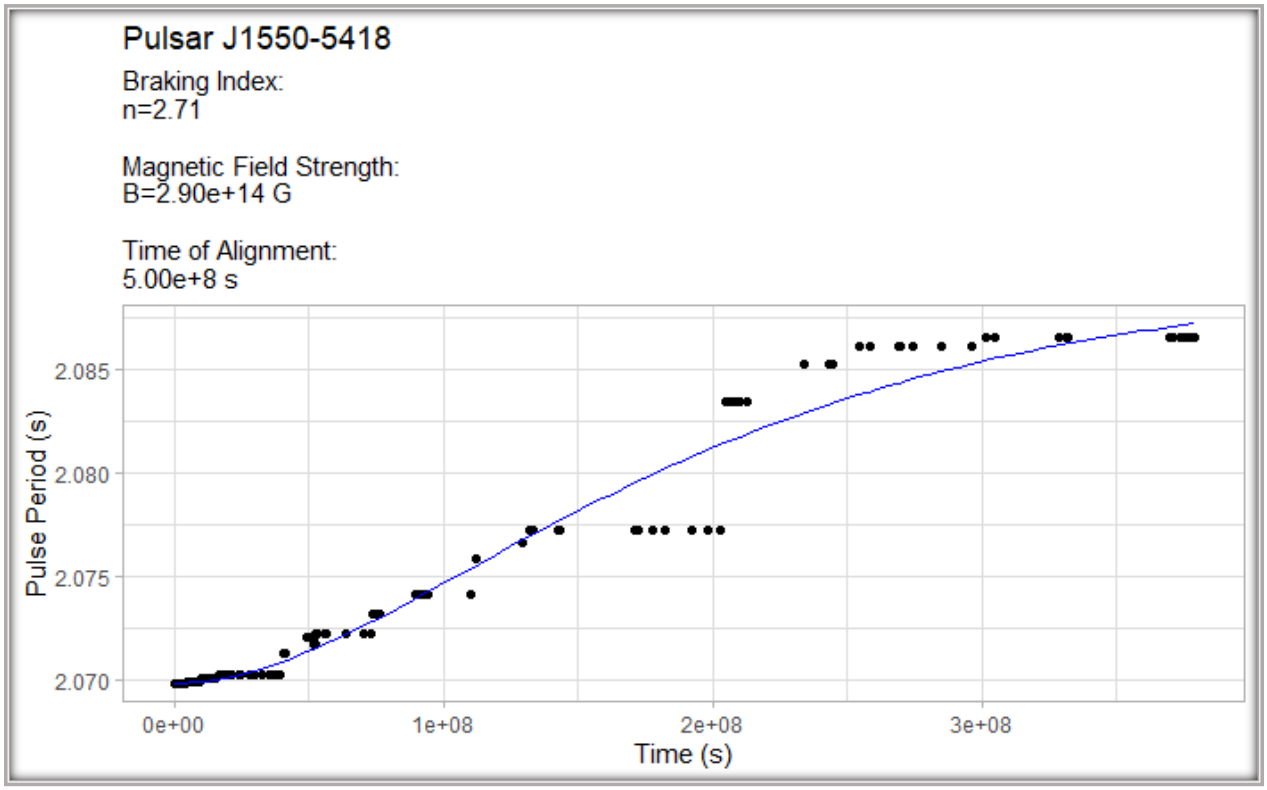

Figure 22: Running our model with n=2.71

```
Formula: P ~ (P0^(n - 1) + ((n - 1)/2) * ((td * k * B^2)^((n - 1)/2)) *
    (sin(X0 * (1 - exp(-2 * t.seconds/td))))^2)^(1/(n - 1))

Parameters:
    Estimate Std. Error t value Pr(>|t|)
B  2.901e+14  1.730e+12  167.68   <2e-16 ***
td 5.003e+08  1.341e+07   37.31   <2e-16 ***
---
Signif. codes:  0 ‘***’ 0.001 ‘**’ 0.01 ‘*’ 0.05 ‘.’ 0.1 ‘ ’ 1

Residual standard error: 0.001023 on 223 degrees of freedom

Number of iterations to convergence: 5
Achieved convergence tolerance: 1.265e-06
```

Figure 23: Statistics from curve with n=2.7

Again, we see that the magnetic field has been estimated to be slightly larger than our calculation using equation (10), but we still have a strong fit. So, which is it? The question seems to come down to which do we trust more, equation (10) or equation (23)? And of course, this is all assuming our governing equation (equation (9)) is a proper representation of the physics that is occurring at and within the pulsar. This will be an active area of exploration going forward with this project. For instance, we are using a rather "extreme" pulsar in that our governing equation is attempting to model a magnetar that has a strange data structure. There are areas where the pulsar slows down rapidly and then maintains this new pulse period in a stable manner for long stretches of time. For now, we can go off of the statistics being presented for the model. If we compare Figure 19 and Figure 23, we can look at the statistics pulled from each curve for our estimated parameters. We can summarize them below in a quick table:

n	$B\ (G)$	t-value
2.53	2.23×10^{14}	164.88
2.71	2.90×10^{14}	167.68

Table 5: Comparing t-values for each magnetic field estimation

Going off of the significance of the magnetic field estimates alone, we see that we have slightly more significance when our braking index is approximately 2.7.

If we look at how equation (23) works, it was derived from equation (9), meaning that they are linked, and making adjustments to one will of course change things for the other. That is why we opted to use an independent calculation for the magnetic field in equation (23) to arrive at our minimized value for n. We can use equation (9) and manually adjust the braking index to have the model predict the magnetic field to match the independent calculation like we did at the beginning of our analysis, or we can use that independent calculation in equation (23), and then work on fitting the data with that value for n and ensure that the t-value for our estimated parameters are large enough to imply significance. This is all done assuming t_d is roughly equivalent (same order of magnitude or close) to the length of your dataset or doesn't vary significantly when you adjust your magnetic field parameter.

The other area of issue here is in justifying our analysis for the approximation in (16). We used estimated values to calculate $\beta = \frac{\sqrt{\Lambda}}{P_0}$. The magnitude of β is proportional to the values we used for Λ, meaning that if our braking index of 2.7 is correct, we must adjust this term and again check to see if our approximation is valid. A quick calculation with our new estimate for β is

$$\beta = 0.097967496$$

If we recall from our maximization analysis that our function reaches a maximum when

$$m = -\frac{1}{\ln(b)}$$

and that $b = \beta$, then we get

$$m = -\frac{1}{\ln(0.097967496)}$$

$$m = 0.395469577$$

Recall that

$$f(m) = amb^m$$

where $a = 0.5$ and $b = 0.097967496$, we get

$$f(m) = \mu = 0.078901755$$

We set our critical value that μ could not exceed as $f_{critical} \approx 0.3$, so even with this more significant estimation for the magnetic field, we arrive at

$$\mu < f_{critical}$$

which means that our approximation

$$\ln(1 + \mu) \approx \mu$$

is still valid.

This process and our equations we are using to model the data and estimate the parameters will be an area of focus moving forward. Being that each parameter estimate is linked, changing one implies a change in the others. As a general starting point for future analysis, we can summarize the process going forward, and then adjust if necessary. First, we will collect each equation that plays a significant role here:

$$P(t) = \left[{P_0}^{(n-1)} + \left(\frac{n-1}{2}\right)\Lambda^{\frac{(n-1)}{2}} \sin^2\left(\phi_0\left(1 - e^{\frac{-2t}{t_d}}\right)\right)\right]^{\frac{1}{n-1}} \quad (9)$$

$$n = \frac{1}{aN}\sum_{k=1}^{N} F(t_k) - \frac{1}{aN}\sum_{k=1}^{N} G(t_k) + \frac{b}{a} + 1 \quad (23)$$

$$B_s = 3.2 \times 10^{19}\sqrt{P\dot{P}} \quad (10)$$

recalling that

$$\beta = \frac{\sqrt{\Lambda}}{P_0} \qquad , \qquad \Lambda = \mathrm{k}\, t_d B^2$$

For a given pulsar, we first use (10) to get a rough estimate of what the magnetic field of the pulsar is. Using that and an estimate for t_d being on the same order of magnitude as the length of your dataset (or if available an independent calculation), we can use (23) with our collected data to estimate the braking index of the pulsar. From there, we can run our nonlinear curve fitting with the braking index calculated by (23) to arrive at a curve of best fit with new parameter estimates for both B and t_d. We can check their significance by also using equation (9) and the estimated magnetic field from (10) to run a nonlinear curve fit, and them compare the output t-values.

For this preliminary analysis and proof-of-concept, it has worked out rather well in providing a curve of best fit and good parameter estimations. Our model has identified this pulsar as a magnetar, which is a good sign that our model is headed in the right direction. Of course, this model is assuming the physical interactions in and around the pulsar to be only a varying rotation-radiation angle. Future research would need to examine other models that assume different interactions, such as local gas and dust,

companion systems, or variable magnetic fields on timescales less than what our data spans. The eventual goal would be to potentially merge these models into an even more generalized model that can account for all these factors to some degree, for which our braking index estimation may become even more accurate.

5.2.3.1: Future Analysis to Consider for General Pulsars

Equation (23) appears promising as a way to estimate the braking index for pulsars. However, our analysis above was using specific values measured and estimated for our magnetar. This is not quite a generalized model as there are various things that could invalidate this procedure. Things such as having the physical values of the pulsar evaluate to a number that wouldn't allow us to use the approximation shown in (16), or values that would result in physically impossible scenarios. We are using measurements taken as a snapshot in time of this pulsar to try and model its current behavior given our data. The values for our parameters would be different depending upon the pulsar being measured and the dataset being used.

A quick general analysis of β can help us see why we must proceed carefully. We mentioned previously that we are using parameters estimated from our data. However, what if this were not a magnetar but instead a typical pulsar where we must consider the estimated value for alignment to be on the order of $10^{14} - 10^{15}\ s$? Again, this is assuming a pulsar with a magnetic field roughly three orders of magnitude lower than our pulsar. If we were to calculate using this time for alignment, we would also need to adjust our magnetic field strength to match that of a typical pulsar. If we do this calculation, we see that we get

$$\Lambda_{Typ} = k{B_{Typ}}^2 t_{d_{Typ}}$$

where

$$k \approx 10^{-40}, \qquad B_{Typ} \approx 10^{11}\ G, \qquad t_{d_{Typ}} \approx 5 \times 10^{14}\ s$$

If we assume that the initial pulse period $P_{0_{Typ}}$ that will be used for a typical pulsar to be

$$P_{0_{Typ}} \approx 0.5\ s$$

(this was estimated using Figure 1 in the paper by Igoshev et. al., 2021)

then we can calculate β_{Typ} as

$$\beta_{Typ} \approx .139771357$$

Carrying out the same maximization analysis to justify the use of approximation (16), we get

$$\mu_{Typ} \approx 0.093477305$$

Again, recall our critical value to invalidate (16) was $f_{critical} \approx 0.3$, so even with a typical pulsar,

$$\mu_{Typ} < f_{critical}$$

However, our approximation is still heavily dependent upon the magnitude of the magnetic field and the alignment time. For instance, increasing the magnitude of the magnetic field strength without decreasing the alignment time results in problematic values for m, and as such μ. For instance, if we keep our time of alignment the same, but increase the magnetic field by one order of magnitude, we end up with

$$\beta = 1.397713572$$

Recall our generalized relationship between m and β from before,

$$f(m) = amb^m \quad (24)$$

where $a = \frac{1}{2}$ due to maximizing our sine term at 1, combining it with the constant $\frac{1}{2}$ from equation (14) and $b = \beta$. If we plot (24), we can see the issue whenever we let $\beta > 1$:

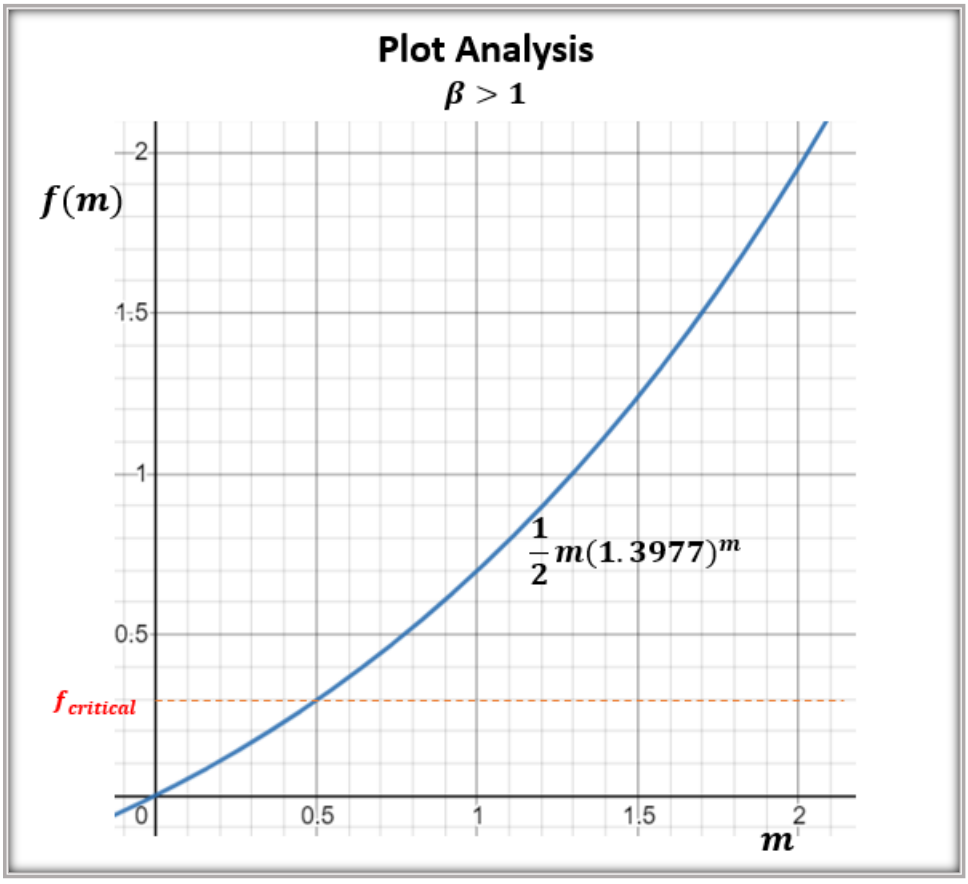

Figure 24: Graphical behavior of our μ term with β>1

This issue is that as m grows, there is no localized maximum and our function blows past our critical value rather quickly. In fact, if β is allowed to go past 1, we end up in dubious territory in general as it turns our maximizing value for m into a minimum that is negative. Now remember, this critical value was only set up so that we could use the approximation $\ln(1 + x) \approx x$ for $0 < x \ll 1$. Because of this, we can actually estimate what the maximum value for β can be in order to use this approximation.

Recall,

$$f_{critical} = 0.3$$

We will use a graphical method to pinpoint approximately what value of β will cause our function to exceed our critical value $\forall\, m$:

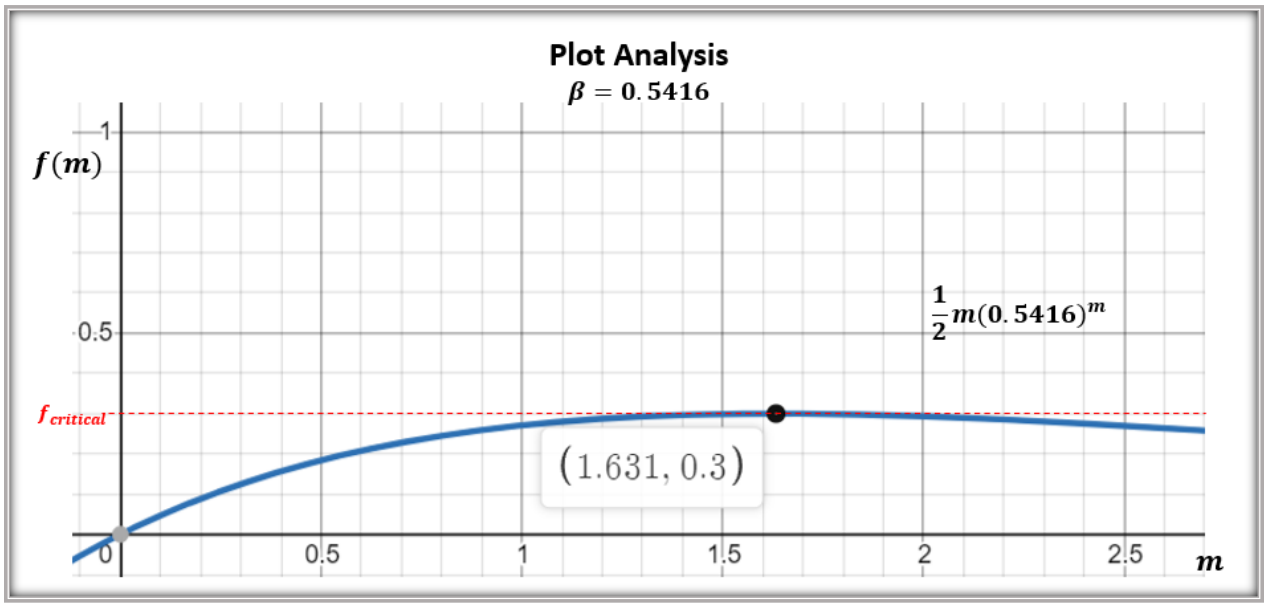

Figure 25: Finding the value that our β term cannot exceed $\forall\, m$

Figure 25 illustrates that we have a maximum limit for β if m (and as such n) is allowed to grow arbitrarily large. What that means is the relationship between the magnetic field, the alignment time, the rotation-radiation angle, and the initial pulse period are crucial in determining if we can use the approximation in (16).

If in future analysis we calculate a β larger than what is in Figure 25, we no longer can use that approximation and would have to estimate the braking index using (13):

$$m \ln(P_T) = \ln\left[1 + \frac{m}{2}\beta^m \sin^2\left(\Phi_{(t)}\right)\right]$$

With some algebra and arrive at

$$m = \frac{\ln\left[1 + \frac{m}{2}\beta^m \sin^2\left(\Phi_{(t)}\right)\right]}{\ln\left(P_T\right)} \qquad (25)$$

Minimizing (25) would require careful analysis, but it would still be possible to get a numerical solution. We will save this exercise for future work to be done on this project.

In general, there may be more information to pull from the way the mathematics works out in the above analysis. Perhaps there is a strong relationship between the strength of the magnetic field and how quickly the rotation-radiation axes align. This may further be tied together in how long the pulsar itself lives, in which the stronger the fields, the shorter its life in general. Mathematically speaking, to avoid strange braking index behavior, it would appear that if you make changes to one parameter, the others must change to ensure the braking index itself is preserved within a domain that physically makes sense.

Or this may just be an artifact of the mathematics. As our project continues and our research deepens, we may eventually find out.

Furthermore, this model is assuming that the rotation-radiation angle is changing and this provides the primary mechanism by which the pulsar slows over time. There are other models that propose different mechanisms for slowing, and in reality, it is more than likely a mixture of things that cause a pulsar to slow down. Take for instance the weird interplay between what our model yields as a good value for the braking index, and what our minimization does. This may mean there are other mechanisms present slowing J1555-5418 down faster that our model isn't accounting for, such as local gas and dust or perhaps a variable magnetic field. We are also assuming that the pulsar's decay curve is dictated by a variable rotation-radiation angle, which it may not be. Our model suggests that this angle plays a role, but the degree to which it does will be left for future analysis. We must keep in mind that what we are doing is taking a snapshot in time of this pulsar and trying to find values for parameters that deliver a curve of best fit and that make accurate predictions about what said parameters are.

5.2.4: Modeling the Raw Data

As one final means of exploration, we want to use our model on the raw data with the outlier measurements included. This exercise is being done to test the robustness of the model when dealing with a potential glitch (anti or otherwise). If those outlier datapoints were in fact glitches and a part of the magnetar's behavior, we want to run our model with those pulse periods to see how they affect the output. Our model being able to provide accurate measurements even with glitched behavior (or bad data) will demonstrate how well our assumed equation captures the physical behavior of our selected pulsar. A successful model should be able to ingest the raw data so that the invention's Glitch Processor is more easily able to work with the bad data all while not sacrificing too much accuracy in timing predictions.

Utilizing our governing equation (9) with our calculated braking index ($n = 2.71$), we get the following results:

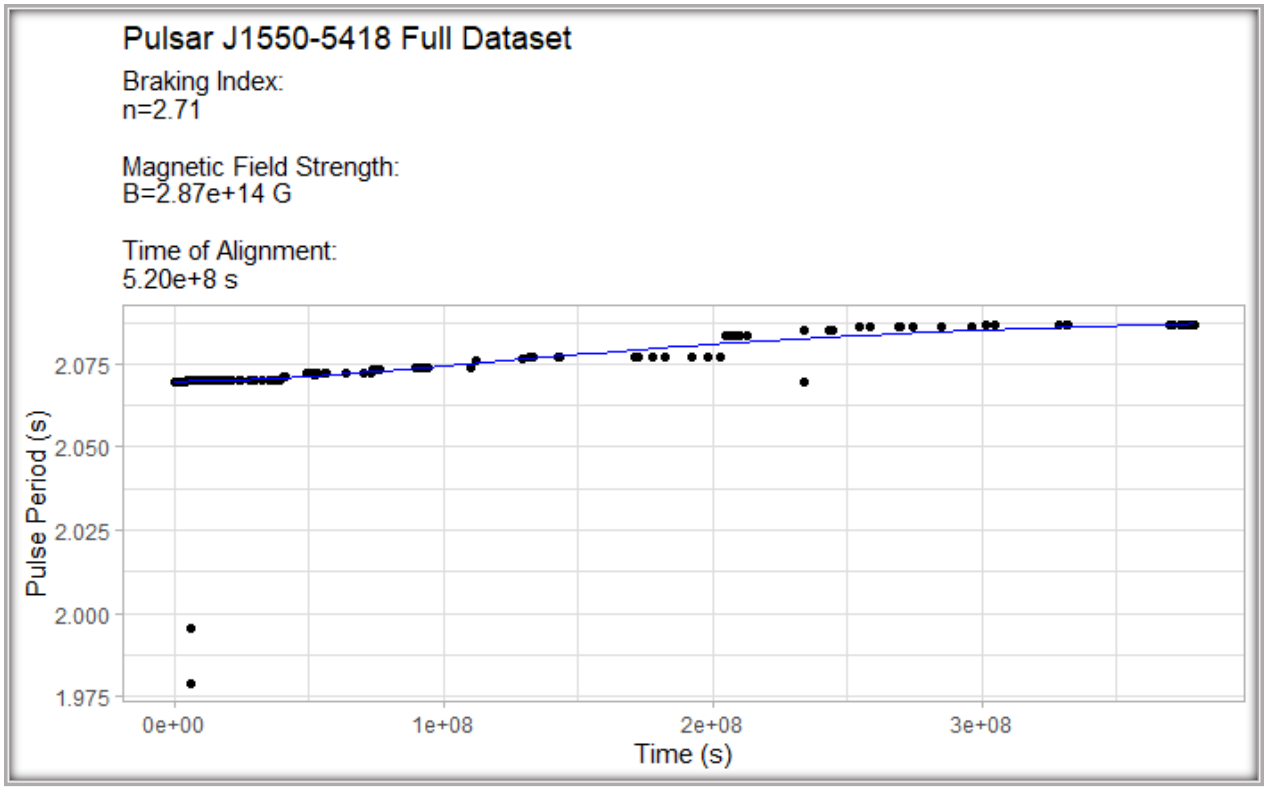

Figure 26: Curve of best fit with full dataset

```
Formula: P ~ (P0^(n - 1) + ((n - 1)/2) * ((td * k * B^2)^((n - 1)/2)) *
    (sin(X0 * (1 - exp(-2 * t.seconds/td))))^2)^(1/(n - 1))

Parameters:
    Estimate Std. Error t value Pr(>|t|)
B  2.865e+14  2.987e+13   9.593   <2e-16 ***
td 5.197e+08  2.562e+08   2.029   0.0436 *
---
Signif. codes:  0 ‘***’ 0.001 ‘**’ 0.01 ‘*’ 0.05 ‘.’ 0.1 ‘ ’ 1

Residual standard error: 0.01822 on 234 degrees of freedom

Number of iterations to convergence: 4
Achieved convergence tolerance: 4.568e-06
```

Figure 27: Statistics from fit using full dataset

As you can see, those outliers definitely play a role in affecting our t-values and the corresponding significance. Whereas our magnetic field estimate remained very significant, our alignment time dropped in significance. This is a good lesson in understanding the alignment times for our model in that a pulsar with a lot of strange behavior may not be the best object to use to make timing predictions from. Even so, our model appears to handle the full dataset well, with a strong fit and significant

magnetic field estimate. The largest error that we can see from our curve fit appears to be approximately 4ms. This is definitely a promising result, but even an error that small can be disastrous when attempting to make a timing prediction using this model. For instance, if you look at the data, the pulsar has long stretches of time where the pulse period barely moves, meaning that if our predictions cannot be accurate to less than 1ms, making a reference time prediction won't be possible. At least not to the accuracy needed for networked systems or any sort of positioning system. This will be briefly demonstrated in the following section.

5.2.4.1: Time Prediction and Future Work

Whereas our model appears to do well at estimating the magnetic field of a given pulsar, the eventual goal of this invention will be to calculate a reference time based on a pulse period measurement (see Component 5- Time Processor in Section 1 or Appendix A). As we've seen above, our estimated pulse period values for the magnetar J1550-5418 were off by about 4ms at its worst if our parameter estimations are accurate. This may not seem like all that much, but it could translate to vastly over or underestimated time values. This brief section is meant to solve our general model for *t* and illustrate why even being off by a few milliseconds is bad when trying to estimate a time using a pulsar. The following analysis is provided for others to review to ensure accuracy:

$$P(t) = \left[{P_0}^{(n-1)} + \left(\frac{n-1}{2}\right)\Lambda^{\frac{(n-1)}{2}} \sin^2\left(\phi_0\left(1 - e^{\frac{-2t}{t_d}}\right)\right)\right]^{\frac{1}{n-1}}$$

Simplify with the following:

$$(n-1) = m, \qquad \left(\frac{n-1}{2}\right)\Lambda^{\frac{(n-1)}{2}} = \Upsilon, \qquad \frac{2}{t_d} = \lambda$$

then,

$$P = \left[{P_0}^{m} + \Upsilon \sin^2\left(\phi_0\left(1 - e^{-\lambda t}\right)\right)\right]^{\frac{1}{m}}$$

where we are suppressing the *t*-dependence on *P* for simplicity.

We now solve for *t*:

$$P^m = {P_0}^m + \Upsilon \sin^2(\phi_0(1 - e^{-\lambda t}))$$

$$\frac{P^m - {P_0}^m}{\Upsilon} = \sin^2(\phi_0(1 - e^{-\lambda t}))$$

$$\sqrt{\frac{P^m - {P_0}^m}{\Upsilon}} = \sin(\phi_0(1 - e^{-\lambda t}))$$

$$\phi_0{}^{-1}\sin^{-1}\left[\left(\frac{P^m - P_0{}^m}{\Upsilon}\right)^{\frac{1}{2}}\right] = 1 - e^{-\lambda t}$$

$$e^{-\lambda t} = 1 - \phi_0{}^{-1}\sin^{-1}\left[\left(\frac{P^m - P_0{}^m}{\Upsilon}\right)^{\frac{1}{2}}\right]$$

$$t = -\lambda^{-1}\ln\left\{1 - \phi_0{}^{-1}\sin^{-1}\left[\left(\frac{P^m - P_0{}^m}{\Upsilon}\right)^{\frac{1}{2}}\right]\right\}$$

Substituting our simplifications back in, we arrive at

$$t_{(P,n)} = -\frac{1}{2}t_d\ln\left\{1 - \phi_0{}^{-1}\sin^{-1}\left[\left(\frac{P^{(n-1)} - P_0{}^{(n-1)}}{\left(\frac{n-1}{2}\right)\Lambda^{\left(\frac{n-1}{2}\right)}}\right)^{\frac{1}{2}}\right]\right\}. \quad (26)$$

Notice that our equation requires the pulse period to be entered into an arcsine function. The arcsine function can only ingest values $\psi\epsilon[0,1]$, so we must normalize our input so that it is scaled between 0 and 1. To do this we calculate the argument in the arcsine's maximum, which occurs when *P* is at its maximum since all other values within the argument are constants. Once we have this maximized value, we can input other pulse periods and then divide that value by this maximized value. This always ensures that our argument stays within the valid domain of arcsine. More mathematically speaking:

$$\psi(P) = \left(\frac{P^{(n-1)} - P_0{}^{(n-1)}}{\left(\frac{n-1}{2}\right)\Lambda^{\left(\frac{n-1}{2}\right)}}\right)^{\frac{1}{2}}$$

$\psi_{(P)_{max}}$ occurs when our pulse period measurement is at its largest, so our final measurement of *P* within our dataset. For J1550-5418, our largest measurement for the pulse period is $P = 2.086549s$. We know the initial pulse period in the dataset, our estimated braking index, the magnetic field strength, and other constants contained with the Λ term. When we calculate this value, we get

$$\psi_{max} = 0.918064126$$

Now, we want to scale our arcsine inputs by this value so that all other pulse period measurements, when calculating $\psi(P)$, range between 0 and 1. That way our function's domain remains valid and we can obtain an output for time. Our new scaled equation is

$$t_{(P,n)} = -\frac{1}{2}t_d\ln\left\{1 - \phi_0{}^{-1}\sin^{-1}\left[\frac{\psi_{(P)}}{\psi_{max}}\right]\right\} \quad (27)$$

The above equation will warrant further study and analysis to determine if it truly is the direction we need to proceed in. The argument inside the arcsine function is what is cause for caution in its current derivation. For making future timing predictions, we will need a more complete picture of the pulsar's

constants, as well as determining how to apply this (or perhaps another version of this) equation. For instance, we will need a good estimate for the true age of the pulsar, a decent estimate of how long we believe it will take for the rotation and radiation axes to align (t_d), as well as calculating when the pulsar will "die" (we can use an estimate on when the pulsar should go radio silent for this). These are needed so that we can perform the same type of analysis as above for our arcsine function that will allow us to make future time predictions based on pulse period measurements.

To illustrate how the time predictions deviated a great degree over time, we applied our timing equation (27) to our dataset and then plot the outputs in an Actual Time-Predicted Time plot:

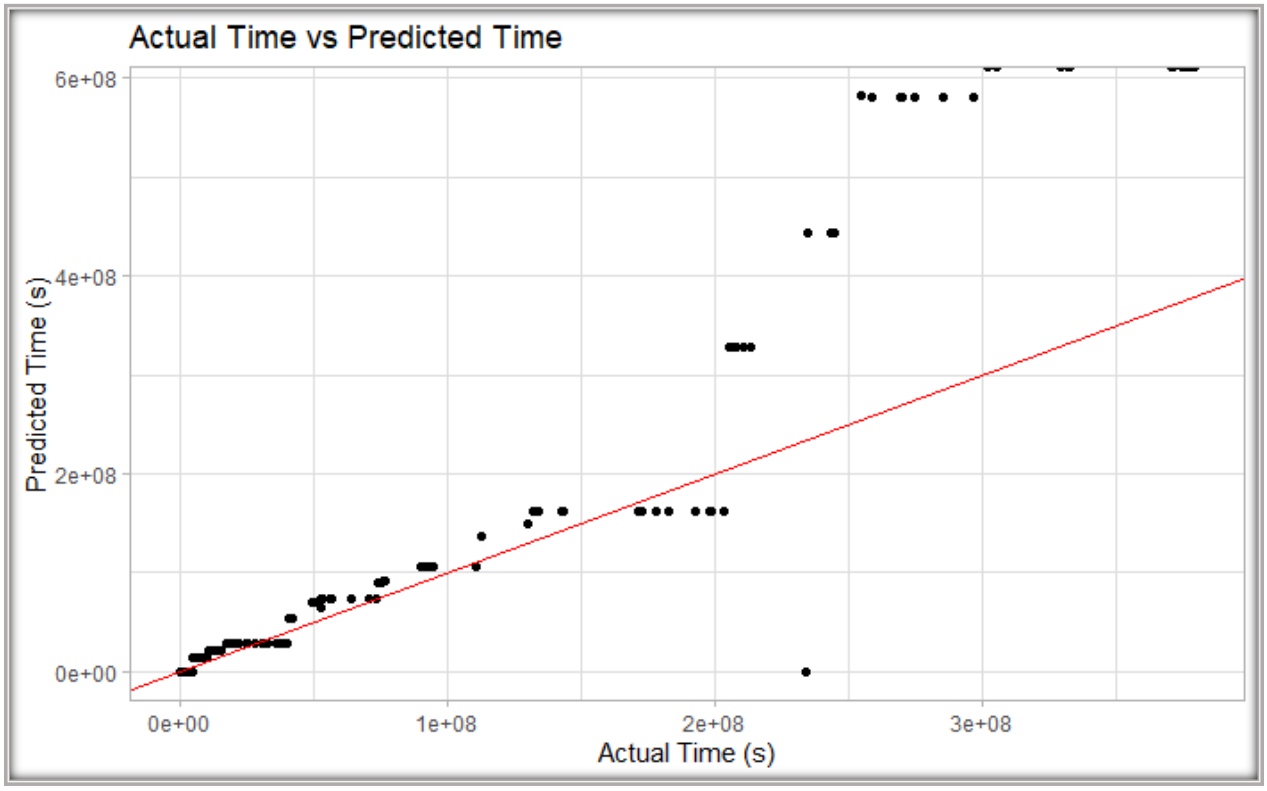

Figure 28: Looking at the how the predicted times deviate from the actual times

The red line in Figure 25 represents the line $f(t) = t$, which is where we would want all of our outputs from equation (27) to land on if our model were to perfectly predict the time each measurement of the pulse period was made. As an example, if we made the pulse period measurement at $t = 1.00 \times 10^8\ s$, then a perfect model would also have the output be at $t_{predicted} = 1.00 \times 10^8\ s$. Therefore, the further from the red line the datapoints are, the worse the prediction is. You can see that early on in the measurement period, we have fairly accurate predictions, ranging from a few days of error to a month or two. However, after we move past the first half of the data, the predicted times vary significantly, where they can be off by as much as 9 years at their worst. Recall what we discussed in the previous section; even being off by 5ms in our pulse period estimation could yield errors in our time prediction by years. As it is, this model is clearly not in a state that is ready to serve within the Time Processor of the invention. For a copy of the RStudio script used to find these values, see Appendix D.

However, this doesn't necessarily mean that our invention or this model is "dead in the water". We have very promising results and have definitely advanced our ideas forward proving that modeling a pulsar's decay curve dynamics, while difficult, is possible. Another thing to consider is that we may have unfortunately picked a very difficult pulsar to model. Not only is our pulsar a magnetar, but the data structure itself is quite peculiar. The knowledge gained in this analysis will help our invention in that we may now know what to look out for when identifying "clock-worthy" pulsars. In the next phase of this project, we will look to expand our data to include different pulsars with some of them being pulsars with well-studied and well-estimated parameters so as to gain better reference time predictions.

6: Further Work and Business Strategies

Now that we've gone through the theoretical background and the results of our analysis, we'll want to identify the work needing to be done to continue this project and briefly analyze business objectives so that we can move forward. Whereas our proof of concept has provided promising results, we are far from being ready to take this technology to market. In order to quantify our business objectives, we will employ a system that NASA has used for years; the Technology Readiness Level (TRL). Being that NASA is one of our potential customers for the end product, adopting this quantification method will bode well for us if and when we put together a grant proposal for joint research and/or a sale. If we are able to justify a TRL that aligns with how they assess future technologies, it will make our bid for collaborative work and business all that more robust and appealing.

6.1: Technology Readiness Level

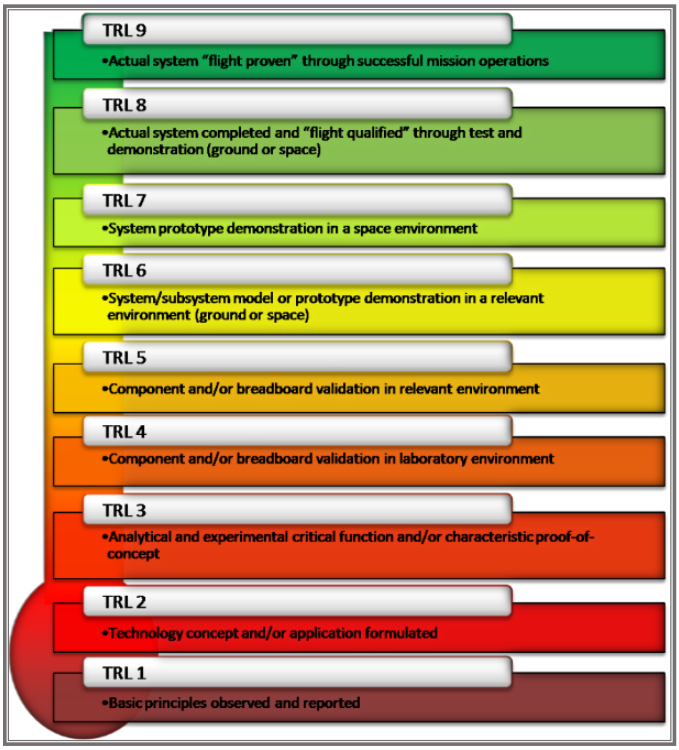

Figure 29: NASA Technology Readiness Level (TRL) chart
Credit: NASA

NASA has employed a system to assess future technologies and their progress when being actively researched. Each piece of technology that they invest in is assigned a TRL value and then tracked as work is done, steadily moving the new technology through these levels as they meet research and testing outcomes. A TRL of 1 would mean that the new piece of technology is in its infancy, normally just a theoretical concept that one has thought of. A TRL of 9 means that this piece of technology has been extensively tested, proven to work in multiple scenarios, and is "ready to fly".

As far as our invention that we are working on, we have broken down the TRL levels that it has gone through up to date, and then we will identify what needs to occur in order to advance it forward as a business option for Booz Allen Hamilton.

TRL	Project Phase	Description of Work
1	Proposed theoretical concept	A suggested use of pulsars as a potential timing source for network communications.
2 (level we were at)	Patent proposal	A patent proposal was drafted that outlined the concepts and illustrated the various components of the technology and their theoretical capabilities. A literature review

		was completed for the necessary research and background knowledge, as well as some initial assessment of methods for data gathering and curve fitting.
3 (current level)	Initial proof of concept	Real data was collected on a selected pulsar, a governing equation was selected and adapted for said data, and initial curves were fit with basic predictions made to assess the model.
4 (in progress)	Multiple tests of current model and other selected models needed with more pulsars	In order to move to this level, we will need to work with other models and collect data on multiple pulsars. Consideration of machine learning/AI driven code to evaluate and advance the use of other models may also occur.

Table 6: TRL Advancement Table

As noted in the above table, the invention was at TRL 2 when we began. After the initial assessment of background literature and a cursory mathematical analysis to identify what we needed to pursue, we began the data collection and curve fitting using our adapted governing equation. This paper illustrates the process of moving into TRL 3 and identifying the business objectives for Booz Allen to advance into TRL 4. With a proof of concept for the mathematics that will be necessary to make timing predictions, we can assess what needs to occur in order to refine the analysis and continue this research.

6.2: Work Needed to Advance to TRL 4

The blow sections will briefly illustrate the path that Booz Allen is recommended to take if wanting to continue research and development on this project. These are suggestions in ways we can pursue results that will be more marketable for the Firm and could lead to lucrative collaborations with interested third parties.

6.2.1: Model Accuracy

The first hurdle that must be overcome is the selected governing model's accuracy. As mentioned in 5.2.4.1, our timing estimates are vastly off and in no state to be used for network timing. When looking at how our model is predicting time, having errors in the 4ms range can lead to this vast inaccuracy of predictions. Part of the issue here could be due to the strange data structure this pulsar exhibits as

discussed in 5.2.1 in that our selected pulsar appears to go through some rapid spin-down periods followed by long stretches of slower spin-downs. Looking at the various curve fits done throughout this analysis, our curve of best fit matches the data much closer early on, and then begins to vastly deviate after that first major spin-down event which could point towards this pulsar not being an ideal candidate to make reference time predictions with.

Furthermore, terrestrial clocks in their current form are more accurate than any astrophysical timing source on shorter timescales (approximately 2 years). In fact, there have been direct comparisons between terrestrial clocks (atomic clocks in laboratory settings) and astrophysical timing sources that show that our terrestrial clocks offer better resolution and accuracy than that of observed astrophysical sources (Hartnett & Luiten, 2011). Hartnett and Luiten utilize statistical measures of timekeeping stability, namely the Square Root Allan Variance (SRAV) and the Sigma Z statistic. These taken together provide a robust measure of timing stability for various sources (see Figure 1 and 2 in Hartnett and Luiten's paper) which demonstrates that localized terrestrial clocks are far more stable on timescales that we are more likely to use. However, astrophysical sources may prove useful in maintaining accurate timekeeping on longer timescales, or during scenarios where spacecraft far away from earth need to maintain the same time as on Earth but have no means of communicating with earth in a timely manner. This paper discusses how we do not have sufficient statistics collected on longer timescales for both terrestrial and astrophysical timing sources to characterize this usefulness, however the main idea arises from the fact that a pulsar never requires an external power source to maintain its pulse period. As such, over very long timescales pulsars may prove to be a more robust, if slightly less accurate, source for timing. As far as maintaining the same time as on Earth when direct contact is not available, using a "pulsar time" may prove useful if only to ensure all clocks read the same time during deep-space mission events.

The first major hurdle will be the accuracy and resolution of the pulse period measurements of a selected pulsar. When observing the frequency of a given pulsar, we will need to ensure accuracy of the measurement out to between the microsecond to nanosecond range. Making accurate calculations at this level will require us to employ either clever scaling techniques, or moving towards more accurate systems of finite precision (quad as opposed to double). As discussed, our introductory generalized model is off by around 4ms at its worst for the selected pulsar. This may seem like a small amount of error, but if you consider that a pulsar can maintain a frequency to the millisecond for years, being off by even a few milliseconds will expand your time prediction by a few years. Considering that networks rely on timing to be accurate to within tens of milliseconds, that level of variance is unacceptable as a primary source for timing predictions. However, this is not a death note for our idea, but rather an area for further evaluation of both our model, our chosen data, and the potential uses for predicting a reference time using pulsars.

6.2.2: Including More Pulsars and Models

This model is one of a few that could be describing the physical situation of our selected pulsar. Our model assumes that the rotation-radiation angle changes over time and this interaction contributes to the slowing rotational period of the pulsar. As seen with our curve, our model fits the data fairly well,

but is still off by around 4ms. This could be due to the strange data structure we have mentioned a few times, but what does that structure suggest? Perhaps magnetar J1550-5418 has other features causing the spin-down to slow more rapidly than just a spin-down induced by a changing rotation-radiation angle. What if there was a local event that caused a large amount of gas and dust to begin to interact with the magnetar that then caused it to slow much more rapidly than in the first 5 years of observations? Events such as these are hard to predict, but it means that our technology will need to be able to account for things such as this.

Scenarios such as there being more local interactions around the pulsar or even the magnetic field varying aggressively could be contributing factors that is causing J1550-5418 to slow faster than our model can predict. As a first course of action in continuing our research and development for this technology, we need to begin to evaluate other mathematical models that describe the above-mentioned interactions. A potential path for Booz Allen to take would be to expand our mathematical algorithm to include more models, each representing a different physical situation. The same type of analysis can be done to fit a curve for each model with the knowledge of the parameters as inputs and then observe which model (if any) has a better fit. What this would look like from a business perspective would be to include an astrophysics expert to validate our model selection and to ensure our theoretical reasoning is sound. We could consider reaching out to pulsar experts and contracting them as advisors on our research so as to ensure that our models accurately can account for the latest knowledge we have on pulsar behavior.

Along with expanding our model selection process, we need to expand our pulsar data. As it stands for our proof of concept, we have selected only one pulsar. Selecting multiple pulsars will allow us to begin to test how well our governing equation does with pulsars that have different physical properties, such as non-magnetars. In fact, right now it is tough to characterize how well our model will work given various datasets from less-rare rotating bodies. If we pair this idea with also including more models that can each capture the different physical situations we believe play a role in a pulsar's spin-down, we will gain immense amounts of knowledge that can shape the direction our research takes. This could even lead to a more generalized model that is able to account for multiple types of interactions. This could take the form of a probabilistic model that will give us the probability measure if a given pulsar is slowing down more due to, say, the magnetic field aggressively changing, or it having strong interactions with its local environment. The business potentials for developing a software package that does this may prove lucrative if we are able to validate its findings.

What this would look like from the project level would be potentially selecting pulsars that are well-measured so we aren't relying on canonical values for our models. For our proof of concept, we are taking for granted the assumption of specific values such as our alignment time (t_d) or the canonical values for pulsars. As already mentioned, this is all done to simulate the long-term behavior of the pulsar's rotation as well as to ensure our model is able to fit an appropriate curve given that we are limiting ourselves to a snapshot in time of this pulsar's behavior. For instance, having a better understanding of t_d would require we have a good estimate for a pulsar's true initial pulse period (P_o) and sufficient data on the pulsar to allow for a good fit. Furthermore, knowledge of the actual age of the pulsar and a deeper understanding of the magnetic field could prove useful as a standard measure that we can adjust our model off of. Selecting well studied pulsars, such as the Crab pulsar, is a must for continuing this project. These pulsar's can be used as "measuring sticks" to validate how well our models' estimate pulsar parameters.

6.2.3: Machine Learning and Other Software

As we refine our mathematics to include more physical situations and expand our pulsar data, we would also want to employ more robust code that can analyze our fitted data. One such approach could be to employ someone with extensive knowledge of machine learning that could train a program to look at our generated curves and select the best one for each. We could work to develop a way to provide the probability of which physical situation best fits a selected pulsar and then categorize that pulsar with the appropriate model. The Time Server in our invention would index that pulsar and its data with that particular model, and when we collect new data on that pulsar, the code will again evaluate the predicted reference time with its paired model.

This will require Booz Allen to identify and allocate time for someone with this sort of coding background. As it stands, this research is being conducted without cost to Booz Allen, but if we wish to continue this work, bringing someone on that is familiar with work such as this could provide us with the means to really gain some ground as far as attaining timing accuracy that is marketable. Before we pursue this, we would expand our data to include more pulsars, with some of them being well studied to provide a useful measure of our model(s). If we can show that both expanding our data and our model selection provides useful input, pursuing someone with machine learning experience would be the next step to push this technology into TRL 4.

Along these same lines, there are software packages available that allow us to accurately time pulsars that exist. Packages such as TEMPO 2 (Hobbs, Edwards, & Manchester, 2006) are used to obtain incredibly accurate astrophysical parameter estimates when trying to calculate the frequency/pulse period of a measured pulsar. This package is extensive in that it can account for relativistic effects present that can skew timing, and is able to accurately measure the Time of Arrival (TOA) of pulse signals that allow for very accurate measurements. As mentioned in the paper by Hobbs et. al. characterizing the TEMPO 2 package, when timing a pulsar for data collection purposes are to be used with Modified Julian Dates (which our project would be very much interested in), the TOA measurement would need to be accurate to 19 significant figures for nanosecond accuracy.

If Booz Allen is seeking to collect data and measure pulsar frequencies independently of observatories that routinely collect this data and perform the necessary corrections to obtain an accurate TOA, employing packages such as TEMPO 2 would be a must. In looking over this package, this would require procuring an astronomer and/or a computer scientist that is familiar with this package, to include the coding languages of FORTRAN and C++ for which this package is based on. It may also prove useful in working with the TEMPO 2 package to gain a better understanding of the intricacies of timing pulsars, which may well help with our model selection and adjustments. However, if Booz Allen is only seeking to collect data from observatories that do this sort of collection and correction, employing TEMPO 2 wouldn't be necessary, but we would be relegating our abilities to provide reference timing to that of a passive role reliant on observatories. This may not be the negative that it sounds like. Observatories are far better equipped to do this sort of data gathering and corrections, and if we are using their finished product, it would bode well in that we know our data is representing any selected pulsar accurately. A deeper review of the TEMPO 2 package should be completed regardless of the direction we choose to

go for this technology as understanding how it works would be greatly beneficial for this project. It is our recommendation at this time, however, to use data collected and corrected by observatories as we further refine our own intrinsic model ideas.

6.3: Approach to the Market

It is not surprise that the space industry is expanding at a rapid rate. According to an article by John Koetsier, a Senior Contributor to Forbes, the space industry is valued at over $4 trillion, with over 10,000 companies vying for market space (Koetsier, 2021). In this article, Koetsier illustrates how the real money in these space market ventures is in communication. A decent source that Koetsier uses in his article for tracking the space technology market is SpaceTech Analytic, which tracks overall investments in space technology and captures the market space from multiple angles (Deep Knowledge Analytics, 2021). This dashboard reveals the trends in monetary value of space technology markets, which can allow for targeted marketing by Booz Allen Hamilton, as well as illustrate how lucrative making a space technology play is today.

Take for instance SpaceX's Starlink which is set to introduce easy access to broadband internet for anyone on Earth. According to an article in PCMag, as of May 2021 over 500,000 people have pre-ordered Starlink. (Kan, 2021) We mention this as one example of how fast the space industry is expanding into various market sectors, and particularly in the communications industry. Space-based communication technology is nothing new, however, the seemingly large shift to space-based technologies is reaching a fever pitch as many companies vie for top spots.

The global space economy rose to $447 billion in 2020 (Space Foundation Editorial Team, 2021) which is seeing a continuing trend of growth over the last 5 years. Traditionally, this market space has been dominated by government spending (and still is), but with the explosion of the commercial space industry the market is gaining new access to this frontier. For instance, a new exchange-traded fund was introduced in 2019 (titled appropriately "UFO") that included 30 companies to give everyday investors a way to invest their money in this new commercial space market (Sheetz, 2019). The appearance of ETF's signal that the private market is breaking into this space and as such we will see the market cap many companies making space-based technology plays. In fact, given that this ETF was introduced in 2019, we've actually seen this increase as the private sector becomes a larger player.

These funds are a nice snapshot of the major players that are positioned to make moves within the space-based technology market. Of the two major ETFs that are focused on space, Procure Space (UFO) and ARK Space Exploration & Innovation (ARKX), some of Booz Allen Hamilton's major competitors within aerospace are listed. In Procure Space's ETF, Northrop Grumman, Lockheed Martin, and Raytheon are all listed. This is all brought up as a means to elucidate the fact that the new space race is private and our competitors are already being included in funds that allow common, everyday investors to buy in. Being that our invention is exploring network communication for space-based platforms as well as potentially deep-space (beyond the Moon's orbit) applications, it falls within the domain of the space market being discussed. The bottom line is that there is a massive interest in new technologies around this sector, and with introduction of ETFs and the increase in attention on space exploration and tourism, now may be the time to start expanding our research and work efforts in this market.

6.3.1: Potential Market Applications

In the book *Inside the Tornado*, the author discusses the behavior of technological markets and how they act different from traditional markets (Moore, 2005). Typically, new technologies exist in hypergrowth markets in which the way a company positions itself determines the success (measured by the market's adoption of said technology) of the company. This can be seen with an example in the standardization of a specific type of networking language, as we see with Cisco and networking communications. Cisco emerged from "the tornado market" (described by Moore in his book) as a major leader and as such became the standard for networking communications. There are other players in the networking game, but Cisco is by far the standard for most government and business ventures that need large-scale networking for their computer systems. The idea for any new emerging technology is to move fast and establish their methods and applications so that integration and use of said technology becomes seen as a standard. With our technology, the idea would be to position our work for use in the exploding private and public space markets as a means to offer potential timing sources for both space and earth-based networks.

6.3.1.1: Where to Focus this Technology

Whereas our technology is very much in its infancy (TRL 3), we can extrapolate where this may be of use by exploring some ideas. The first area of exploration is of course network timing. Keeping a networked timed is incredibly important for communication to work. We can imagine a deep-space spacecraft needing to keep its computer systems timed with networks on Earth, so keeping the same reference time is important. Using pulsars for this provides a means to achieve this regardless of distance between Earth and the spacecraft, or even two separate spacecrafts on deep-space missions. The accuracy needed for this, as discussed in our analysis in Section 5, would need to be incredibly precise (on the order of magnitude of nanoseconds).

However, even without this achievement of accuracy, one could see this technology being adapted in a way to provide an "assisted timing source". This could work similarly to something in use today called Assisted GPS or A-GPS. This is used primarily in cell phones (but sees use elsewhere) as a means to speed up locating your position via our GPS constellation of satellites. For normal GPS location services, what is required is that the location of each GPS satellite being used has to be calculated in order to locate your position on the Earth's surface. The time period needed to find the orbital and timing data of a GPS satellite before it can provide your location is called the Time to First Fix (TTFF). This is usually dependent upon local conditions, in which if they are unfavorable can extend TTFF to be upwards of a few minutes. For cellphones, Assisted GPS is a special piece of technology that uses other signals, such as local cellphone towers, to help locate the phone and as such cutting down on how many satellites are needed to provide an accurate location. This cuts down on the computational time and data transfers that need to happen in order to provide an accurate location.

If we want to expand this idea into a way to calculate a reference time, it may be useful in helping to calculate a reference time faster. Using pulsars as a source to calculate the reference time down to the day or even hour may help save time and processing power for a time server that will only need to worry about calculating from the hour down to the millisecond. This is not something that has been tested, but could be a potential avenue for research and applicability. A-GPS requires a specific chip to be installed in any device wanting to use it, which means our technology may also become integral to any network timing source as a means to provide not only as a backup reference time or an alternate reference time if needing to communicate at vast distances, but also as a means to ease the time of calculation of a local reference time.

Another application for this sort of technology beyond that of space-based usage would be network timing security. As mentioned in Section 2.3.1, having a backup source for a reference time is among the best ways to detect if your system is under attack. Approaching the market from this perspective could enable Booz Allen to supply a way to secure network timing servers so that a system would easily be able to detect if they are the subject of a NTS attack.

6.3.2: Market Competition

As this has been a preliminary investigation into the ability to use actual pulsar data to fit a curve and estimate parameters, we have only started investigating the market landscape around this technology. A patent review has not been completed at the request of Booz Allen Hamilton's legal team to ensure we do not arrive at any legal issues when it comes to the ideas and methods explored throughout this paper. However, we have done a cursory exploration into the market space to identify if this idea has been expressed by any potential competitors. One such company has been identified as having explored this topic with potential market applications and has published a paper as a result.

Aster Labs has explored this topic in the paper *Spacecraft Navigation and Timing Using X-Ray Pulsars* (Sheikh, Hanson, Graven, & Pines, 2011) in collaboration with Cross Trac Engineering Inc, Microcosm Inc, and the University of Maryland. This paper explores the ideas of using pulsars as both navigation and timing sources for various platforms, particularly spacecraft. It would appear that as far as Booz Allen is concerned when it comes to competition, this is the only instance in which we could identify a company that has published any work along the lines of what we are suggesting. In reviewing their paper, they highlight the various needs that would be required for a technology such as the one our patent proposal is suggesting, however they have not gone into any analysis yet. For instance, they discuss using the Time of Arrival of pulse signals from various pulsars, but there is no mention of utilizing a decay curve as a means to provide any reference time calculations either for timing or location. We performed a simple SWOT analysis with respect to the proposed technology and this company in order to identify potential paths forward for Booz Allen. However, further research into their patents would be needed to ascertain further details.

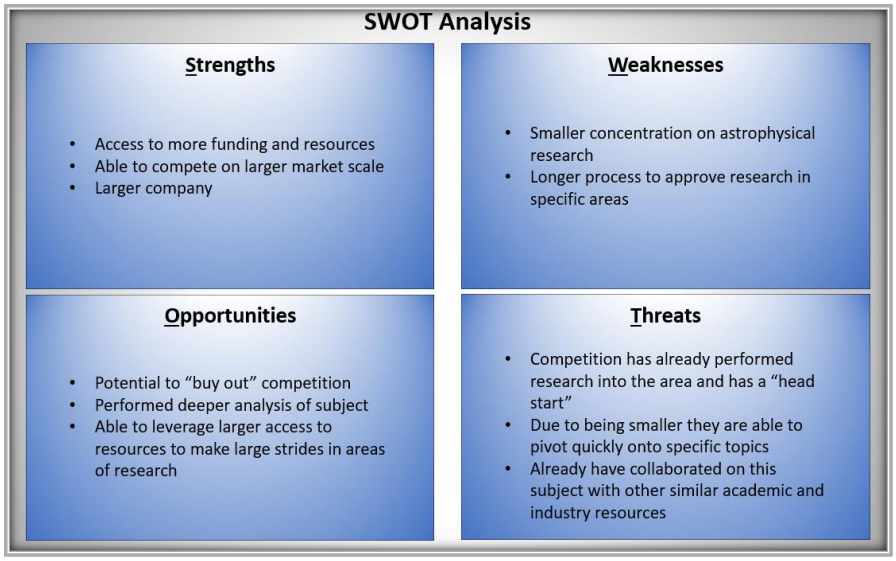

Figure 30: SWOT analysis for Aster Labs

The above SWOT points out some basic ideas behind how we can handle the sort of competition that Aster Labs presents. In particular, we draw our attention to the Opportunities section. This line of reasoning is being presented as a potential outcome for Booz Allen Hamilton to break into the space technology and research. As discussed above in Section 6.3, the space technology market, especially along the lines of commercial application, is very lucrative and is not going anywhere. In fact, as this market expands and access to space becomes more common, we would want Booz Allen Hamilton positioned to take advantage of the wealth available. Technologies such as the one proposed in this paper clearly have been thought about by other players and could work as a "beachhead" research opportunity for a dedicated astronomical research and development division. If Booz Allen decides that this sort of work is a direction they wish to go (even beyond the technology we are performing this analysis for), making a move into a pure R&D division dedicated to space technology would signal the market that we are a contender for future contracts and collaborations.

In reviewing the Aster Labs company, they have dedicated themselves to reselling nano-satellite parts and performing research into future technologies that can be used both on orbital and deep-space platforms. When reviewing press around their company, they have been awarded various governmental contracts, to include a Phase I STTR contract from NASA dealing with satellite swarm localization and control. If this smaller company already has contracts in place with NASA, Booz Allen would immediately gain more visibility for space-based contracts focused around satellites if we moved to collaborate or acquire them, which plays directly into space-based communications. As we mentioned above, communication technology appears to be the primary driver of wealth generation in this market space, so gaining ground in this space could prove lucrative.

All of this is preliminary and much deeper analysis would need to be completed before moving in any given direction. With respect to the invention this paper was written for, it would appear that the work done by Aster Labs would not only be valuable for our research, but complimentary. The principle author for the paper, Suneel Sheikh, has also contributed to textbooks on the topics of GPS and timing, so it would appear that they are a leading expert in topics that would be of interest for this particular

research. Acquiring this level of expertise to continue this research would be incredibly valuable and may help our team make larger strides in pushing this beyond TRL 4.

7: Conclusions

To conclude this research, we will quickly identify the known issues and shortcomings so as to gain a sense of how to move from TRL 3 to TRL 4. The following sections are summaries of the biggest issues our work has revealed that we need to answer in order to advance this idea further, and things we have accomplished during this project.

7.1: Areas Needing Further Research and Development

- Accuracy of predictions for the pulse period
- Accuracy of the reference time predictions
- Better understanding of the physical situation around the pulsars being modeled
- Deeper mathematical analysis around governing equations selected (more generalization and research into pulsar dynamics to justify models used)
- More pulsar data, and data from pulsars with known and/or well-understood parameter values
- Robust datasets that have period measurement accuracy at the nanosecond scale
- Deeper market research around technologies tangential to the one being proposed
- Dedicated research team with access to expertise in fields such as pulsar physics, computational physics, ML/AI experience, mathematical modeling, and GPS/Timing knowledge

The first two points are directly linked, and are the primary focus of our research going forward. These will be heavily dependent on gaining deeper knowledge into pulsar dynamics. The mathematical analysis around our selected governing equation(s) going forward will also follow from deeper research into pulsar dynamics. For instance, our model assumes a variable rotation-radiation angle that provides an extra source for the pulsar to slow. There are other models that assume different physical interactions that also cause them to slow. We may need to employ multiple models, or even build a general model that takes into account all of these interactions. However, the structure and dynamical behavior of pulsars is still an area of active research, so there are assumptions about behavior we are using and making in order to construct our models to align well with the data.

Speaking of the data, as we have mentioned a few times, we are only looking at one pulsar for this initial proof of concept. Not only will we need to expand our pulsar data to include more than one pulsar, we are also happened to select a very “extreme” pulsar in that it is a magnetar with very some strange data structures. Our knowledge around how magnetars behave is still an active area of research as we do not fully understand their dynamics at this time. All of this ties into our points about gaining access to expertise in various areas, stretching from pulsar physics to data analysis. Machine Learning and A.I research would also prove useful as we expand how many pulsars our models are working with. These issues are actually an exciting space to be in, in that we will be working on the edge of known

knowledge, and this may attract various talent pools to try and advance our knowledge in this area. As far as marketing is concerned, we will need to probe deeper into this market space to see where exactly this technology could fit in and gauge interest. The current thought is that we would be targeting "early adopters" and visionaries that invest in gaining more knowledge in areas that will help humanity build a robust society beyond Earth.

7.2: What this Project has Accomplished

- Constructed a Python script to automate the collection, parsing, and tidying of real pulsar pulse period data
- Constructed a script in RStudio that is able to ingest real pulsar data and deliver curves of best fit, decent parameter estimation, and timing predictions.
- Built a mathematical base that justifies our logic, as well as provides a place to continue research from that will help guide our decisions
- Identify general market trends for the market space this technology would play in
- Identify potential competition from other commercial sources that have done similar research
- Identify solutions for said competition that may prove lucrative for Booz Allen Hamilton

When we first started this project, the idea behind using a pulsar for a reference timing source was conceptual. We have now put that idea into action with real pulsar data and as a result we have achieved the first two points above. During this process, it was required that we do our mathematical "due diligence" to identify a governing equation, justify it physically, and then mathematically work with it to ensure it can handle the data we were collecting. This produced a new equation that was generalized for the braking index, and also spawned a way to estimate a braking index while using independent parameter estimates and pulse period measurements. These are good starting points for future model exploration in that we now know what to look for and have base scripts to build off of that didn't exist prior to beginning this project.

As mentioned in 7.1, we have taken a first look at the market that this technology would play a role in and it looks promising. Whereas we have identified that Booz Allen doesn't have a large foothold in pure space-based technology, this technology may provide that. We have found minor competition for technology that appears tangential or even complimentary to what we are proposing, which has presented us a potential opportunity in allowing Booz Allen to announce its presence within this market space. These are, of course, suggestions for how to proceed as further market analysis from the appropriate experts Booz Allen employs would be necessary to determine if this is a move we would want to make. This move could include expanding our research time to include pulsar physics experts, navigation and timing experts, ML/AI-fluent people, and a market research team. Either way, there does appear to be a market interest in technology such as this that already has a player on the field. However, with the resources Booz Allen has available and our work on this project, we have a good opportunity to develop this further.

7.3: Final Thoughts

Overall, this initial analysis and its results are promising in that they have allowed our team to advance this idea past a conceptual phase. We have begun to build a strong theoretical and mathematical base to work from and advanced our knowledge quite a bit. This has more clearly identified areas that need further work, which has in turn given us a stronger direction to proceed in. Knowing what you don't know is much better than not knowing what you don't know. During the preliminary market research, we discovered this is an area of interest by other researchers, which also lends credence to our idea, if only in the sense that there may be a market demand for such a technology. As humanity expands into the solar system and the commercial space industry continues to grow, the need for new technologies, methods, and knowledge will also increase. Timing for communication networks in deep space, or the ability to position a group of satellites that aren't within line-of-sight with Earth will assuredly begin to reveal itself as a necessity. Positioning Booz Allen Hamilton to be at the forefront of that research and providing solutions for these future technologies would not only benefit the company, but benefit humanity as we seek to move beyond Earth.

References

1.65. (2021). Retrieved from ATNF Pulsar Catalogue: https://www.atnf.csiro.au/research/pulsar/psrcat/

Archibald, R. F., Gotthelf, E. V., Ferdman, R. D., Kaspi, V. M., Guillot, S., Harrison, F. A., . . . Tomsick, J. A. (2016, March 01). A high braking index for a Pulsar. *The Astrophysical Journal Letters, 819*(1), 1-5. doi:10.3847/2041-8205/819/1/L16

Archibald, R. F., Kaspi, V. M., Ng, C. -Y., Gourgouliatos, K. N., Tsang, D., Scholz, P., . . . Kennea, J. A. (2013, May 29). An anti-glitch in a magnetar. *Nature*, 591-593. doi:10.1038/nature12159

Arora, P., Awasthi, A., Bharath, V., Acharya, A., Yadav, S., Agarwal, A., & Gupta, A. S. (2014, Februrary 19). Atomic Clocks: A brief history and current status of research in India. *Pramana*, 173-183. doi:10.1007/s12043-014-0709-6

Basu, A., Char, P., Nandi, R., Joshi, B. C., & Bandyopadhyay, D. (2018, October 20). Glitch Behavior of Pulsars and Contribution from Neutron Star Crust. *The Astrophysical Journal*. doi:10.3847/1538-4357/aaddf4

Bates, S. D., Lorimer, D. R., Rane, A., & Swiggum, J. (2014, January 17). PsrPopPy: An open-source package for pulsar population simulations. *Monthly Notices of the Royal Astronomical Society*, 2893-2902. doi:10.1093/mnras/stu157

Burnicki, M. (2019, Februrary 27). Time Service Jamming, Spoofing, and Holdover. *Meinberg Knowledge Base*. Retrieved from https://kb.meinbergglobal.com/kb/time_sync/time_service_jamming_and_spoofing

Camilo, F., Ransom, S., Halpern, J., & Reynolds, J. (2007, July 31). 1E 1547.0-5408: A Radio-emitting Magnetar with a Rotation Period of 2 Seconds. *The Astrophysical Journal*. doi:10.1086/521826

Deep Knowledge Analytics. (2021). *SpaceTech Analytics*. Retrieved from https://www.spacetech.global/dashboard

Goward, C. D. (2016, April). Now Hear This - 'Misnavigation' or Spoofing? *U.S. Naval Institute, 124*(4). Retrieved from https://www.usni.org/magazines/proceedings/2016/april/now-hear-misnavigation-or-spoofing

Hamil, O., Stone, J., Urbanec, M., & Urbancova, G. (2015, March 19). Braking index of isolated pulsars. *Phsyical Review D, 91*(6), 063007. doi:10.1103/physrevd.91.063007

Han, J., Manchester, D., & van Straten, W. (2007, October). (2011): Parkes observations for project P236 semester 2007OCTS.v2.CSIRO.Data Collection. doi:10.4225/08/51EE81874E1CE

Hartnett, J. G., & Luiten, A. N. (2011, January 07). Colloquium: Comparison of Astrophysical and Terrestrial Frequency Standards. *American Physical Society: Review of Modern Physics, 83*(1). doi:10.1103/RevModPhys.83.1

Hobbs, G. B., Edwards, R. T., & Manchester, R. N. (2006, May 26). Tempo2, a new pulsar-timing package - I. An overview. *Monthly Notices of the Royal Astronomical Society, 369*(2), pp. 655-672. doi:10.1111/j.1365-2966.2006.10302.x

Horton, E., & Ranganathan, P. (2018). Development of a GPS spoofing apparatus to attack a DJI Matrice 100 Quadcopter. *Journal of Global Positioning Systems*. doi:10.1186/s41445-018-0018-3

Igoshev, A. P., Popov, S. B., & Hollerbach, R. (2021, September 20). Evolution of neutron star Magnetic Fields. *Universe, 7*(9), 351. doi:10.3390/universe7090351

Jespersen, J., & Fitz-Randolph, J. (1999). *From Sundials To Atomic Clocks.* National Institute of Standards and Technology. Retrieved from https://nvlpubs.nist.gov/nistpubs/Legacy/MONO/nistmonograph155e1999.pdf

Kan, M. (2021, May 04). SpaceX: Over 500,000 People Have Placed Orders for Starlink. *PCMag*. Retrieved from https://www.pcmag.com/news/spacex-over-500000-people-have-placed-orders-for-starlink

Khalajmehrabadi, A., Gatsis, N., Akopian, D., & Taha, A. F. (2018, August). Real-Time Rejection and Mitigation of Time Synchronization Attacks on the Global Positioning System. *IEEE Transactions on Industrial Electronics, 65*(8), 6425-6435. doi:10.1109/TIE.2017.2787581

Khan, S. Z., Mohsin, M., & Iqbal, W. (2021, May 06). On GPS spoofing of aerial platforms: a review of threats, challenges, methodologies, and future research directions. *PeerJ Computer Science*. doi:10.7717/peerj-cs.507

Koetsier, J. (2021, May 22). Space Inc: 10,000 Companies, $4T Value... And 52% American. *Forbes*. Retrieved from https://www.forbes.com/sites/johnkoetsier/2021/05/22/space-inc-10000-companies-4t-value--and-52-american/?sh=7f62e81055ac

Lasky, P. D., Cristiano, L., Rowlinson, A., & Glampedakis, K. (2017, June 23). The Braking Index of Millisecond Magnetars. *The Astrophysical Journal Letters*. doi:10.3847/2041-8213/aa79a7

Lin, L., Gogus, E., Baring, M., Granot, J., Kouveliotou, C., Kaneko, Y., . . . Gehrels, N. (2012, August 14). Broadband Spectral Investigations of SGR 1550-5418 Bursts. *The Astrophysical Journal, 756*(1). doi:10.1088/0004-637X/756/1/54

Lorimer, D., & Kramer, M. (2005). *Handbook of Pulsar Astronomy.* Cambridge: Cambridge University Press.

Manchester, D., Ord, S., Berbiest, J. P., Sarkissian, J., Hobbs, G., Kesteven, M., . . . van Straten, W. (2007, April). (2011): Parkes observations for project P456 semester 2007APRS. v2. CSIRO. Data Collection. doi:10.4225/08/5211D08B64F07

Manchester, R. N., Hobbs, G. B., Tech, A., & Hobbs, M. (2005, April). The Australia Telescope National Facility Pulsar Catalogue. *The Astronomical Journal, 129*(4), 1993-2006. doi: 10.1086/428488

Mills, D. (1989). Internet Time Synchronization: The Network Time Protocol. doi:10.17487/RFC1119

Moore, G. A. (2005). *Inside the Tornado.* HarperCollins Publishers.

Price-Whelan, A. M., Sipocz, M. M., Gunther, H. M., Lim, P. L., Crawford, S. M., Conseil, S., . . . Astropy Contributors. (2018, September). The Astropy Project: Building an Open-science Project and Status of the v2.0 Core Package. *The Astronomical Journal, 156*(3), 19. doi:10.3847/1538-3881/aabc4f

Robitaille, T. P., Tollerud, E. J., Greenfield, P., Droettboom, M., Bray, E., Aldcroft, T., . . . Streicher, O. (2013, September 30). Astropy: A community Python package for astronomy. *Astronomy and Astrophysics, 558*. doi:doi.org/10.1051/0004-6361/201322068

Rowlatt, J. (2014, October 04). Caesium: A brief history of timekeeping. *BBC News*. Retrieved from https://www.bbc.com/news: https://www.bbc.com/news/magazine-29476893

Ryden, B., & Peterson, B. (2010). *Foundations of Astrophysics.* San Francisco, California, United States: James Smith.

Sheetz, M. (2019, April 24). Debut of 'UFO' ETF gives invesotrs another way to invest in the growing space industry. *CNBC*. Retrieved from https://www.cnbc.com/2019/04/20/how-to-invest-in-space-companies-ufo-etf-adds-another-way.html

Sheikh, S. I., Hanson, J. E., Graven, P. H., & Pines, D. J. (2011). *Spacecraft Navigation and Timing Using X-ray Pulsars.* Retrieved from https://www.asterlabs.com/publications/2011/Sheikh_et_al,_ION_Navigation_2011.pdf

Space Foundation Editorial Team. (2021, July 15). Global Space Economy Rose To $447B In 2020, Continuing Five-Year Growth. *Space Foundation*. Retrieved from https://www.spacefoundation.org/2021/07/15/global-space-economy-rose-to-447b-in-2020-continuing-five-year-growth/

van Eysden, C. A., & Melatos, A. (2010, December 11). Pulsar glitch recovery and the superfluidity coefficients of bulk nuclear matter. *Monthly Notices of the Royal Astronomical Society, 409*(3), 1253-1268. doi:10.1111/j.1365-2966.2010.17387.x

Appendix A

Official Patent Proposal

PATENT PREPARATION DOCUMENT:

RTFP

A SYSTEM AND METHOD FOR DERIVING REFERENCE TIME FROM PULSARS' ROTATIONAL DECAY

PRINCIPAL AUTHOR: WILLIAM MACLEOD
SUPPORTING AUTHOR: JAMIE TER BEEST
SUPPORTING AUTHOR: GIDEON BASS

EXECUTIVE SUMMARY / INVENTION BACKGROUND

The invention determines reference time at high precision without input from human sources. Reference time is determined by adding units of time, such as seconds or days, to a communally agreed upon reference point. In common usage this can be a date-time group such as 11:06 PM EDT, June 7th, 2018. In order to configure a new clock to maintain the communally agreed upon reference time, the new clock must be set to the same time as a previously configured clock that holds that reference time. If a clock loses its reference time, as happens when it loses power, it needs to be resynchronized with a clock that still has the communally agreed upon reference time.

This invention removes the requirement for a second clock, with which to resynchronize reference time when it is lost, by observing the rotational decay of one or more pulsars. Pulsars are a special class of neutron star that emit a rotating beam of electromagnetic radiation that is observable as a series of pulses. The beam rotates at a very stable rate making it suitable for maintaining the time of a clock. While the rate of rotation does decay, it does so at a very slow and very predictable rate. By knowing the rate at which one or more pulsars rotated at a communally agre ed upon date-time group, and the rate at which those pulsars' rotation decays, an observer can determine the date time group of an observation made of a pulsar by calculating the pulsar's current rate of rotation. This invention is useful for spacecraft that have lost reference time and are too far from other previously configured clocks to resynchronize their clock with reference time.

INVENTION DETAILS TECHNICAL PROBLEM

For a technical system to know the present date and time it requires two things: a clock that correctly increments the date and time forward in sync with the communally recognized progression of time, and a communally agreed upon reference point upon which to increment the time. In the mundane case this can be accomplished by setting the time of one clock (e.g. a wrist watch) to the to that of a clock with

known-good reference time (e.g. a clock tower). In this case, the watch and the clock tower both increment their seconds hand at the same rate, and beginning when the watch's time was synchronized with the clock tower's, their clocks will read the same reference time. In more advanced information systems this can be accomplished by directing a client system to a Network Time Protocol (NTP) server which will provide the correct reference time to the client system's clock. In each case, a clock that does not carry the correct reference time must have access to a clock that does in order to receive and maintain the correct reference time.

In situations where access to a clock with known-good reference time is not possible, this task presents a problem. Examples of these situations could be a spacecraft that has lost power for an unknown period of time and upon powering back on needs to resynchronize reference time. Another example could be a GNSS client that suspects itself the victim of a time spoofing attack and requires an alternative source of reference time with which to synchronize its clock.

SOLUTION TO THE PROBLEM

The solution to this problem is to identify a source of reference time that is not maintained by a manmade clock, that is accessible from remote locations, and is difficult to spoof. The source identified by this invention is a type of rotating neutron star called a pulsar.

All stars have a lifespan within which they consume matter as fuel in fusion reactions and release energy. When their fuel is expended, they reach the end of their lifespan and they can die in different ways depending on their size. Smaller stars turn into dwarf stars and simply radiate off their remaining energy without producing any more through fusion. Larger stars collapse into black holes. Between these two extremes lies a third option, wherein the star's gravity is enough to compress its constituent protons and electrons into neutrons, but not enough to create the singularity characteristic of a black hole, the resultant object is called a neutron star. A neutron star is considerably denser than the star that created it and consequently has a smaller radius. Through the conservation of angular momentum, this translates to a much higher rotational speed. Although most of the neutron star's matter is electrically neutral, what charge remains is moving very fast and creates very powerful magnetic fields which eject matter from the fields' poles at very high energy, creating beams of electromagnetic radiation. If these magnetic poles are on a different axis from the neutron star's axis of rotation, the beams will rotate in a cone shape. An observer on or near one of these cones will observe the beam of radiation only when the beam passes over them, which will appear as though the neutron star is blinking or pulsing, hence the name pulsar.

Because there is very little friction in space to slow their rotation, pulsars maintain the periodicity of their pulsing very well. This makes them very good for time applications and there are examples of pulsar clocks using the stable periodicity of pulsars to maintain timing. Pulsars do however slow down over time at rate that is dependent on their age. By modeling this decay as a function of time from a communally agreed upon reference, an observer can use a measurement of a pulsar's rotational period to infer the time. The observer can improve the precision of their inference by taking measurements from multiple pulsars for which they have modeled decay functions.

RTFP DETAILED PROCESSES

The first component of the invention is the Database of known pulsars containing the Coordinates and Decay Function for each pulsar. The Database is periodically updated by the Decay Function Processor to provide new Decay Functions for known Pulsars, and by the Time Processor to provide the last known pulse rate. The Database communicates the coordinates for each pulsar to the Orientation Unit to direct the one or more sensors toward the pulsar it is attempting to observe. The Database also communicates the Decay Function to the Time Processor to calculate the reference time for a given measured pulse rate.

The second component of the invention is a high-precision clock used to increment the measured reference time and the estimated reference time with units of time, e.g. seconds or milliseconds. This clock could be implemented as a chip-scale atomic clock or as a pulsar clock, observing the pulses of pulsars with very little rotational decay.

The third component of the invention is a set of one or more sensors to detect the electromagnetic radiation emissions of a pulsar. Pulsars emit electromagnetic radiation across multiple bands, so the type of sensor may vary based on the type of radiation being observed and pulsar being measured for time data. Examples of sensors could be an antenna for detecting pulsar emissions in the radio spectrum or a camera to detect emissions in the optical spectrum. The sensor is connected to a subsystem for orienting the sensor toward the pulsar to maximize antenna gain in the received signal. This orientation can be implemented physically through the use of a gimbal or implemented in software as in a phased-array antenna. The sensor orientation unit receives the coordinates for each pulsar from the Database and can optionally correct for the relative motion of the pulsar to the sensor.

The fourth component of the invention is a signal processor that isolates the signal of the pulsar from noise, such as background radiation, and interference, such as other emitters operating in the same frequency as the observed pulsar. The method for isolating the pulsar's signal is implementation-specific, but in general, the signal processor begins with a low-pass filter to remove all noise above the observed signal's frequency. It then down-modulates the signal to a frequency more manageable by hardware, typically the baseband but some implementations may include a phased demodulation scheme through an intermediate frequency. It can then send the signal through a band-pass or low-pass filter, depending on the demodulation scheme, to further isolate the pulsar signal from other sources of radiation. It can then optionally increase the signal strength further, by passing the signal through a frequency-dependent, time-only filter to mitigate the effect of pulse dispersion caused by differing arrival times of a pulse's various frequency components. It then folds the pulsar's signal at the frequency of the pulsar's rate of rotation to generate a running average or pulse profile of the pulsar. The initial value for the pulsar's rate of rotation can be pulled from the Database's record of the pulsar's last known pulse rate, or by direct measurement of two pulses in the signal. To determine the current rate of rotation, the signal processor varies the frequency over which the signal is folded in small increments. Small changes in this frequency will result in changes to the strength of the folded signal, maximizing the signal strength at the pulsar's exact frequency of rotation.

The fifth component of the invention is the Time Processor which takes each pulsar's frequency of rotation, measured by the Signal Processor, and uses it to determine the current reference time. It does this by maintaining a set of Decay Functions in the Database that each represent the rate of decay for a

particular pulsar over time. These functions can be initially seeded by human observations, but over the life of the system, the Decay Function Processor establishes new functions. By solving the function for the measured frequency of rotation, the Time Processor can calculate the reference time at which the measurement was taken. The Time Processor maintains rotational Decay Functions for multiple pulsars monitored by the invention and averages their calculated reference time. The more pulsars the system is able to observe, the more precise the measurement of reference time becomes and the more efficient the Glitch Processor can detect spin-up events. This averaged reference time is provided to any client system that requires it.

The sixth component of the invention is the Glitch Processor that detects changes in a pulsar's rate of rotation that are not accounted for by the mathematical Decay Function used by the Time Processor to predict the decay of the pulsar. While the exact mechanism of these glitches is not well understood and we are not able to predict them, their effect on the rate of rotation is obvious enough that we can detect them and respond. When a glitch occurs in a pulsar, its Decay Function is no longer valid for measuring reference time and so must be re -baselined. The method for identifying a glitch is implantation-specific, but an example would be for the Database to provide the individual reference times of each pulsar to the Glitch Processor, which would calculate the standard deviation of the individual reference times. If a particular pulsar's reference time is outside of a configurable number of standard dev iations from the average, the pulsar is assessed to have experienced a glitch and its rotational Decay Function is flagged to be re-baselined by the Decay Function Processor.

The seventh component of the invention is the decay function processor. When the Glitch Processor identifies that a Decay Function is no longer valid for a given pulsar, it directs the Decay Function Processor to generate a new one. As collecting enough measurements to plot a curve of best fit for the Decay Function may take a while, the Glitch Processor can flag the pulsar in the Database to be excluded from Time Processor's calculations of average reference time. This flag can be removed when the re-baselined Decay Function has been established. The Decay Function Processor receives pulse profiles and the frequency of rotation from the signal processor for the identified pulsar. It uses these measurements to predict a new function that describes the decay of the pulsar. The method of predicting a new Decay Function is implementation specific, but the general procedure would be to accumulate data over a period of time that correlates the pulsar's measured frequency of a rotation to the Time Processor's estimated reference time when the measurement was taken. When enough data is accumulated to plot a curve of best-fit, the new Decay Function for the pulsar is written to the Database. The precision of the Decay Function increases with the quantity of data collected and the period of time over which the data was collected.

ADVANTAGES OF THE INVENTION

The invention provides highly reliable reference time without requiring resynchronization with the communally recognized reference time after initiation. It also allows clocks to recover reference time automatically after losing it. Its sources for reference time are numerous and uniquely challenging to spoof or jam. It is scalable in that the precision of reference time can be improved by incorporating observations of as many pulsars as the system can locate and manage in its database. Increasing the number of pulsars used to derive reference time also benefits the security of the provided data, in that pulsar radiation can be highly direction. The time resilience created by this invention has applicability in very remote use cases and very secure use cases.

APPLICABILITY OF THE INVENTION

Use invention has applicability in remote and secure time systems. In the remote use cases, spacecraft are a natural beneficiary of this capability. Such spacecraft might reasonably lose reference time as a result of powering off for extended periods of time. A spacecraft far enough from earth to make re-establishing reference time from a terrestrial clock would need an alternative source. Since pulsars are so numerous it is difficult to imagine a location in space where the spacecraft could not readily find as many as are necessary to re-establish reference time. Nearer in, a satellite system is close enough to receive reference time from terrestrial clocks, but for critical systems this process must be hardened against attack. A satellite implementing this invention would not need to orient its antenna toward earth or other satellites, where interference or spoofed signals might originate. It would instead point away from these potential sources and could further mitigate their associated risk by making use of the pulse signal in the higher spectrum. BRIEF

DESCRIPTION OF THE DRAWINGS

Figure 1: An Observer Receiving Pulsar Radiation as the Cone Rotates– This diagram shows the offset between a pulsar's axis of rotation and its magnetic poles. As the pulsar rotates, its magnetic poles revolve around the axis, changing the direction of the pulsar's cone of radiation. The observer receives the pulse of radiation only when it is within the cone. When the observer is outside the code, the observer receives the lull between pulses.

Figure 2: Subsystems of the Reference Time from Pulsars System– This diagram shows the component subsystems of the RTFP System and their logical interconnections.

Figure 3: Flow Diagram of the Reference Time for Systems Method- The diagram shows the sequence of events for the RTFP Method

Figure 4: Received Pulsar Radiation Expressed as a Function of Signal Strength over Time– The diagram shows a notional stream of received Pulsar Radiation distorted by noise. Within the stream, discreet pulses are discernable, but the pulse profile is distorted.

Figure 5: Folding Received Pulsar Radiation over the Pulse Period to Establish a Pulse Profile– The diagram shows a high-level explanation for how a pulse profile is established. The received signal is folded over its pulse period and normalized. The resultant pulse profile mitigates the distortion of noise and allows the observer to work with a more stable received strength value than any single pulse could provide.

Figure 6: Maximizing Signal Strength of the Pulse Profile by Folding on the Pulse Period– The diagram shows how changing the period over which the signal is folded changes the established pulse profile. The pulse profile's signal strength is optimized when it is folded over the pulse period. When it is folded over a longer or shorter period, the pulse's signal is spread out over a wider period of time.

Figure 7: Solving a Pulsar's Decay Function for a Measured Pulse Period– This diagram presents a notional decay function for a single pulsar, in which reference time progresses forward as the pulse period increases. The red lines indicate a point on the function for which the reference time is calculated for measurement of the current pulse period.

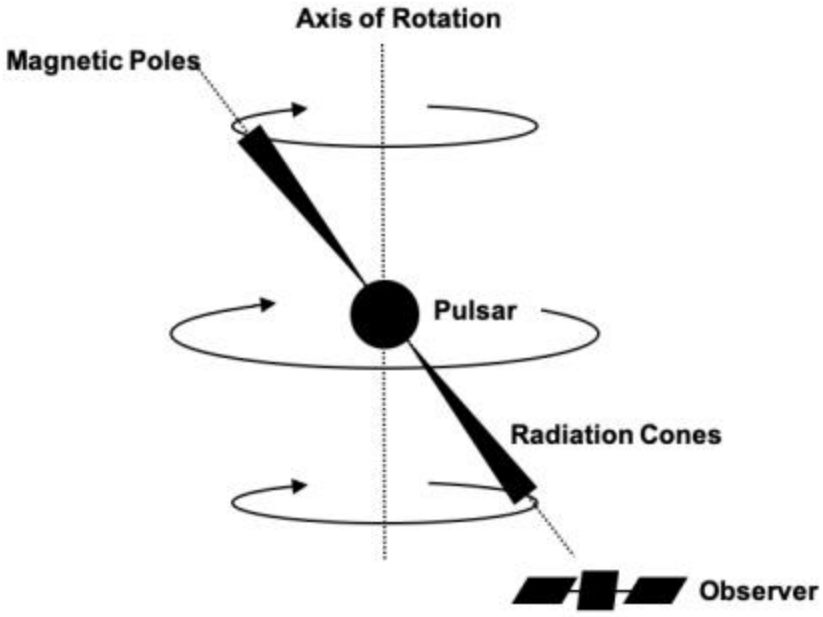

Figure1: An Observe Receiving Pulsar Radiation as the Cone Rotates

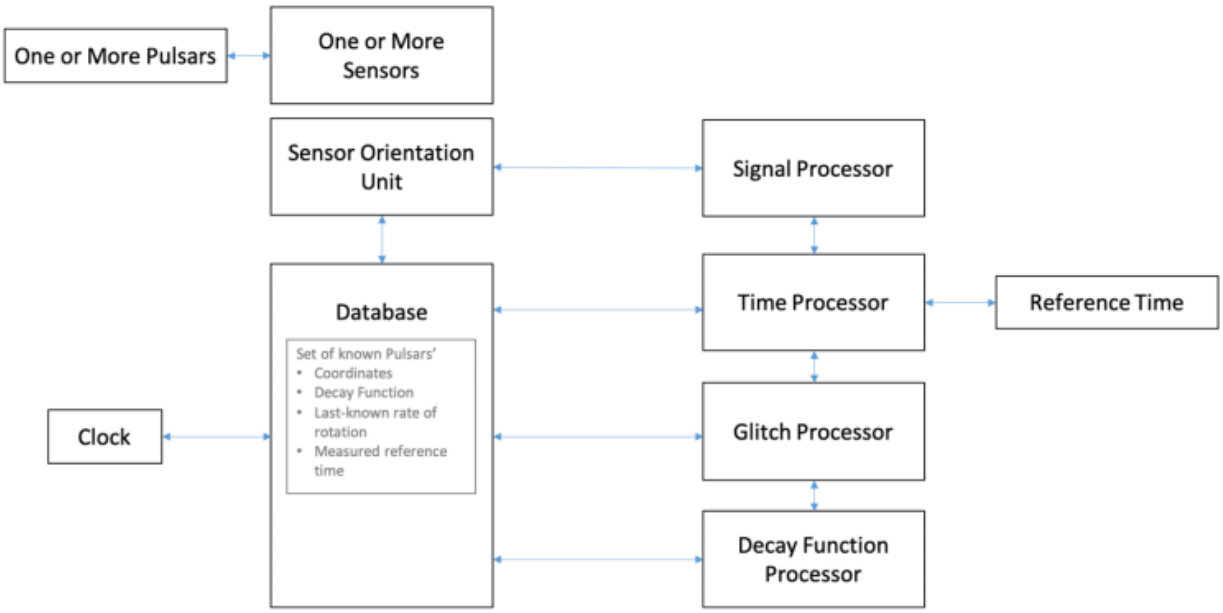

Figure2: Subsystems of the Reference Time from Pulsar System

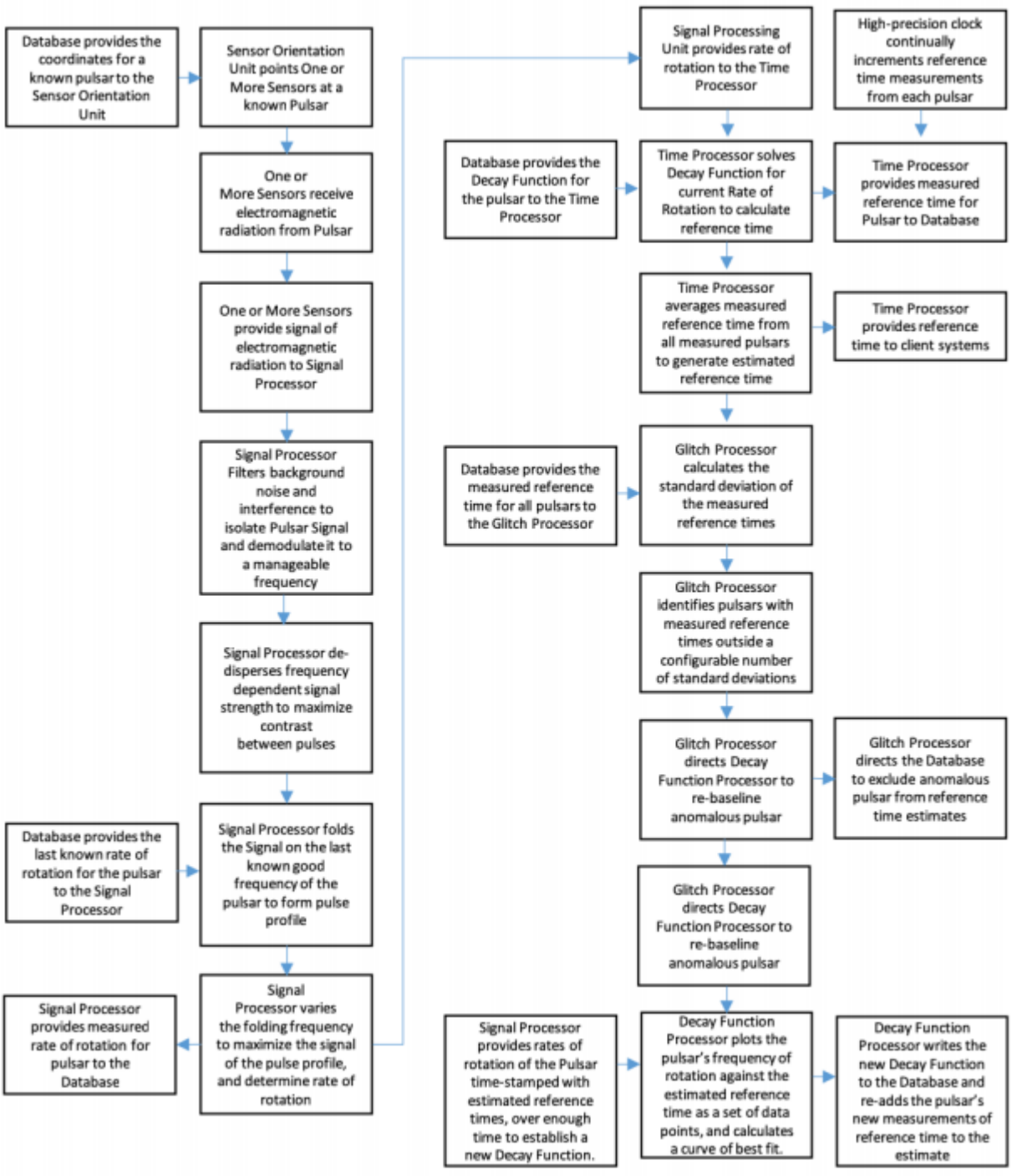

Figure 3: Flow Diagram of the Reference Time for Systems Method

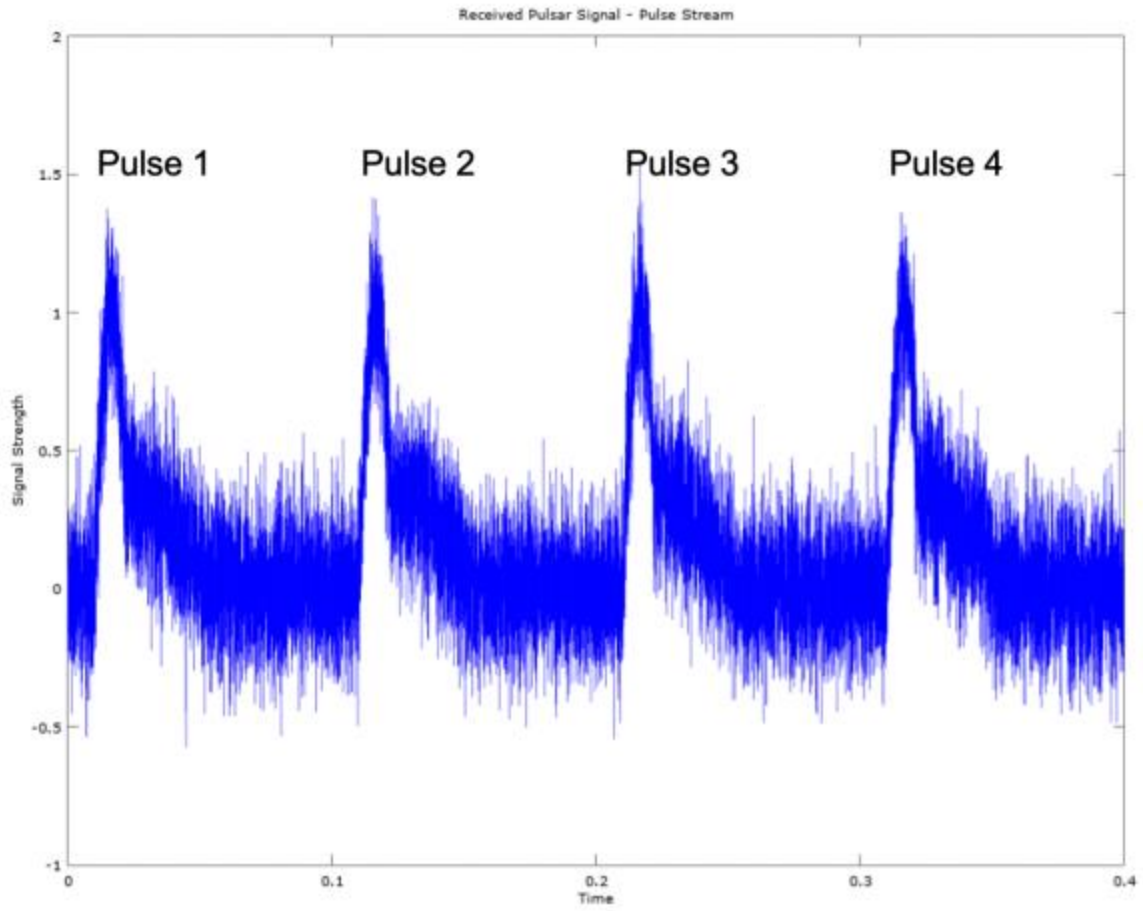

Figure 4: Received Pulsar Radiation Expressed as a Function of Signal Strength over Time

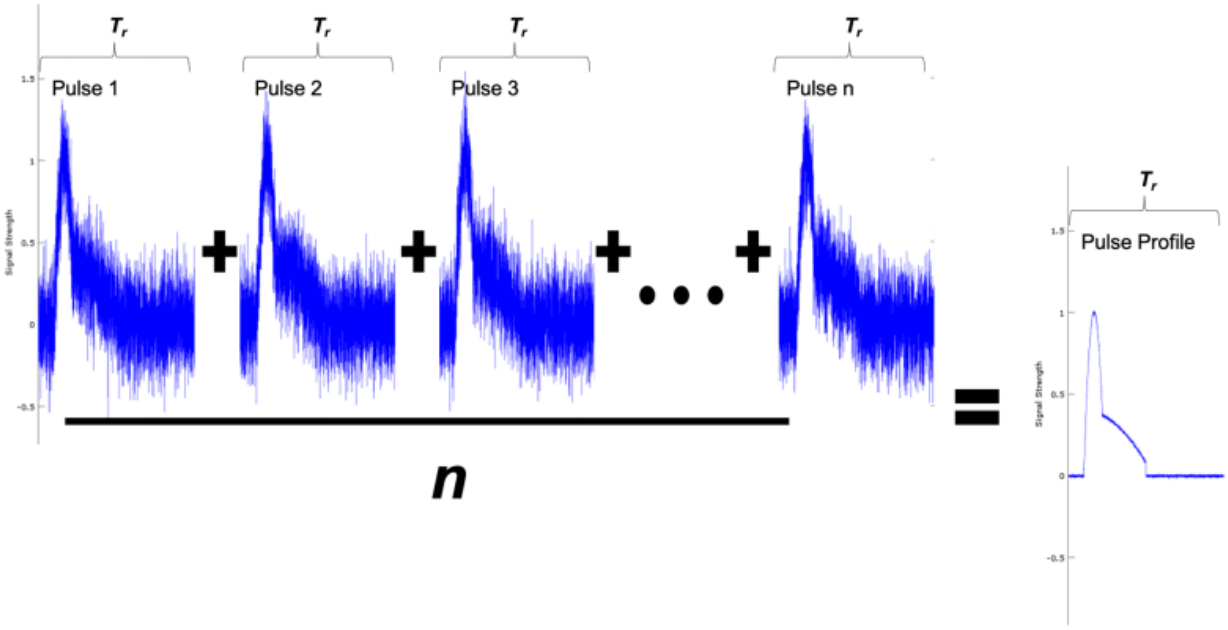

Figure 5: Folding Received Pulsar Radiation over the Pulse Period to Establish a Pulse Profile

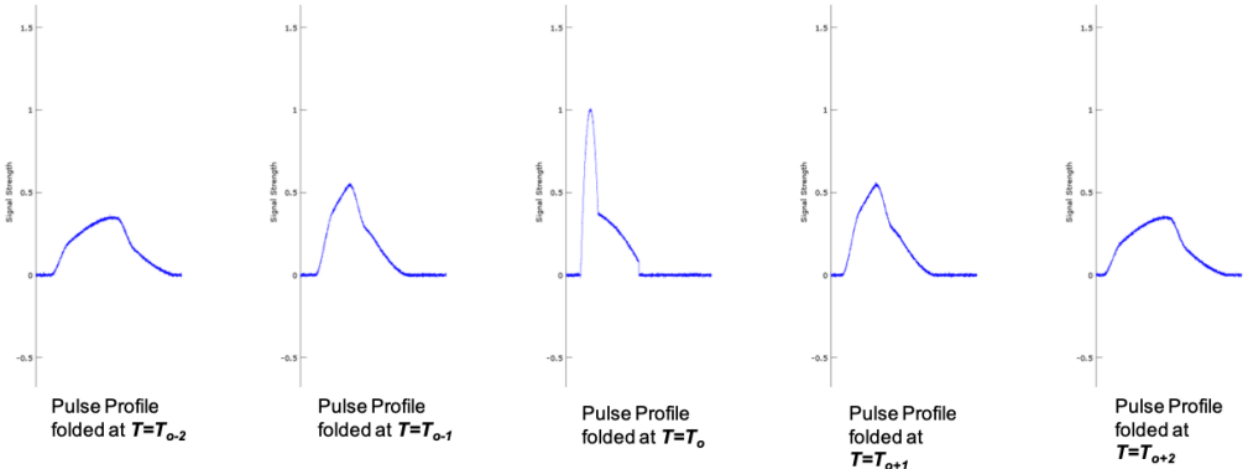

Figure 6: Maximizing Signal Strength of the Pulse Profile by Folding on the Pulse Period

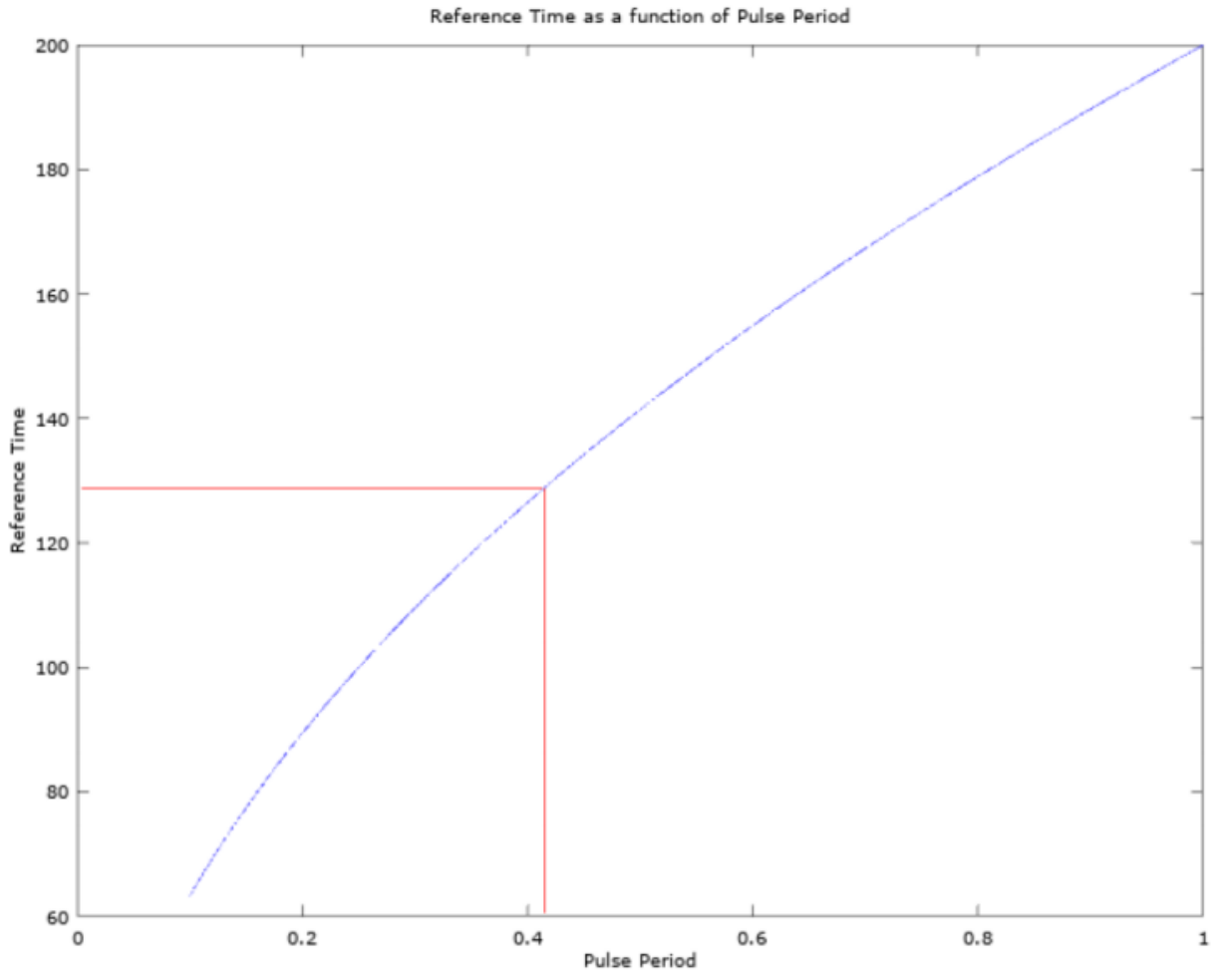

Figure 7: Solving a Pulsar's Decay Function for a Measured Pulse Period

Appendix B

Python Script for Data Collection and Parsing

```
import json

import openpyxl
import requests
import datetime
import os

from astropy.io import fits
from openpyxl import Workbook
from openpyxl.chart import (
    ScatterChart,
    Reference,
    Series,
)

pulsar_name = input("Which Pulsar would you like to query the database for?\n")



#####       Query the database for a collection with this pulsar
base_of_api_url =
"https://data.csiro.au/dap/ws/v2/domains/pulsarObservations/search?observationMode=Al
l%20without%20calibration%20files&p=1&pulsarName="
end_of_api_url = "&rpp=1000&showFacets=false&so=ASC"
api_url_for_pulsar = base_of_api_url + pulsar_name + end_of_api_url
headers = {"Accept": "application/json"}
r = requests.get(api_url_for_pulsar, headers=headers)
print(r.url + "\n")
result_page = r.json()
files = result_page.get("files")
# print(json.dumps(files,indent=2))
downloadable_files = len(files)
files_to_download = input(
    "There could be as many as {} files to download.  How many would you
like?\n".format(downloadable_files))
# files_to_download = 50 ###################REMOVE
if files_to_download == '':
    files_to_download = downloadable_files
else:
    files_to_download = int(files_to_download)
files_downloaded = 0

##### Making Directory to store files
parent_dir = 'Pulsar Data/'
folder_path = parent_dir+str(datetime.datetime.now()).replace(' ','-
').replace(':','.')
print("Making new directory:  " + folder_path)
os.mkdir(folder_path)
download_base_url = 'https://data.csiro.au/dap/ws/v2/collections/'
download_file_url = '/downloadfile?fileName='
```

```
#### Cycle through the downloadable files to download them all
for file in files:
    if (float(file.get('fileSize')) <= 1000000.0) and (str(file.get('mountStatus'))[
                                                       1:] == 'rue'):  ### the first
character of the mountStatus is sometimes capitalized
        try:
            file_name = file.get('filename')
            file_path = file.get('filepath')
            data_collection_id = file.get('dataCollectionId')
            files_downloaded += 1
            #            print("found one")
            full_download_url = download_base_url + str(data_collection_id) +
download_file_url + str(
                file_path).replace('/', '%2F')[3:]
            g = requests.get(full_download_url)
            print(full_download_url)
            open(folder_path + '/' + file_name, 'wb').write(g.content)
        except:
            print("Found a bad egg.")
    else:
        print("Found a bad egg.")
    if files_downloaded >= files_to_download:
        break
print("Only {} files might be useful.\n".format(files_downloaded))

##############################################################################################
########   Switching over to the extraction task
##############################################################################################


# This section generates an array of all of the FITS files by filepath, so that later
on, we can open them up what at a time
list_of_files = []
for roots, dirs, files in os.walk(folder_path):
    for x in files:
        if x.endswith(
                '.FTp'):  # We may need to revisit this if we want to start looking
at file extensions other than .FTp
            list_of_files.append(os.path.join(roots, x))
print(list_of_files)  # This is an array of filepaths to the FITS (.FTp) files
print(len(list_of_files))  # This is how many FITS files you have

# This section opens an Excel doc
wb = Workbook()
ws = wb.active
excel_row = 2

# This section cycles through all of the FITS files and pulls out the Pulsar Name
(SRC_NAME), Date-Time Group of the Observation (DATE-OBS), and Pulse Frequency (F)
ws['A1'].value='Pulsar J-Name'
ws['B1'].value='Time'
ws['C1'].value='Frequency (1/s)'
ws['D1'].value='Frequency Derivative'
ws['E1'].value='Project ID'
ws['F1'].value='Front End'
```

```
ws['G1'].value='Back End'
ws['H1'].value='BE Config'
ws['I1'].value='Observation Frequency'
ws['J1'].value='Pulse Period'


for each_file in list_of_files:
    try:
        print(each_file)
        open_file = fits.open(each_file)
        #        open_file.info()
        print('------------------')
        print('SRC_NAME = ' + open_file[0].header['SRC_NAME'])
        ws['A' + str(excel_row)].value = open_file[0].header[
            'SRC_NAME']  # Sets the value of the worksheet in column A for this row
        print('SRC_NAME = ' + open_file[0].header['SRC_NAME'])
        ws['A' + str(excel_row)].value = open_file[0].header[
            'SRC_NAME']  # Sets the value of the worksheet in column A for this row
        print('DATE-OBS = ' + open_file[0].header['DATE-OBS'])
        dtg_str = open_file[0].header['DATE-OBS']
        year = int(dtg_str[0:4])  # we assume that the laout of the DATE-OBS is
always the same YYYY:MM:DDTHH:MM:SS
        month = int(dtg_str[5:7])
        day = int(dtg_str[8:10])
        hour = int(dtg_str[11:13])
        minute = int(dtg_str[14:16])
        second = int(dtg_str[17:18])
        dtg = datetime.datetime(year, month, day, hour, minute,
                                second)  # Creates a datetime object with the values
we just pulled out.
        ws['B' + str(
            excel_row)].value = dtg  # Sets the value of the worksheet in column B
for this row to the datetime object we just created.
        for x in open_file[2].data.field(
                0):  # There must be a better way of doing this, but this FOR loop
removes the 'F       ' or 'F0          ' at the beginning of the string and removes
the uncertainty value at the end.
            if (x).startswith('F ') or (x.startswith('F0')):
                x = x[2:]  # remove either the 'F ' or 'F0' that precedes each entry
                for y in x:
                    if y == ' ':  # removes all ' ' at the beginning of the string
                        x = x[1:]
                    else:
                        break
                print('F0(x) = ' + x)
                F0 = x
                if ' ' in x:
                    F0 = x[:x.find(' ')]  # cuts off all ' ' and the uncertainty
value in the string
                if 'D' in F0:
                    F0 = F0.replace('D',
                                    'E')  # converts the 'D' to an 'E' so that the
scientific notation is more easily understood by excel or other libraries
                print('F0 = ' + F0)
        ws['C' + str(excel_row)].value = float(
```

```
            F0)  # Sets the value of the worksheet in column C for this row to the
floating point version of the pulse frequency we just isolated.

        for x in open_file[2].data.field(
                0):  # There must be a better way of doing this, but this FOR loop
removes the 'F1       ' at the beginning of the string and removes the uncertainty
value at the end.
            if (x).startswith('F1'):
                x = x[2:]  # remove the 'F1' that precedes each entry
                for y in x:
                    if y == ' ':  # removes all ' ' at the beginning of the string
                        x = x[1:]
                    else:
                        break
                print('F1(x) = ' + x)
                F1 = x
                if ' ' in x:
                    F1 = x[:x.find(' ')]  # cuts off all ' ' and the uncertainty
value in the string
                if 'D' in F1:
                    F1 = F1.replace('D',
                                    'E')  # converts the 'D' to an 'E' so that the
scientific notation is more easily understood by excel or other libraries
                print('F1 = ' + F1)
        ws['D' + str(excel_row)].value = float(
            F1)  # Sets the value of the worksheet in column C for this row to the
floating point version of the pulse frequency we just isolated.

        ws['E' + str(excel_row)].value = open_file[0].header['PROJID']
        ws['F' + str(excel_row)].value = open_file[0].header['FRONTEND']
        ws['G' + str(excel_row)].value = open_file[0].header['BACKEND']
        ws['H' + str(excel_row)].value = open_file[0].header['BECONFIG']
        ws['I' + str(excel_row)].value = open_file[0].header['OBSFREQ']
        ws['J' + str(excel_row)].value = 1 / float(F0)
        excel_row += 1  # Increments forward to the next row in the excel
spreadsheet.
    except:
        print("Found another bad egg.")
print("Only {} files were useful.\n".format(excel_row))

#####   Make a Scatter Plot

chart = ScatterChart()
chart.title = pulsar_name + " Decay Curve"
chart.style = 13
chart.x_axis.title = 'Time'
chart.y_axis.title = 'Pulse Period'

xvalues = Reference(ws, min_col=2, min_row=2, max_row=excel_row)
yvalues = Reference(ws, min_col=10, min_row=2, max_row=excel_row)
series = Series(yvalues, xvalues)
# series.marker = openpyxl.chart.marker.Marker('x')
series.marker = openpyxl.chart.marker.Marker('x')
series.graphicalProperties.line.noFill = True
chart.series.append(series)
```

```
# print(dir(series))
# print(dir(series.graphicalProperties))
ws.add_chart(chart, "J10")

wb.save(folder_path + '/pulsar_freqs.xlsx')  # Saves the Workbook to this location
```

Appendix C

RStudio Curve Fitting Script

```
---
title: "J1550-5418_General_Model"
author: "Joshua Carroll"
date: "11/1/2021"
output:
  word_document: default
  html_document: default
---

```{r setup, include=FALSE}
knitr::opts_chunk$set(echo = TRUE)
```

#Load proper libraries
```{r}
library(tidyverse)
library(lubridate)
```

#Import Pulsar Data
```{r}
library(readxl)
J1550_5418_Output <- read_excel("J1550-5418 Output.xlsx") %>%
  arrange(t) %>%
  rowid_to_column() %>%
  mutate(t.seconds = as.numeric(t - min(t)))
```
```

```

#Plot the original dataframe:

```{r}
J1550_5418_Output %>%
  ggplot(aes(t.seconds, P)) +
  geom_point() +
  labs(title = "Pulsar J1550-5418", subtitle = "Raw data plot", y = "Pulse Period (s)", x = "Time (s)" ) +
  theme_light()
```

#Subset dataframe without apparent outliers:

```{r}
J1550_5418_Subset <- J1550_5418_Output[-c(35,36,37,38,39,40,41,42,43,44,201), ]

```

#Plotting the subset data:

```{r}
J1550_5418_Subset %>%
  ggplot(aes(t.seconds, P)) +
  geom_point() +
  labs(title = "Pulsar J1550-5418", subtitle = "Data plot with outliers removed", y = "Pulse Period (s)", x = "Time (s)" ) +
  theme_light()
```

#Define model constants

```{r}

c = 2.99792458*10^10 # Speed of light (cm/s)

R = 10^6 # Canonical radius of a pulsar (cm)

I1 = 10^45 # Moment of inertia

X0 = pi/2 # Assumed initial angle of dipole beam

k = (8*pi^2*R^6)/(3*I1*c^3) # Pulsar constant (cgs)

k

```

#Potential Parameter Values

```{r}

n = 2.706 # Braking index

#B = 2.231*10^14 # Estimated Magnetic flux (Gauss)

P0 <- as.numeric(J1550_5418_Output[1,5]) # Initial pulse period of pulsar

td0 <- as.numeric(J1550_5418_Output[236,6]) # Age of star/time of star observation

P0

td0

```

#Generalized Model

$$
```

P(t) = \left [P_0^{n-1} + \frac{n-1}{2} (t_d k B^2)^{\frac{n-1}{2}} \sin^2 (\chi_0 (1 - exp(-2t/t_d))) \right]^{\frac {1}{n-1}} \qquad \textrm{where} \qquad k = \frac{8 \pi ^2 R^6}{3Ic^3}

$$

#Generalized Model and Function:

```{r}

Gen_Pulsar_Model <- P~(P0^(n-1)+((n-1)/2)*((td*k*B^2)^((n-1)/2))*(sin(X0*(1-exp(-2*t.seconds/td))))^2)^(1/(n-1))

gen_pulse_period_function <- function(B, n, td, t.seconds){

  (P0^(n-1)+((n-1)/2)*((td*k*B^2)^((n-1)/2))*(sin(X0*(1-exp(-2*t.seconds/td))))^2)^(1/(n-1))

}

```

#Generalized Model Curve Fit

```{r}

CrvFit <- nls(formula = Gen_Pulsar_Model, data = J1550_5418_Output, start = list(B=2*10^14, td=td0), trace = TRUE)

summary(CrvFit)

```

#Extracting the calculated magnetic field strength and alignment time

```{r}

Bval <- summary(CrvFit)$coefficients[1,1]

td1 <- summary(CrvFit)$coefficients[2,1]

Bval

td1

```

```{r}

J1550_5418_Output %>%

  ggplot(aes(t.seconds, P)) +

  geom_point() +

  geom_function(fun = gen_pulse_period_function, args = list(B = Bval, td=td1, n=2.706), colour = "blue")
+

  labs(title = "Pulsar J1550-5418", subtitle = "Curve fitting using nls()\n\nn=2.706 \n\nB=2.87e+14 G", y =
"Pulse Period (s)", x = "Time (s)" ) +

  theme_light()
```

#Simplified Term Calculations

```{r}

LAM <- k*((Bval)^2)*td1

LAM2 <- sqrt(LAM)

A<-LAM2/P0

LAM

A



```

Appendix D

RStudio Time Prediction Script

```
---
title: "Time Prediction Model"
author: "Joshua Carroll"
date: "12/4/2021"
output:
  word_document: default
  html_document: default
---

```{r setup, include=FALSE}
knitr::opts_chunk$set(echo = TRUE)
```

#Load proper libraries
```{r}
library(tidyverse)
library(lubridate)
```

#Import Pulsar Data
```{r}
library(readxl)
J1550_5418_Output <- read_excel("J1550-5418 Output.xlsx") %>%
  arrange(t) %>%
  rowid_to_column() %>%
  mutate(t.seconds = as.numeric(t - min(t)))
```
```

J1550_5418_Output

```

#Define model constants

```{r}

c = 2.99792458*10^10        # Speed of light (cm/s)

R = 10^6                    # Canonical radius of a pulsar (cm)

I1 = 10^45                  # Moment of inertia

X0 = pi/2                   # Assumed initial angle of dipole beam

k = (8*pi^2*R^6)/(3*I1*c^3)  # Pulsar constant (cgs)

k

```

#Parameter Values

```{r}

n = 2.706                   # Braking index

B = 2.9*10^14               # Magnetic flux (Gauss)

P0 <- as.numeric(J1550_5418_Output[1,5])      # Initial pulse period of pulsar

td <- as.numeric(J1550_5418_Output[236,6])

P0

td

```
```

#Generalized Timing Model

$$

t_{(P)}= -\frac{1}{2}t_d \ \ln \left [1-\chi_0^{-1} \sin^{-1} \left [\left(\frac{P^{n-1}-P_0^{n-1}}{ \left (\frac{n-1}{2} \right)\Lambda^{\frac{n-1}{2}}} \right)^{\frac{1}{2}} \right] \right] \qquad \textrm{where} \qquad \Lambda = k \ t_d \ B^{2}

$$

#Simplifying Terms

```{r}

a=(k*td1*Bval^2)^((n-1)/2)

A=((n-1)/2)*a

A

```

#Calculating Y maximum

```{r}

Pf <- as.numeric((J1550_5418_Output[236,5]))

Y=(((((Pf)^(n-1))-((P0)^(n-1)))/A))^(1/2)

Pf

Y

```

#Generalized Timing Function:

```{r}

gen_time_function <- function(P){
  (-td1/2)*log(1-(X0^(-1))*asin(((((P^(n-1))-(P0^(n-1)))/A)^(1/2))/Y))
}

```

#Test the timing model:

```{r}
v=212

Pt <- as.numeric(J1550_5418_Output[v,5])

Actual_time <- as.numeric(J1550_5418_Output[v,6])

tt <- gen_time_function(P=Pt)

t_error <- abs(tt-Actual_time)

min <- t_error/60
hour <- min/60
day <- hour/24



tt
Actual_time
t_error
```

min

hour

day

```

#Import Pulsar Data

```{r}
J1550_5418_Output_Predictions <- read_excel("J1550-5418 Output.xlsx") %>%
  arrange(t) %>%
  rowid_to_column() %>%
  mutate(t.seconds = as.numeric(t - min(t)))%>%
  mutate(T_Predict = gen_time_function(P=P))%>%
  mutate(LOG_ACT_T = log(t.seconds))%>%
  mutate(LOG_PRD_T = log(T_Predict))%>%
  mutate(T_error = abs(T_Predict-t.seconds))
J1550_5418_Output_Predictions
```

#Plotting Time estimate versus actual time:

```{r}
J1550_5418_Output_Predictions %>%
  ggplot(aes(t.seconds, T_Predict)) +
  geom_point() +
  geom_abline(intercept = 0, slope = 1, size = 0.5, color="red" ) +
  labs(title = "Actual Time vs Predicted Time ", y = "Predicted Time (s)", x = "Actual Time (s)" ) +
  theme_light()
```
```